Condition Assessment of Electrical Contacts of Disconnectors

F.K. Mensah

Master of Science Thesis

Electrical Engineering Mathematics and Computers Science

Department of High-Voltage Components and Power Systems

Delft University of Technology

February 2011

Supervisor: Dr. ir. S. Meijer

Abstract

Electrical power supply system consists of three major parts: generation unit, transmission unit and distribution units. Each of these units consists of much high voltage equipment such as disconnectors. To ensure the reliability of the electricity supply, this equipment must be maintained. For TenneT TSO bv, the primary electricity transmission operator of the Netherlands, the need is to have insight into the condition of this equipment without taking them out of operation. In other words, to be able to perform online condition assessments of disconnector contacts.

A contact is characterised by its temperature and resistance therefore the conditions of the contact can be determined either by its temperature or resistance. The temperature of the contact can be measured on-line by means of infrared camera; infrared thermography. Infrared thermography is a non-contact and non-destructive technique well suited for devices operating under high voltage or carrying high current. Unlike the contacts temperature, the resistance of the contact can only be measured off-line. Measuring the contacts resistance online will mean physically connecting the measuring equipment to the high voltage system which is not only dangerous to the employees but also cause damage to the measuring equipment. The advantage of resistance measurements is that, it is more accurate as it directly describes the condition of the contact.

A widely used method to evaluate the results from thermography is the delta-T temperature ratings; a qualitative method used to assess the severity of overheating of the contact. Although this technique is safe and easy, it has the disadvantage of not accounting for the load current which is crucial in temperature measurements. The aim of this research is to use the thermal data obtained online to determine the offline numerical value of contacts resistance.

To fulfil this goal two models where developed, a thermal model and a resistance model. The thermal model is used to investigate the factors that affect the temperature of the contact such as wind, sun and load current and also assess the contacts condition based on its temperature rise. The resistance model is based on a steady state heat transfer analysis and uses the data obtained from online measurement to determine the numerical value of the off-line contacts resistance. The two models were tested on samples in the high voltage laboratory of Delft University. Next to this the thermal model was tested on the on-line disconnectors at two substations of TenneT TSO bv. One of which was an outdoor substation and the other an indoor substation.

The results found were that the resistance models can estimate the off-line numerical value of the contact with 6% accuracy provided that the resistance of the contact is high. On the other hand the model fails to predict the off-line resistance value when the contact has low resistance. This is due to the fact that when the resistance is low, the temperature

of the surfaces in the neighbourhood of the contact, on either side is higher. Next to this finding is the fact that the convection heat transfer correlations specified for horizontal are for Rayleigh number in the range of 10^5 to 10^{10}. The values found for the calculation were in the range of 262-807 for the very low resistance and 551-10^3 for the high resistance

The measurements performed in the substations were less accurate because of the limitations of the infrared camera. This was because too many factors affect the temperature measurements such as reflections, distance from object to camera and emissivity which is the most vital material property for radiation. Furthermore there were no way of assess the condition with the resistance model due to the fact that the dimensions of the contact were unknown.

Table of content

1. Introduction

Electrical power supply system consists of three major parts: generation units, to produce electricity, transmission units to transport electricity from the generating plant to the area to be used and distribution units, to connect the individual customers to the electrical power system[1]. These three parts in turn consist of many types of high voltage equipments, such as: transformers, switchgears, disconnectors, cables and many more. These equipments are interconnected to make power supply possible i.e. each device is coupled with an electrical contact to the next one. Hence there are many electrical contacts in the electrical power grid. An example of an electricity grid is shown in figure 1.1.

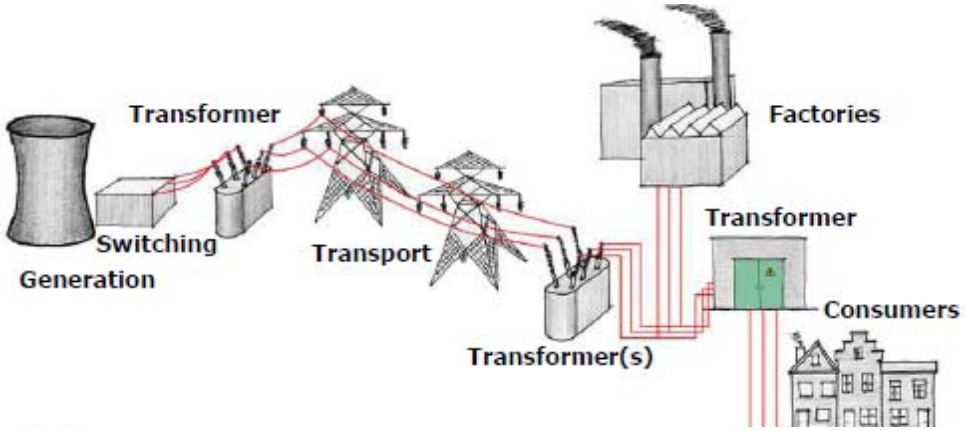

Figure 1.1 Electricity grid

The electrical contacts in the electrical grid are not only between two different equipment, but also can be between parts of the same equipment to create a current path One such equipment where there is an electrical contact between its parts is the disconnector , shown in Figure 1.2. The figure also shows the contact points of the disconnector , A and B are the contact points for other devices. C is the main contact zone which connects the two parts of the disconnector. Disconnector contact is the main topic of this thesis and will be addressed in more details later on in this report. But first the function and types of diconnectors are addressed in the next section.

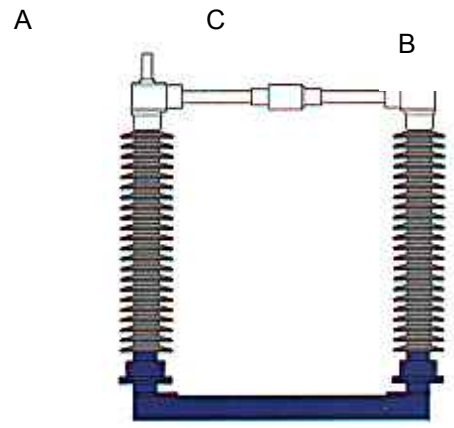

Figure 1.2 a centre break disconnector

1.1 Introduction to disconnectors

This section addresses briefly the main function of disconnectors and also provides a short out line of the most common types of disconnectors in practise.

General function Disconectors

One of the devices encountered in substations are disconnectors. The main function of disconnectors is to isolate one part of the system for operational reasons or for maintenance and repair purposes. In closed position disconnectors must be able to carry their rated load current as well as their rated short circuit current. In open position they must provide isolation against the rated power frequency voltage and overvoltage due to switching or lighting impulse voltages[2]. Therefore the reliability of disconnectors is very important for the personnel safety as well as for operational reasons.

Types of disconnector

Disconnectors come in a variety of types. For this report only the four most common types encountered are briefly reviewed: Centre break, double break, Pantograph and Vertical break types.

- *Centre break type*
  Figure 1.3 illustrates a centre break disconnector. This type is the most commonly used. The active parts are the two blades which make and break at the centre. The centre break disconnector requires lager inter-phase distance than standard values due to the fact that the blades rotate horizontally. On the upside, it is simple to construct and can be easily mounted to fit station profile.

Figure 1.3 centre break disconnector in closed position [Hapam website].

- *Double side break type*
  The double side break disconnector, see figure 1.4 is a variant of the centre break disconnector. The active parts consist of two jaw assembly, one at each end and a rotating blade. The centre rotates to open or close the disconnector. Contrary to the centre break type, this type provides two breaks in series, requires minimal inter-phase distance and allows higher loads on high voltage terminals.

Figure 1.4double break disconnector in closed position

- *Pantograph type*
  The pantograph type is shown in figure 1.5. The active parts consist of fixed

arrangements attached to a busbar, a blade and a hinge. This type requires the least inter phase spacing compared to the two types mentioned previously.

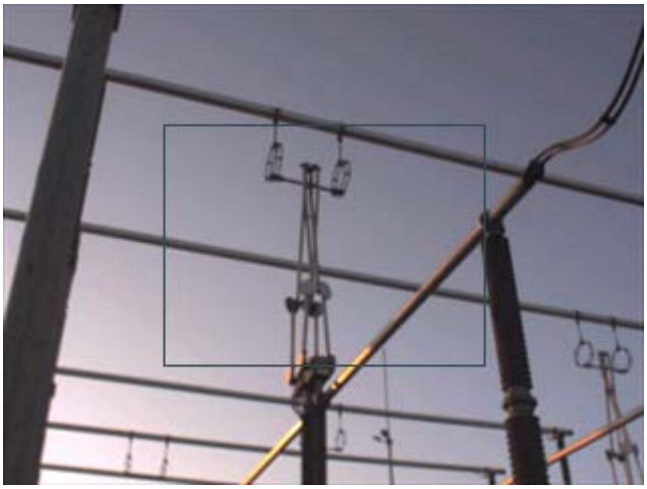

Figure 1.5 pantograph disconnector in closed position

- *Vertical break type*
  Figure 1.6 shows a vertical break disconnector in open positions. The active parts are the hinge end assembly, the blade and the jaw end assembly. Just like the pantograph type this type is used in places where there is enough overhead space to accommodate the vertically rotating blade.

Figure 1.6 Vertical break disconnector in open position [Hapam website].

In the introduction of this section it was mentioned that because of safety reasons disconnector must be reliable. In order to achieve highly reliable disconnectors, they must

be maintained on a regular basis. In practise there are different maintenance strategies and diagnostics tools available; this subject is briefly reviewed in the coming paragraph.

1.2 Available diagnostics for disconnectors

To ensure that disconnectors fulfil the function of isolation and thus, guarantying the safety of the workers, and eliminating any malfunctioning or failure of the component, it is essential that they are properly maintained. There are fundamentally three different maintenance strategies in practise[3, 4]:

- Corrective maintenance: This is done after failure of the equipment.
- Time-based maintenance or preventive maintenance: maintenance done at predefined time intervals to avoid failure.
- Condition based maintenance also known as predictive maintenance: Condition assessment is performed on equipment followed by appropriate action to avoid the consequence of the failure.

The purpose of diagnostic is to provide information about the state of the equipments. The information obtained from diagnosing the equipments can be used to asses the condition and in case of any abnormalities that can cause failure to the equipment, the adequate action can be undertaken to prevent that failure. For disconnectors, some of the parameters and diagnostics used in maintenance strategy to test the functionality are summarised here below [5].

Table 1.1 diagnostic techniques for disconnerctors

Functionality	Parameter	Method
Mechanical operation	Operating time	Motor running time
Conducting ability	Contact resistance	Four point resistance measurements
	Temperature of contacts and breaker units	Infrared imaging Temperature profiling Temperature at a point
Switching function	Contact travel characteristic measurements	Dynamic position sensor with: • Analogue output • Digital output

1.3 Problem definition

Poor or defected contacts have been claimed to be responsible for the majority of faults occurring in disconnectors[6, 7]. These faults often result in failure of the equipment which in turn can lead to the interruption of the electricity supply for part of the power system. Examples of a failed disconnector contact which lead to a total system failure were found in the Swedish transmission system. The two blackouts in Sweden were caused by failed disconnector contacts[6] . It is therefore important that electrical contacts of electrical equipment are maintained at high levels.

Due to ageing, overheating and wear the contact resistance will increase during its service life time .Therefore, the contacts condition can be assessed by measuring this resistance. The contacts resistance is the most suitably characteristic of the contacts because it directly describes the contacts condition [7-9]. This direct approach, although accurate is less favourable due to the fact that, it is not possible to measure the contact resistance on-line. In particular, the measuring equipment will have to be physically connected to the high voltage system which is not only dangerous to the employees but also cause damage to the measuring equipments.

It is known that when current passes through a resistance, heat is generated. The temperature of the contact will rise because of this heat generation. The temperature rise not only depends on the magnitude of the current but also on the magnitude of the contact resistance. The higher the contact resistance or current the higher the temperature rise. This makes the temperature of the contact a suitable parameter to assess the contacts condition [7, 9]. Even if the contacts temperature indirectly describes the contact resistance, it is more favourable than the contacts resistance, as temperature can be measured remotely which makes it easier to measure it on line.

Therefore, to be able to assess the contacts condition on-line a model is needed to relate the temperature rise at the contact to the contacts resistance. The classical approach with regard to infrared temperature measurements is to utilize the delta- T temperature ratings to assess the severity of the overheating. The main question now is, is it possible to use the temperature data to determine the contact resistance? Hence the problem definition of this thesis is:
Investigate the possibility to establish a relationship between contact resistance and infra-red temperature measurement to assess the condition of electrical contacts.

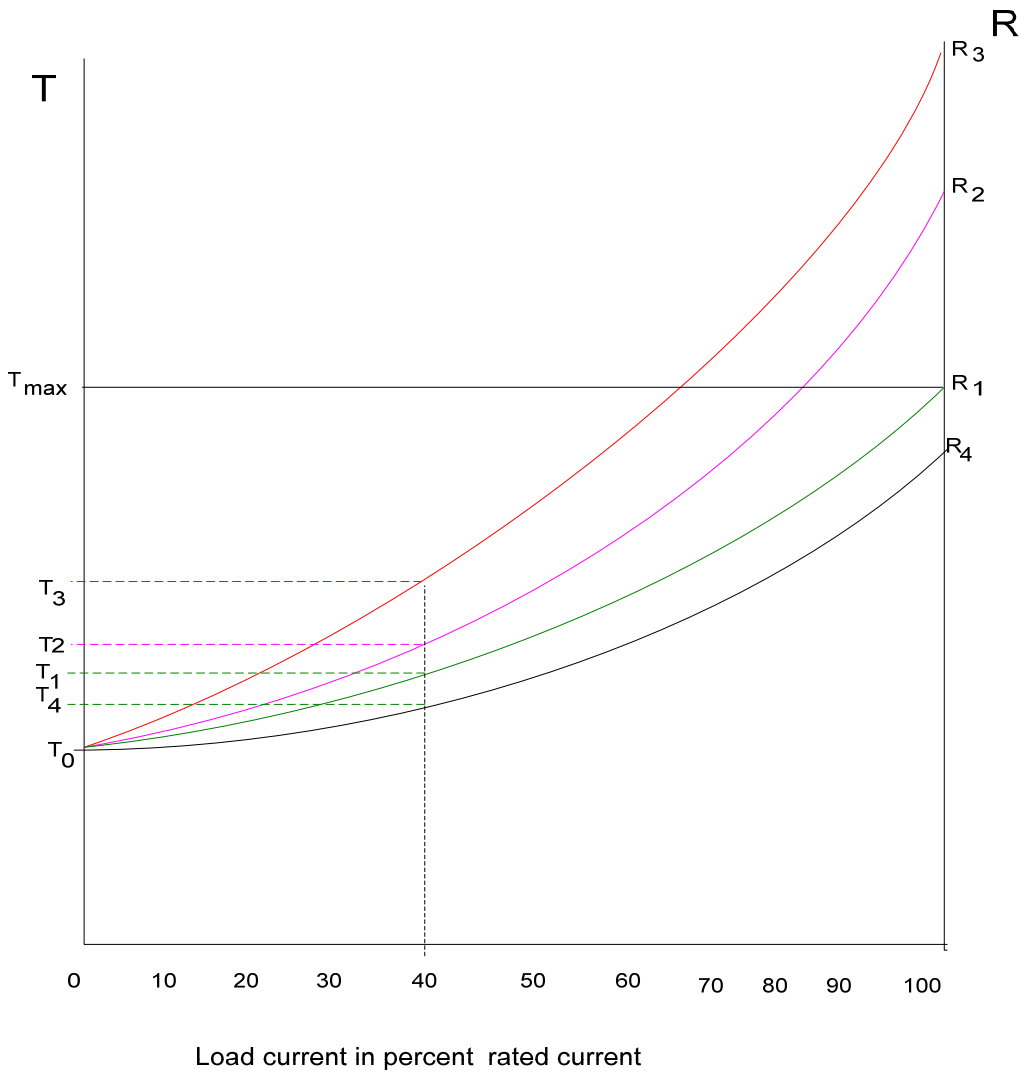

Figure 1.7 idea to be that will be studied in this thesis

Figure 1.7 illustrates the idea behind the proposal of this thesis. The green curve in the plot represents the initial resistance and T_0 is the no load temperature. For example at 40 % rated current the temperature of the contact should be T_1. If the temperature however, is T_2 then from this knowledge it should possible to determine R_2.

2. Disconnector contact

To be able to asses the condition of the disconnector contact it is necessary to understand the subject of electrical contact. The diagnostic methods and parameters will be discussed after briefly reviewing some of the fundamental concepts of electrical contacts

2.1 Electrical Contact

An electrical contact is defined as an electrical connection between two conducting elements [8]. The purpose of contacts in an electrical circuit is not only to provide current path between conducting elements or isolate current paths from each other. But also, when closed, to carry current and to interrupt current when open. Especially in close position, it is essential that the contact is tight. For this to happen, the connection between the two contact parts must be good. Depending on the operation, electrical contacts can be divided into three major categories[10] :

- Static contacts: Static contacts are the ones with permanent electrical connections over their entire life span.
- Switching contact or make- and- break contacts: Switching contacts consist of pair of contacts that open and close on demand.
- Sliding contacts: Sliding contacts consist of at least one fixed part and one moveable part that slide over the fixed part.

Disconnector contacts are of the make and break type, and are often made of silver-plated copper contacts designed to carry load currents without excessive temperature rise. Figure 2.1 shows a typical disconnector contact.

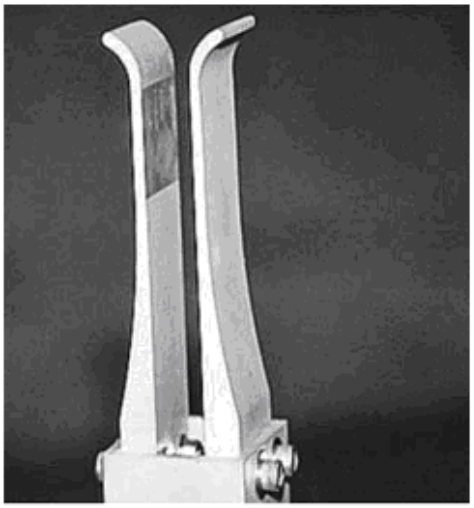

(a) Silver plated jaw

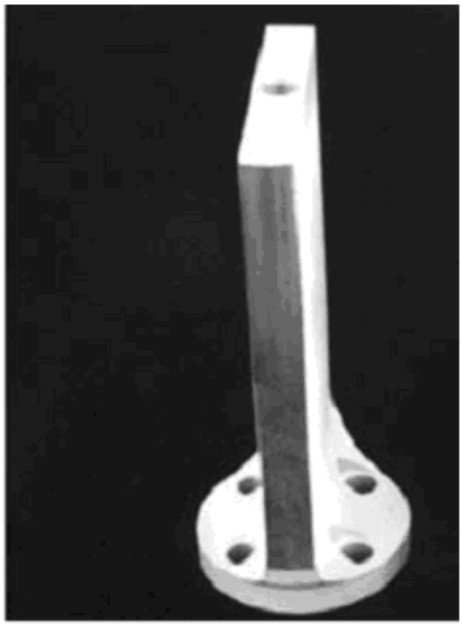

(b) Silver plated blade

Figure 2.1 typical example of disconnector contact

2.2 Contact behaviour

Regardless of the category, the contact resistance primarily depends on [11, 12]

- Condition of the surface
- The mechanical force applied (contact pressure)
- Type of material

Every surface has a roughness, thus when two metals are brought together to form a contact, not the whole surface will contribute to the conducting path of the contact. The actual contact between the two surfaces takes place at limited number of spots making the actual contact area smaller than the theoretical area. These spots form the conducting or electrical path, therefore when electrical current is applied to the contact it will flow through these spots. When there is enough pressure on the contact the connection between the two surfaces will be tight and hence the contact resistance will be small, contact is good, (e.g. new contact). In this case, the conducting area or electrical path is

larger and so the current will be evenly distributed over the entire area (fig2.2a). On the other hand, when the connection between the two metals is not good or tight enough the conducting area becomes smaller which will cause the current to pass through a smaller surface (fig 2.2b). During the operating life of the contact, the contacts resistance will increase. The increase in resistance is caused by chemical compounds or oxides present at the contacts surface. An increase in resistance will lead to more heat generation and hence causing substantial temperature rise at the contact. A rise in temperature in turn will accelerate the oxidation process at the contact surface and lead to additional resistance. This process will eventually lead to the failure of the contact.

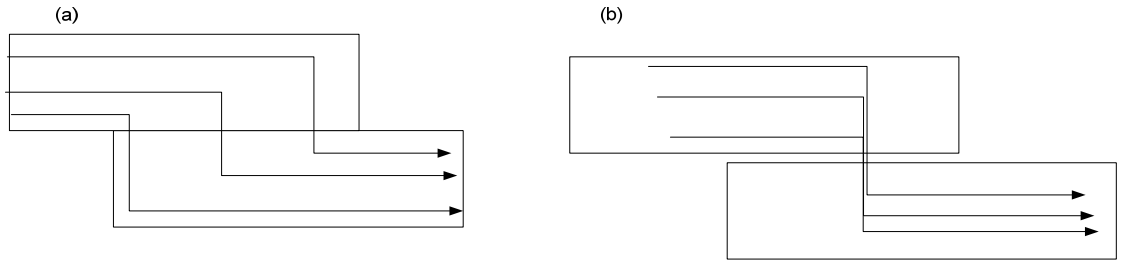

Figure 2.2 current flow through contact of two metals a) good contact b) bad contact

In case of disconnectors, the contacts open and close on demand. Especially in the open position due to chemical reaction with the environment a tarnish layer is formed on the surface which will cause a significant increase of the resistance at the contact. The total resistance of the contact is the resistance of the layer formed at the surface which has a higher resistance because of the non-conducting nature plus the actual contacts resistance. Due to thermal stress caused by load application the contact will show signs of degradation over its life time. The contact degradation is slow at first but at some stage this process will rapidly accelerate to a final stage that will eventually lead to the failure of the contact [13]. It is therefore important to diagnose the contact, because it provides information about its condition. The information obtained from diagnostic can be used to support decision making about operation, repair and replacements of the disconnector before the final stage of degradation occurs.

The diagnostic methods and tools applicable to disconnector contacts are reviewed in the next paragraph.

2.3 Contact diagnostics

In order to perform a successful maintenance on equipment, not only the diagnostic tool and associated methods must be determined but, also the parameters that determine the performance and thus contribute to the reliability of the equipment must be identified. Since the object of interest for this thesis is disconnetor contact, only the diagnostic methods used in this particular category are considered.

2.3.1 Condition Parameters

It has been stated previously that the contact is characterised by it resistance and temperature. The condition of the contact can be determined either by on-line diagnostics or off-line diagnostics. For on-line diagnostics, the temperature of the contact is measured; off-line diagnostics usually consist of resistance measurements. A good contact has a lower resistance value than a bad contact. Furthermore, the contacts temperature depends initially on the contact resistance. An excessive temperature rise or resistance increase clearly indicates abnormalities at the contact. Therefore parameters describing the condition of electrical contacts are:

- Temperature
- Resistance

2.3.2 Resistance measurements

Contact resistance measurement is one of the methods used to test the current carrying ability of disconnectors [5]. The electrical resistance of a contact is more suitable characteristic to evaluate the condition of the contact as it directly describes the condition of the contact. This method can only be done off-line, as it is impossible to measure on line because measurements done under high voltage conditions pose great danger. Traditionally, the four-point measuring method is used when measuring low resistance values. The object whose resistance is to be measured, in this case the disconnector contact, has to be taken out of service, apply current from a separate current source to it and physically measured through wires, ammeter and volt meters (see figure 2.3). The problem with these types of measurements is that they can only be done off –line which means that part of the system must be taken out of service. The advantage is that, the measurements are accurate. The measured resistance(R in ohm) is the ratio of the voltage drop across the contact (V in volts) to the current (I in amps):

$$R = \frac{V}{I}$$

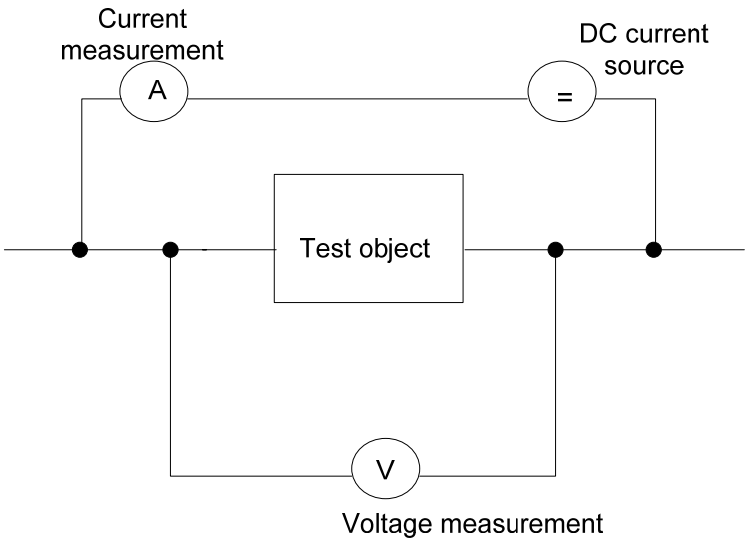

Figure 2.3 circuit for resistance measurement

2.3.3 Temperature measurement

Unlike resistance, the temperature is observable through the help of a measuring device such as infrared cameras. Overheating at the contact can be detected by thermal methods. These methods can be dived into two categories:

Contact Method: The temperature at the contact is measured by thermocouples and thermometers

Non- contact: The temperature at the contact is measured by means of infrared sensors and imaging system, and optical fibre measurements.

Infrared cameras can be used to measurements temperature variation on energized equipment. As oppose to resistance measurements, this method can be performed at any given time because these types of measurements can be done while the system is still in service. One of the great advantages of this technique is the fact that it is a non-contact and non –destructive technique well suited for devices operating under high voltage or carrying high current [3]. This technique however has the disadvantage of not being as accurate as the contact resistance measurements.

In this chapter a limited overview of the basic principles and aspects of electrical contacts that are important in the analysis of their condition state have been given. Electrical contacts in the electrical power grid are essential components and therefore must be maintained at high level. Maintenance of the contact is carried out by measuring the contacts temperature or resistance. Through diagnostics failure of the contact can be prevented. The next chapters will provide more details about the evaluation methods for the temperature and resistance measurements

3. Infrared Thermography

Infrared radiation was discovered in the 1800 by F.W.Herschel [9, 14]. His experiments showed that the region just beyond the red region, invisible to the human eye had the highest temperature. Herschel's discovery has led to many applications using infrared radiation, such as infrared thermography.

Although Infrared radiation is not visible to the human eyes, there are equipment such as thermal imaging cameras which can detect radiation in the infrared range of the electromagnetic spectrum and convert it into visual images called thermograms. This process is known as infrared thermography. Since all objects emit thermal radiation at temperatures above absolute zero, and the amount of emitted radiation increases with increasing temperature, thermography makes these temperature variations at the surface of the object visible. Infrared thermography is commonly used as a part of a preventive maintenance program, because it is safe and easy to use on electrical power equipments operating under high voltage conditions. Another advantage of this technology is the fact that it is a non-contact and non-destructive inspection technique [15].The inspection can be carried out over a wide area, while the equipment are under operation. A third advantage of this technique is, a poor or bad contact can be easily and quickly detected.

The basic principles of infrared thermography are based on the fundamental laws of thermal radiation as described next.

3.1 Background thermal radiation

Infrared thermograghy is based on the principle of thermal radiation, which is, all object emit energy as a result of having a temperature above absolute zero degrees Kelvin [12, 16, 17]. The intensity of the energy emitted by an object varies with temperature and wavelength. The wavelength of the thermal radiation is between 0.1 and 100 micrometers. This range is often subdivided into three categories in accordance with their wavelengths: a portion of the ultraviolet range, the whole visible range and the whole infrared rang as shown in figure3.1.

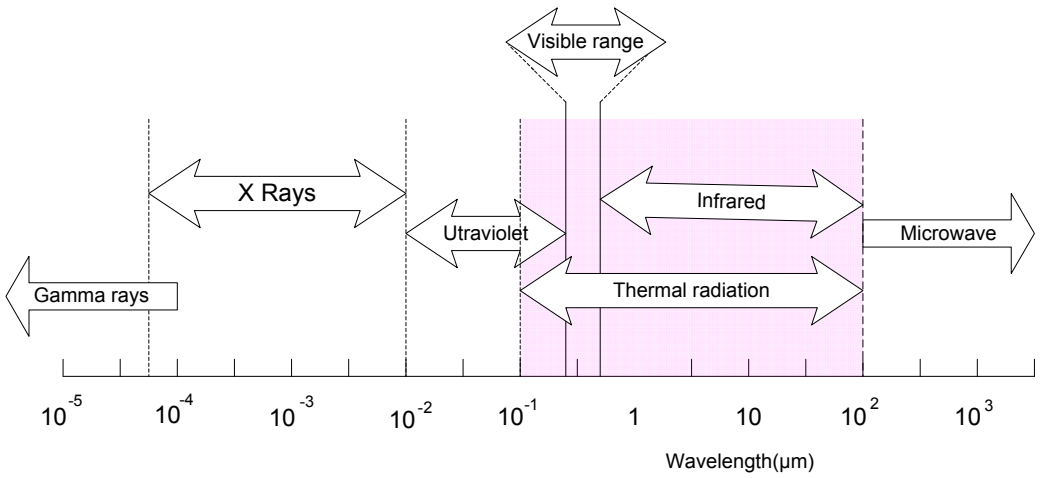

Figure3.1 Illustration of the thermal radiation part of the electromagnetic spectrum

To be able to understand the radiation properties of real surfaces a theoretical concept called blackbody is introduced .The theory of blackbody is described below.

3.1.1 Black body radiation laws

A blackbody is a perfect surface that absorbs and emits all incident radiation regardless of the wavelength, direction and the temperature. It was Planck who first determined the relation between wavelength, temperature and emitted energy. Planck determined that, a black body at temperature T, emits radiation power according to the following expression [12, 16, 17].

$$W_{b\lambda} = \frac{2\pi hc^2}{\lambda^5[e^{(hc/\lambda kT)} - 1]} \qquad (3.1)$$

Where h is the Plank constant (h = 6.6256 x 10^{-34} Js), c is the speed of light (c= 2.988 x10^8m /s), k is Boltzmann constant (1.3805x10^{-23} J/K) and T the absolute temperature (K). The relationship between temperature, wavelength and the emissive power of a blackbody is depicted in figure 3.2.

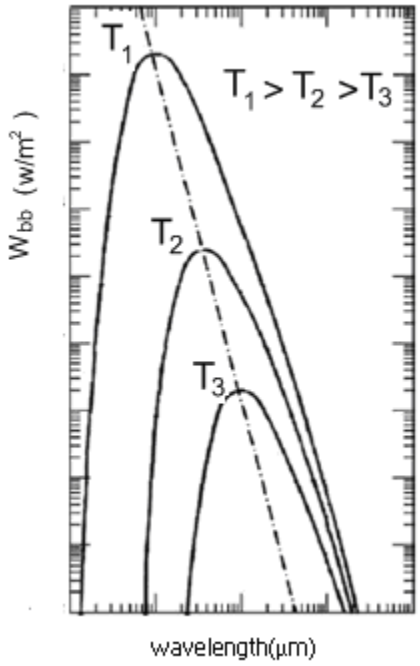

Figure 3.2 Black body emissive powers according to Planck's law

The figure shows that as the temperature increases the total emitted energy per unite area increases and the maximum emissive power shifts to shorter wavelength. The wavelength corresponding to the maximum radiation energy is given by formula 3. 2 and is known as Wien's displacements

$$\lambda_{max}T = 2.898x10^{-3} \text{ [12]} \quad (3.2).$$

Where, λ_{max} is the wavelength of maximum radiation.
The dashed line in the figure shows the location of the maximum emitted power, and the corresponding wavelength with increasing temperature.
From Planck's law the total radiated energy from a blackbody at temperatureT can be obtained by integrating formula 3.1 over the entire wavelength range. The result of the integral is given by Stefan-Boltzmann law:

$$W_{bb} = \sigma T^4 \text{ [12]} \qquad (3.3)$$

Where σ is the Stefan-Boltzmann's constant ($\sigma = 5.67 \times 10^{-8}$ W/m^{2}K^4)

Unlike black bodies, most surfaces encountered in power systems are not perfect radiators or emitters. However, there are ways to characterize the radiation properties of non-black bodies. For example to able to describe the surface emission of a non-black body, a dimensionless quantity known as emission coefficient or emissivity (ε), is introduced. This radiation property is described in the next section because of its importance later on in this report

3.1.2 Emissivity

Emissivity is defined as the ratio of the radiation intensity of a nonblack body to the radiation intensity of a black body. This explains the importance of the black body law, because it serves as a standard to which the radiation properties of real life surfaces can be compared. The mathematical expression for emissivity is given by equation 3.4 [9, 18].

$$\varepsilon = W_o / W_{bb} \qquad (3.4)$$

Where W_o is the total radiant energy emitted by a non-black body at a given temperature (T) and W_{bb} is the total radiant energy emitted by a black body at the same temperature and is always less than one or equal to one.

The emissivity of real surface is not constant and varies with temperature of the surface, direction of emission and wavelength [12, 16, 17].

Dependency of the emissivity on the nature of surface

The emissivity value also depends strongly on the nature of the surface. A bright shinny surface has lower emissivity than a rough dull surface. The influence of the surface finish on the emissivity value is shown in figure 3.3. Looking at this figure it is seen that polished copper has very low emissivity value. This value is increased by the presence of an oxide layer, achieving a value of almost 1 for black oxidized copper.

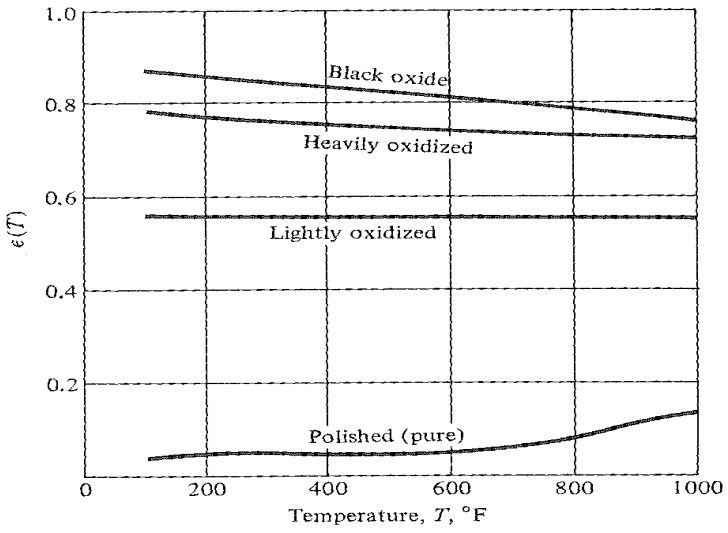

Figure3.3 Effect of oxidation on emissivity of copper [12]

Temperature dependency of the emissivity

The emissivity values of selected material in the temperature range that is of interest to this project are listed in table 3.1. These values are taken from the camera specification and [12, 17] . In table 3.1 some of the emissivity values are missing. This is because different authors give different values for different temperature and most values are often limited to one temperature, the state of the surface is also different in each table. This table is constructed from the different values from different sources to show the temperature dependency of the emissivity. Even though it is not clear from table 3.1 how the emissivity value is affected by the temperature, some authors state the emissivity of conducting materials increase with increasing temperature, but for non-conducting materials the emissivity may increase or decrease with temperature depending on the specific material [12, 17, 19].

Table 3.1 Effect of temperature on emissivity of selected metals

Emissivity (ε)							
metal	Surface state	Temperature[°C]					
		0	20	23	27	40	100
Alumimum	Highly polised				0.04[12]		
	Polihsed	0.05[20]		0.04[12]			0.06[14]
	Rough	0.07[20]					
	oxidized		0.11[21]				
	Strongly oxidated	0.25[20]					
Copper	High polished			0.03[22]			
	polished	0.01[20]	0.03[12]			0.02[14]	
	Oxidized	0.65[20]			0.78[14]		
	Black oxidized	0.88 [20]	0.78[12]			0.76	
Nickel	Polished	0.05[20]					0.045
	oxidized			0.42[21]			0.41[12, 22]
Silver	Polished		0.025[12, 22]				0.03[12]

Dependency of emissivity on the wavelength

Figure 3.4 shows how the emissivity of aluminium varies with wavelength. For polished

aluminium, the emissivity decreases with increasing wavelength. For anodized aluminium the emissivity fluctuate with the highest value between 8-10μm.

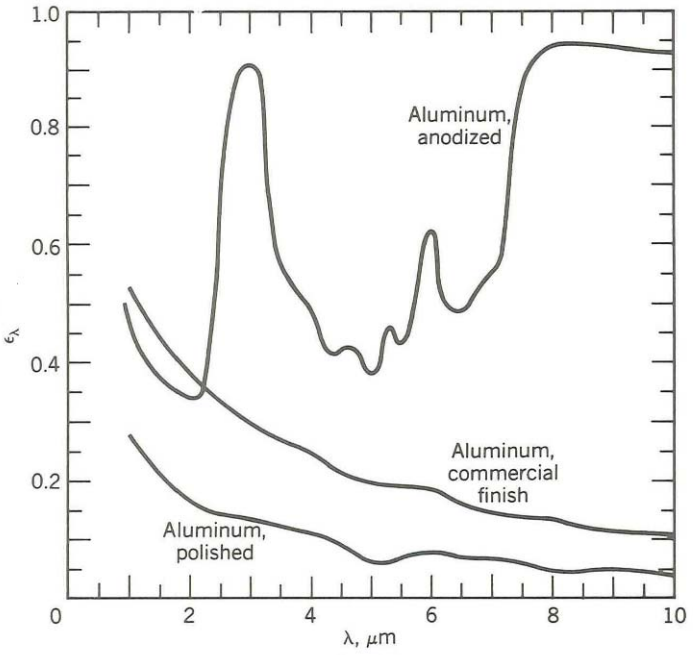

Figure3.4 Wavelength dependency of emissivity of aluminium[16]

The variation of the emissivity with the wavelength depends on whether the object is a conductor or non-conductor as well as the surface coating.

Dependency of emissivity on the direction of radiation

In figure 3.5 the directional dependency of emissivity of conductors and non-conductors are shown. It is observed that, for conductors the emissivity is constant between 0 and 40 degrees. After 40 degrees it will increase with increasing angle and then decay to 0. For non-conductors the emissivity is constant between 0 and 70 degrees after which it decreases sharply with increasing angle to 0.

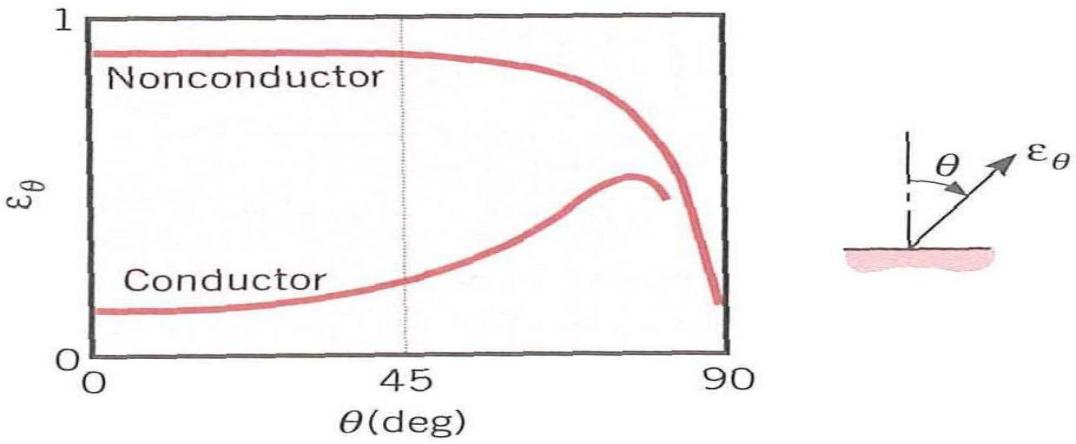

Figure3.5 Directional dependency of emissivity of conductor and non-conductor[17]

Emissivity is the most important surface property that affects the amount of emitted radiation energy from the surface. The importance and role of this property in the infrared thermography will be clearer in the following paragraphs, but first a brief description of infrared radiation is given.

3.2 Infrared Radiation

In the preceding paragraphs the basic concepts of thermal radiation have been discussed. It was also stated that infrared radiation is part of thermal radiation and the radiated energy is caused by the motion of atoms and molecules on the surface of an object having a temperature above absolute zero degrees Kelvin. The wavelength of the infrared radiation falls in the range 0.7 to 100 micro meters. Hence the principles of thermal radiation can also be applied to infrared radiation. Emissive power of an object varies with wavelength of radiation, direction of radiation and temperature of the object.
Since infrared themography operates in a limited spectral range it is convenient to carry out calculations using total properties. These are properties averaged over all wavelength and directions. The emissivity is therefore assumed to be constant over the entire wave length. Objects with constants emissivity at all wavelengths and direction are called gray bodies.
The total emissive power of a blackbody is given by formula 3.3 for real surface at the same temperature as the blackbody the total emissive power is less. The radiating power of a real surface are addressed in the proceeding subparagraph

3.2.1 Radiation energy balance of a real surface

The law of total radiation states that, when radiation is incident on a real surface, some of it is absorbed, some of it reflected and the rest is transmitted through the body[12, 16, 17]. Illustration of this statement is shown in figure 3.6.

The mathematical formulas governing the law of total radiation are given by equation 3.5 and 3. 6.

$$W_{incident} = \alpha W_{incident} + \tau W_{incident} + \rho W_{incident} \qquad (3.5)$$

Dividing each term in equation 3.6 by $W_{incident}$ gives

$$\alpha + \tau + \rho = 1 \qquad (3.6)$$

Where $W_{incident}$ is the total radiation energy incident on the surface of the object, αW the absorbed energy, τW the transmitted energy and ρW the reflected energy. The material properties α, τ, ρ are absorptivity , transmissivity and reflectivity respectively.

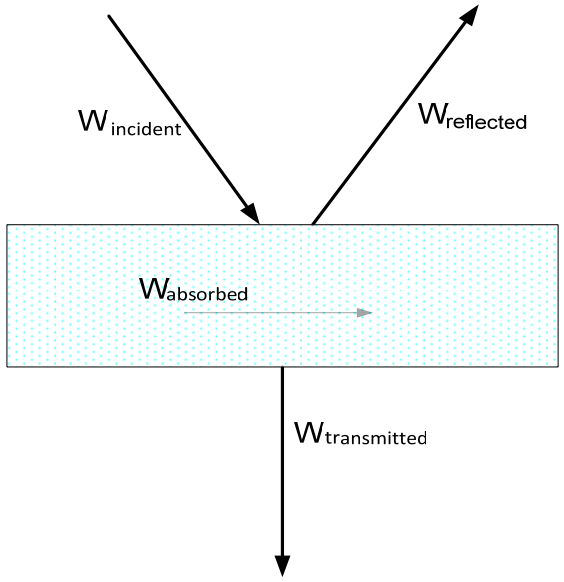

Figure 3.6 illustration of radiation energy balance

Although the energy balance equation as present here above is the general case. It forms the basis for determining the total amount of energy leaving the surface of the object and reaching the infra camera. This is done in the next paragraph.

3.2.2 Infrared temperature measurements

For this thesis one of the devices used to measure the temperature of the test object is the infrared camera. To be able to perform accurate temperature measurements, the energy received by the camera must be investigated. This is due to the fact that, the infrared camera measures the temperature of the target object; by measuring the amount of energy radiating from its surface.

From the thermal radiation law, an object with temperature higher than the absolute temperature will radiate energy. Combing this law with the energy balance equation, the total energy leaving the surface of the test object can be derived. In addition to the emitted energy from its surface, it will react to the incident radiation from its surroundings by absorbing a part of it, reflecting a part of it and transmitting the rest. The amount of energy radiating from the surface is therefore a combination of emitted energy, transmitted energy and reflected energy. On the basis of this theory the total radiation incident on the camera lens come from three sources:

- Radiated energy emitted directly from the target object (W_o)
- Radiated energy from other objects surrounding the target object which is reflected onto the target's surface (W_{amb})
- And radiated energy from other objects surrounding the target object which is transmitted through the target to the camera. ($W_{backgroud}$)

The amount of energy leaving the surface of the object is shown figure 3.7.

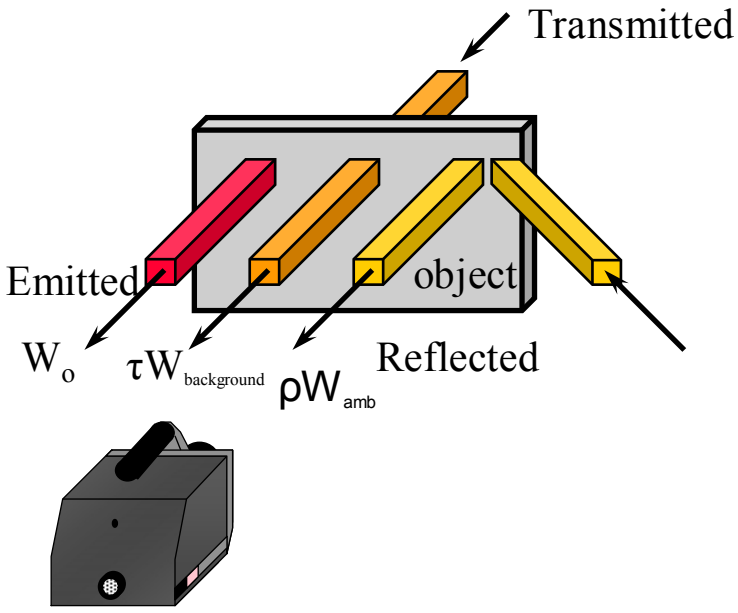

Figure 3.7The radiant energy leaving the surface of test object unto the camera lens

The total radiation energy received by the infrared camera can be derived as:

$$W_{cam} = W_o + \rho W_{amb} + \tau W_{backgrond} \quad (3.7)$$

Kirchhoff's law state that, the emission coefficient is equal to the absorption coefficient for any surface:

$$\varepsilon = \alpha \quad [12] \qquad (3.8)$$

Opaque objects are object that don't transmit energy through their body, thus the transmission coefficient of opaque bodies is:

$$\tau = 0 \quad [12] \qquad (3.9)$$

Using Kirchhoff's law and given there is no transmitted radiation from opaque objects equation 3.6 becomes:

$$\varepsilon + \rho = 1 \quad (3.10)$$

Or

$$\rho = 1 - \varepsilon \quad (3.11)$$

From equations 3.7 and 3.11 the radiant energy received by the camera from an opaque object can be written as:

$$W_{cam} = W_o + (1 - \varepsilon) W_{amb} \quad (3.13)$$

Figure 3.4 shows the radiant energy coming from an opaque object.

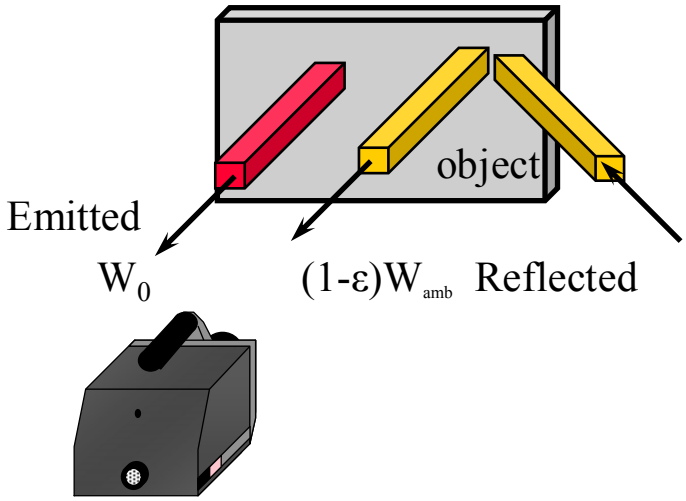

Figure 3.9 the radiant energy from an opaque object to IR camera

For a real life object the Stefan-Boltzmann law of emissive power takes the form:

$$W_o = \varepsilon \sigma T^4 \quad (3.14)$$

The emission from the ambient is

$$W_{amb} = \sigma T^4_{amb} \qquad (3.15)$$

Where W_0 and W_{amb} is the emissive power of the object and ambient respectively [W/m2] .

Therefore, the temperature of the object from a calibrated camera output can be calculated as:

$$W_{cam} = \varepsilon \sigma T^4 + (1- \varepsilon) \sigma T^4_{amb} \qquad (3.16)$$

Where T_{amb} , is the temperature of the air surrounding the object and ε the emissivity of the object. The first term on the right hand side of equation 3.15 is the radiation energy emitted by the object and the second term is the radiation energy reflected off of the target. If the object is colder than its background the camera will see more reflected energy than emitted energy.

It is clear from the camera output formula that, the infrared camera calculates the temperature of the object based on the amount of radiation it receives and the emissivity

of the object. Consequently, to be able to arrive at the correct temperature of the object, the camera will require input of the correct value of the emissivity of the object and the ambient air temperature. The ambient temperature can be measured with thermometers, measuring the value of emissivity is not as easy as the temperature and therefore will be considered in more details in the next section.

3.2.3 Determining the emissivity value of the object

There are various methods to determine or measure the emission coefficient of real life object whose temperature is to be measured.

The first method is the easiest; the value of the emissivity is read directly from tables often given by the manufacturer. The problem with this method is, it doesn't always work. From earlier discussion of the emissivity it was mentioned that, the value of emissivity depends on temperature as well as on the nature of the surface. In these tables the value of emissivity is given for a specific temperature and the nature of the surface is defined as highly polished to heavily oxidized surface. But how much oxides should be at the surface to satisfy heavily oxidized is not mentioned and thus is left to the thermogragpher's discretion.

A second method applies [14]:
Black tape or paint of known and high emissivity (e.g. 0.95) is placed upon a small surface of the target object. The surface temperature of the area marked with known emissivity is measured with the IR camera. Assuming the object has a uniform temperature distribution on the entire surface, the camera is then moved from the area of known emissivity to a different area of the objects surface. Calibrate the camera until the temperature reading is the same as that of the marked area, which gives the emissivity value of the object.

For TenneT, this method is the most attractive, for obvious reasons. The diconnectors of TenneT have been in operation for a while and embedding temperature sensors in the disconnectors is not a feasible choice from economical point of view. Secondly, thermometer or thermo couples won't solve the problem either because for thermo couples a recorder is needed to display the temperature reading, which will require very long wires to connect the thermo couple read out to the recorder and is not practical.

Another method is a variant of the second method [14]. The temperature of the object is measured by means of contact method (e.g. by thermometer). Then the IR camera is tuned until the temperature on the camera is the same as on the thermometer.

The data acquired from the infrared measurements must be analysed in order to assess the condition of the equipment. A widely used method to evaluate the results is the delta-T temperature ratings as presented in the next section.

3.2.4 Delta –T temperature ratings system

The delta-T rating is a qualitative method used to assess the severity of overheating the equipments. This method is based on the temperature rise of the target object above some predefined reference usually the ambient air surrounding the target or a similar object operating under the same condition as the target object. The temperature difference between the target and the reference are often divided into three or four categories to indicate the maintenance priority [4, 23]. Typical delta –T ratings are given in table 3.2.

Table 3.2 Thermographic Survey Suggested Actions Based on Temperature Rise[4]

Temperature difference based on comparison between similar components under similar loadings	Temperature difference based on comparison between components and ambient air temperatures	Recommended action
1°C–3°C	1°C–10°C	Possible deficiency; warrants investigation
4°C–15°C	11°C–20°C	Indicates probable deficiency; repair as time permits
–	21°C–40°C	Monitor until corrective measures can be accomplished
>15°C	>40°C	Major discrepancy; repair Immediately

The delta-T classification is good way to indicate a relative degree of severity that enables repair priority. However it does not say if the temperature limit of the equipment has been exceeded. Another disadvantage of the delta-T ratings is the fact that they don't account for the actual load and ambient temperature at the time of the infrared inspections [23].

A model which accounts for the load and ambient conditions that influence the temperature of the equipment is discussed in the next chapter.

4. Proposed Model for evaluation of the contacts condition

As stated in the previous sections the contacts condition can be determined by means of temperature or resistance measurements. In order to find the correlation between these two parameters a model is needed to establish the relation between the temperature rise at the contact and the contact resistance. If this relation can be determined, it should be possible to estimate the off line contact resistance numerical value using the temperature data obtained online, see figure 4.1 below.

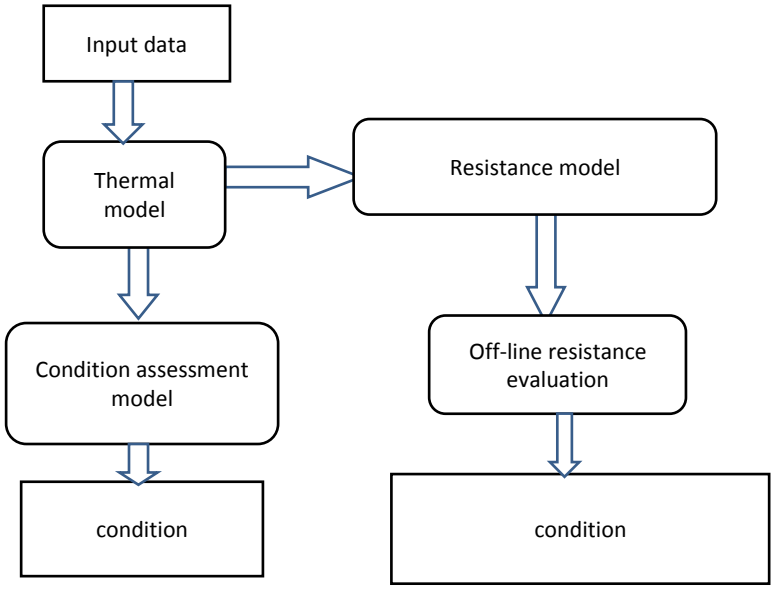

Figure 4.1 abstract block diagram of model

The development of this model will be done in two steps:
The first step is the thermal model, which will be used to calculate the temperature of the contact on the basis of some input data. Chapter 5 will describe the input data and also give a detailed description of this model. Chapter 6 deals with the resistance model, in this chapter the data obtained from the thermal model are used to evaluate the resistance of the contact.

5. Thermal model (On-line method)

As stated in previous sections, the temperature rise of the contact is one of the parameters to assess its condition. Therefore, in this model the factors affecting the temperature rise of the contact will be investigated before deriving a condition assessment of the contact based on its temperature rise.

5.1 Influencing factors

To diagnose the contacts condition based on its temperature behaviour, it is essential to study the factors that affect the temperature rise at the contact. In particular the following will be considered:

- The temperature rise at the contact above the ambient temperature due to the load current (I_{load})
- The effect of ambient conditions (A) such as, wind, sun and rain on the temperature
- The contact resistance - temperature behaviour: $T=f(R_{contact})$.

The temperature rise can then be determined as a function of these factors i.e.
$\Delta T_{contact} = f(R_{contact}, A, I_{load})$

Figure 5.1 shows a block diagram of the thermal model with all the data needed to calculate the contacts temperature.

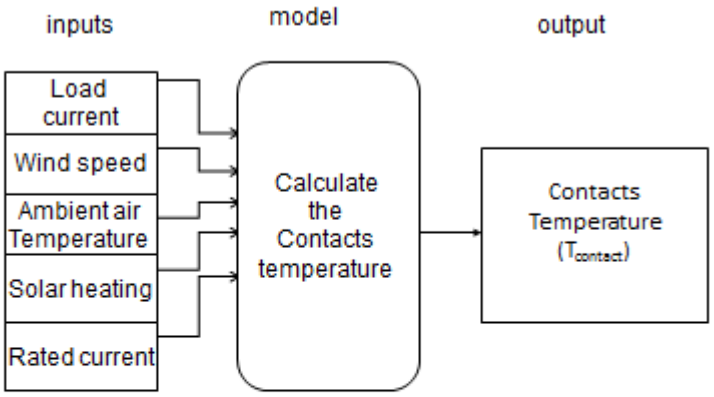

Figure 5.1 block diagram of thermal model

The influences of these parameters on the temperature of the contact are further addressed in the sections here below.

5.1.1 Temperature rise due to current Load

To understand the reason why the load current is an important factor to be considered regarding temperature measurement, it is necessary to consider the heat generation process in electrical device carrying current. When current passes through a resistance it produces power according to Joules' law:

$P=I^2R$ (5.1)

The electrical power input is converted to thermal power: heat. This means that as the electrical power input increases the thermal heat will also increase. The heat loss at the contact will translate to temperature rise at the contact. The heat dissipation according to Joules' law is proportional to the square of the load current. Therefore the temperature rise depends on the electrical current passing through the contact.

If other factors such as wind, rain and solar heating are neglected, then the relation between the maximum allowable temperature at the contact corrected for ambient air temperature at time of measurement and load current can be expressed as [4]:

$$T_{contact} = \Delta T_{\max}(\frac{I_m}{I_r})^n + T_{ma} \qquad (5.2)$$

Where:

ΔT_{max} is (the difference between the total rated temperature and the rated ambient temperature, often taken to be 40[°C]) the maximum temperature rise at full load specified by IEC standards[24].

T_{ma} = measured ambient temperature at time of measurement [°C]

I_r = rated current [A]

I_m = measured load current[A]

n= exponent (1.6-2.0)

Rearranging equation 5.2 yields the equations for the temperature rise at the contact:

$$T_{contact} - T_{ma} = \Delta T_{\max} (\frac{I_m}{I_r})^n \qquad (5.3)$$

$$\Delta T_{contact} = T_{contact} - T_{ma} \qquad (5.4)$$

$$\Delta T_{contact} = \Delta T_{\max} (\frac{I_m}{I_r})^n \qquad (5.5)$$

The temperature ratings as specified by the IEC standards are based on new contacts, operating under specified standard ambient conditions and operating under full load. Formula 5.2 therefore gives the temperature of a new contact which has the maximum temperature rise, corrected for load and ambient conditions different from standard conditions. With this temperature, it can be determine whether or not the contact is operating within its temperature limit. In figure 5.3 the contact maximum temperature and the contact temperature rise are plotted against the percentage of the load current for n=2 (2 is the theoretical value, the actual value of n often differs from this value) and ΔT_{max} is 35 degrees Celsius. It is clear from the graphs that, as the load current increases the temperature also increases. The maximum temperature is a function of the load current and ambient temperature (eq. 5.3). If the ambient for example increases from 20 to 25 degrees Celsius, the total maximum temperature will also be 5 degrees Celsius higher. The contacts temperature rise above the ambient air temperature stays the same. If the load current becomes lager than the rated current the temperature rise at the contact will exceed the limit of the maximum temperature rise (ΔT_{max}). This implies that the contact is overloaded rather than a bad contact. Had the operating current been unknown, one might conclude that the contact is bad; this is one of the reasons why the load current is crucial in temperature measurements and must therefore be included in the temperature calculations. Temperature and temperature rise of the contact due to load variations are depicted in figure 5.2; the results are plotted in figure 5.3.

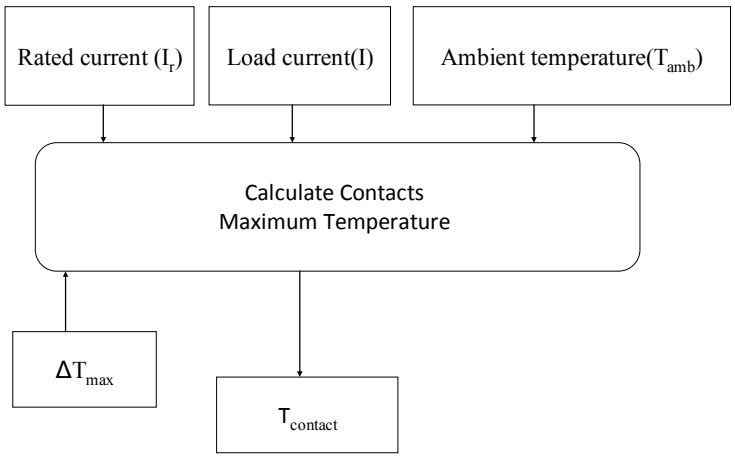

Figure 5.2 block diagram for contact temperature due to load current

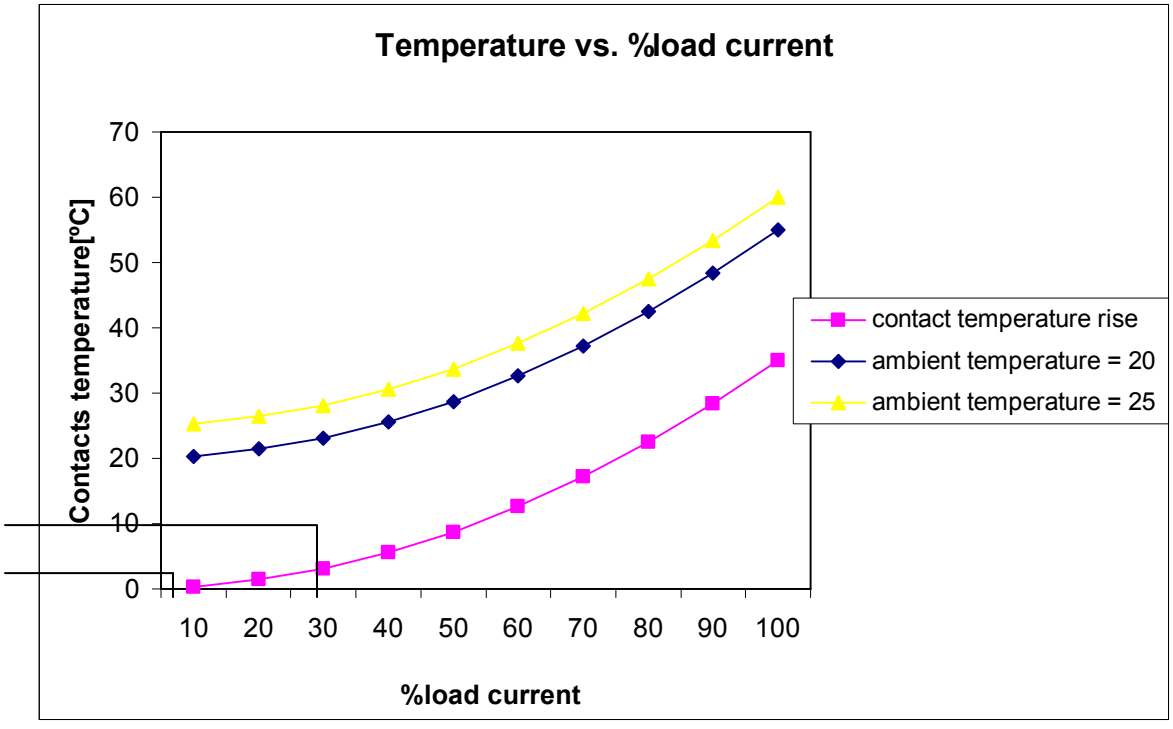

Figure 5.3contacts temperature as a function of percentage load.

Most high voltage equipment in the power systems are used outdoor and as a result are exposed to environmental conditions, such as wind. The effect of the wind on the temperature must be account for when measuring the temperature of such outdoor power equipment. This is the subject of the next paragraph.

5.1.2 Effect of wind on the temperature

When objects are exposed to weather conditions such as rain and wind, their temperature distribution will be substantially affected. The effect of the rain will not be considered the reasoning behind this is the fact that themographic inspections are not conducted during rain fall. Not only will the rain affect the camera vision it might cause damages to the camera as well. However, it can be assumed that the rain will have a cooling effect on the temperature based on some well-known facts that will not be proven here. It is a well-known fact that water in general has a cooling effect on hot objects. The cooling effect of the wind originates from wind induced forced convective heat loss. The amount of cooling depends on the wind speed, orientation of the wind, shape and size of the object and the air temperature [25]. The general equation for heat transfer by convection is given as:

$$P_{convection} = A_s \overline{h_L}(T_{contact} - T_{air}) \quad [12, 16, 17] \qquad (5.6)$$

The key to solving this equation is finding the appropriate value for the average heat coefficient $\overline{h}_L$. This is a very complex process and needs to be done carefully .To understand the nature of convective heat transfer and the evaluation of its coefficient a quick out line of this subject and the correlation equation will be given.

There are two modes of heat transfer by convection, depending on the manner in which the fluid motion is induced, the convection heat transfer can be classified as natural convection or forced convection. In heat transfer engineering the term fluid is used to describe the medium through which the heat transfer occurs, such as air, gases and liquids. If the flow is driven by external forces such a fan, a pump or atmospheric wind then the process is termed forced convection. If the flow is not externally induced then natural convection occurs. Since there are two modes of convective heat transfer equation 5.6 is different for both forced and natural convection. The difference lies in the average convective coefficient which has a different form and value for both transfer modes. In order to derive an equation for each transfer mode and thus solving the convection heat transfer equation the average heat transfer coefficient must be found. This is done by firstly determining whether the flow is laminar or turbulent. The factor that determines the type of flow is the Reynolds number, in the case of forced convection; the Raleigh number determines the type of flow in the natural convection mode. The

second step is to find the appropriate average Nusselt number correlation equations which depends the Reynolds or Raleigh number, the surface orientation and geometry of the object. There are lots of average Nusselt correlation equations in the literature, almost in every thermal science or heat transfer text book. The objective here is not to investigate which is the most accurate as this is beyond the scope of this report, but rather to use the equations that are simple and consistence. The last step is to calculate the heat transfer coefficient based on the geometry and orientation of the object. The object of this thesis is disconnector contacts which can be idealized as a flat plate conductor, and therefore the governing heat transfer equations for a flat plate are given.

The heat transfer by forced convection correlation equations over a flat plate [17]:

$\overline{Nu_L} = 0.664\,\mathrm{Re}_L^{1/2}\,\mathrm{Pr}^{1/3}$ $\quad \mathrm{Re}_L < 10^5$ For laminar flow (5.7)

$\overline{Nu_L} = 0.037\,\mathrm{Re}_L^{4/5}\,\mathrm{Pr}^{1/3}$ $\quad 10^5 \le \mathrm{Re}_L \le 10^8$ for turbulent flow (5.8)

$$\mathrm{Re}_L = \frac{VL}{\nu} \qquad (5.9)$$

The heat transfer by natural convection correlation equations over a flat plate:

$$Gr_L = \frac{g\beta(T_s - T_{amb})L^3}{\nu^2} \qquad (5.10)$$

$$Ra_L = Gr_L\,\mathrm{Pr} \qquad (5.11)$$

<u>Horizontal plate:</u>

<u>Heated surface facing up</u>

$\overline{Nu_L} = 0.59Ra_L^{1/4}$ $\quad 200 \le Ra_L \le 10^4$ (5.12) for laminar flow[19]

$\overline{Nu_L} = 0.54Ra_L^{1/4}$ $\quad 10^4 \le Ra_L \le 10^7$ (5.13) for laminar flow

$\overline{Nu_L} = 0.15Ra_L^{1/3}$ $\quad 10^7 \le Ra_L \le 10^{11}$ (5.14) for turbulent flow

<u>Heated surface facing down</u>

$\overline{Nu_L} = 0.27Ra_L^{1/4}$ $\quad 10^5 \le Ra_L \le 10^{10}$ (5.15) for laminar and turbulent flow

<u>Vertical plate:</u>

$\overline{Nu_L} = 0.59Ra_L^{1/4}$ (5.16) $\quad 10^4 \le Ra_L \le 10^9$ for laminar flow [19]

$\overline{Nu_L} = 0.10Ra_L^{1/3}$ (5.17) $\quad 10^9 \le Ra_L \le 10^{13}$ for turbulent flow

All the material properties can be read from any thermophysical properties of mater charts which can be found in any heat transfer text books. However, these properties must be evaluated at the film temperature T_f for the calculations.

$$T_f = \frac{T_s + T_{air}}{2}$$

$$\overline{Nu_L} = \frac{\overline{h_L} L}{k} \qquad (5.18)$$

$$\Pr = \frac{\nu}{\alpha_t} \qquad (5.19)$$

Where:

A_s = surface area of the object [m^2]

L= characteristic length[m]

V= the wind speed [m/s]

α_t=thermal diffusivity [m^2/s]

ν = kinematic viscosity [m^2/s]

k = thermal conductivity of air [W/mK]

Re_L= Reynolds number [dimensionless]

Pr = Prantl number [dimensionless]

Gr_L= Grahof number[dimensionless]

$\bar{h}_L$ = average convection heat transfer coefficient [W/m^2K]

g = gravitational acceleration ($9.807 m/s^2$)

β= thermal expansion coefficient [K^{-1}]

Rewriting the general heat convection equation for a flat plate, yields equations for forced and natural convection heat loss respectively.

<u>Forced convection heat transfer</u>

$$P_{forced,convection} = 0.664 \frac{k}{L^{0.5}} A_s \left(\frac{V}{\nu}\right)^{\frac{1}{2}} \Pr^{\frac{1}{3}} (T_{contact} - T_{air}) \qquad (5.20) \text{ for laminar flow}$$

$$P_{forced,convection} = 0.037 \frac{k}{L^{0.5}} A_s (\frac{V}{\nu})^{\frac{4}{5}} \Pr^{\frac{1}{3}} (T_{contact} - T_{air}) \quad (5.21) \text{ for turbulent flow}$$

Natural convection heat transfer

$$P_{natural,convection} = 0.54 \frac{k}{L} A_s Gr_L^{\frac{1}{4}} \Pr^{\frac{1}{4}} (T_{contact} - T_{air}) \quad (5.22) \text{ for laminar flow}$$

$$P_{natural,convection} = 0.15 A_s \frac{k}{L} Gr_L^{\frac{1}{3}} \Pr^{\frac{1}{3}} (T_{contact} - T_{air}) \quad (5.23) \text{ for Turbulent flow}$$

The wind correction factor is the ratio of temperature rise without wind to temperature rise with wind, which is the same as the ratio cooling by natural convection to cooling by forced convection. Therefore, equations 5.20 through 5.23 must be solved in order to find the wind correction factor. Solving these equation is a very complex process, because not only must the power dissipation at the contact must be known but also the temperature at the surface of the object, because the fluid properties are evaluated at the film temperature which is the average of the fluid temperature and the surface temperature of the object. For every electrical power input the temperature rise at the contact will be different, and so will the average transfer coefficient as it depends on the film temperature.

The equation for natural and forced convection transfer have the same form, the only difference between them are the values of their average coefficients. Therefore the effect of the wind can be investigated, by studying how it changes the average transfer coefficient. This was done by Santori[26] who simplified equations 5,7 and 5.8 to derive correlation equations for the average transfer coefficient for forced convection at mean temperature of 40 °C as:

$$\overline{h_{L,f}} = 3.83 V^{0.5} L^{-0.5} \quad \text{For Laminar flow (5.24)}$$

$$\overline{h_{L,f}} = 5.74 V^{0.8} L^{-0.2} \quad \text{For turbulent flow (5.25)}$$

What makes Santori's simplification interesting for this project is the fact that the simplification was evaluated a t40 °C. In paragraph 5.1.1 it was stated that the maximum rated ambient temperature is often 40 °C. On the basis of this theory the average natural and forced convection transfer for a horizontal plate with heated side up can also be simplified in the same manner to:

$$\overline{h_{L,n}} = 1.32 (T_{contact} - T_{amb})^{0.25} L^{-0.25} \quad \text{For Laminar flow (5.26)}$$

$$\overline{h_{L,n}} = 1.65 (T_{contact} - T_{amb})^{0.33} \quad \text{For turbulent flow (5.27)}$$

For natural convection

$\overline{h_{L,f}} = 3.78V^{0.5}L^{-0.5}$ For Laminar flow (5.28)

$\overline{h_{L,f}} = 5.56V^{0.8}L^{-0.2}$ For turbulent flow (5.29)

For forced convection

The indexes n and f indicate natural and forced in the above equations respectively. From equations 5.26 and 5.27 it is seen that the average natural convection coefficient depends on the temperature of the contact and its surroundings. Since the contacts temperature depends on the heat dissipation at the contact and therefore on the load, there will be different correction factor for every load. The wind correction factor in the laminar region is:

$$\frac{\overline{h_{L,n}}}{\overline{h_{L,f}}} = \frac{1.32(T_{contact} - T_{ambient})^{0.33}L^{0.25}}{3.74V^{0.5}} \quad (5.30)$$

Formula 5.30 is computed for a contact with characteristic length 70mm, ambient temperature is 20°C. The results are presented in table 5.1.

Table 5.1 effect of wind on the temperature

		Wind Correction factor			
		V=2m/s		V=4/m	
%Load	$T_{contact\ s}$ V=0m/s	$(\frac{V}{\nu_n})^{0.27}$	$\frac{\overline{h_{L,n}}}{\overline{h_{L,f}}}$	$(\frac{V}{\nu_n})^{0.27}$	$\frac{\overline{h_{L,n}}}{\overline{h_{L,f}}}$
10	20.65	1.45	0.90	1.75	0.98
20	22.60	1.45	1.42	1.75	1.55
30	25.85	1.45	1.86	1.75	2.02
40	36.25	1.45	2.24	1.75	2.45
50	36.25	1.45	2.60	1.75	2.83
60	43.4	1.45	3.00	1.75	3.20
70	51.85	1.45	3.24	1.75	3.54
80	61.60	1.45	3.54	1.75	3.87
90	72.65	1.45	3.83	1.75	4.18
100	85	1.45	4.11	1.75	4.48

From table 5.1 it is clear that the wind has a strong effect on the temperature. Observing the table it can be seen that, the wind cooling depends on the load and wind speed. The wind cooling increases with increasing load and wind speed. So when the load and wind speed are given the wind correction factor can be looked up from this table.

The above method shows how to calculate the wind correction in the laminar regions. The turbulent region will have different correction factors. These results also show that a single wind correction factor does not exist as the correction factor depends on the power dissipated at the contact. This is the reason why it is difficult to develop a well-defined wind correction factor for all wind speeds and over the entire load range. This being said, reference[18] proposed a model to correct for the wind by multiplying the temperature

measure during wind by $(\frac{V}{v_n})^{0.27}$ where v_n is the maximum allowable wind speed [m/s] when type testing a disconnector. From the equations for the forced convection heat transfer and its average transfer coefficient, it can be seen that the wind effect is of the form $(V)^m$. So for now, the model as suggested by [18] is used as the wind correction factor. With this correction factor for wind, the temperature rise corrected for wind can be expressed as:

$$\Delta T_{wcontact} = \Delta T_{\max} (\frac{I_m}{I_r})^n (\frac{V}{v_n})^{0.27} \qquad (5.31)$$

Using this correction factor the inputs to investigate the effect of the wind can be given in a block diagram as depicted in the figure below. Note that the input is not the correction factor but rather the wind speed as the correction factor is dependant on the wind speed.

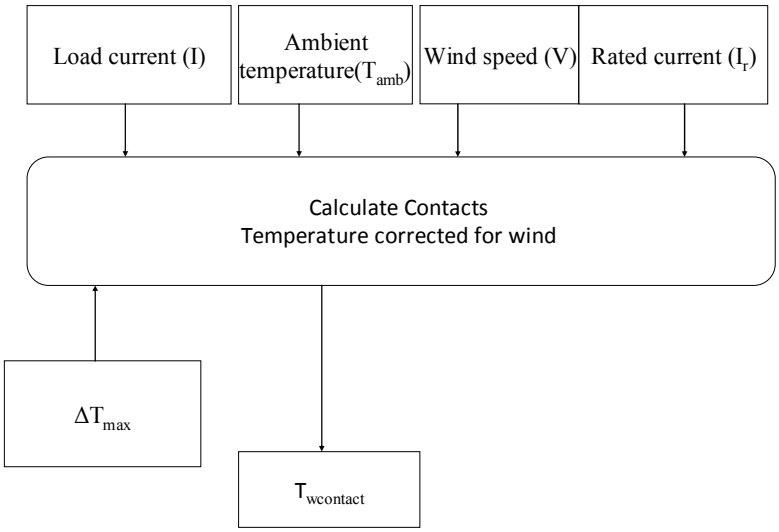

Figure 5.4 Flowchart to investigate the influence of the wind

The wind speed in the Netherlands is on average, 2.2m/s inlands and 5.5 at the cost. Therefore the wind effect will be investigated for wind speeds in the range of 0-5m/s. The value of v_n is chosen from [24] : v_n = 0.5m/s. The effect of the wind on the contacts temperature according to this model is given in columns 3 and 5 of table 5.1.

This method also shows the effect of wind cooling. The assumption made here is that the correction factor only depends on the wind speed (Colum 3 to 5 of table 5.1) which makes the correction factor constant for all loads.

5.1.3 Effect of solar heating

The discussion so far has excluded the effect of the sun. Since some of the power equipment are installed outside (outdoor power stations) and thus exposed to the natural environment, the effect of the sun on the outdoor power equipment must also be considered. When an object is exposed to the sun, it will receive radiant energy from it. In order to differentiate between abnormal temperature rise due to bad contact and abnormal temperature rise caused by solar radiation, the effect of the sun must be investigated. According to the first law of thermodynamics, the power input is equal to the power output for a steady state system. The mathematically expression for this statement is given by the following equation [8, 12, 17] :

$$P_{in} = P_{out} \qquad (5.32)$$

Combing this formula with Joules' law and noting that the solar heating is part of the power input, the energy balance equation for a steady state system can be written as:

$$I^2R + P_{sun} = P_{out} \qquad (5.33)$$

$$P_{sun} = A\alpha_s Q_s \qquad (5.34)$$

Where Q_s = solar energy incident on objects surface [W/m^2], A_s surface area of object [m^2] and α_s = solar absorptivity.

The amount of solar energy received by an object depends on the time of day, surface area of the object, time of the year, atmospheric clarity and altitude of the sun [19, 25, 27]. For example the solar heat gain at noon in the summer with clear atmosphere will be higher than that at noon with the same atmospheric condition in the winter. Table 5.2 shows the total amount of heat received directly from the sun and sky radiation for clear and industrial atmosphere. The incident solar radiation also depends on the solar azimuth angle and is needed for the calculation of the heat gain from the sun. The solar azimuth angle and the solar latitude applicable for this report are given in table 5.3.

Table 5.2 Total heat flux received by a surface at sea level normal to the sun rays[25]

Degrees solar altitude	**Clear atmosphere**	**Industrial atmosphere**
*H*c (deg)	*Q*s (W/m^2)	*Q*s (W/m^2)
5	234	136
10	433	240
15	583	328
20	693	422
25	770	502
30	829	571
35	877	619
40	913	662
45	941	694
50	969	727
60	1000	711
70	1020	809
80	1030	833
90	1040	849

Table 5.3 solar altitude (Hc) and azimuth (Z_c) for annual peak solar heat input for 50 and 60 latitude [25]

	Local sun					
latitude	10:00a.m		Noon		2:00p.m	
Degrees North	***H*c**	***Z*c**	***H*c**	***Z*c**	***H*c**	***Z*c**
50	55	137	63	180	55	232
60	48	143	53	180	48	223

If the sun were to be the only input energy source, the surface temperature rise would have been cause by the heating of the sun. As to what extend it will affect the temperature will depend on the power loss through conduction, radiation and convection. To be able to account for the sun effect, equations 5.23 must be solved which means that the modes of the heat transfer among other factors discussed in the subparagraph 5.1.2 must be known beforehand.

For now a simplified approach will be taking just to make clear that the sun cannot be ignored in some cases. The latitude of the Netherlands is approximately 52 degrees north, which is between 50 and 60 degrees latitude given in the table 5.3. From table 5.2 the solar altitude of the Netherlands can be calculated given the time and day of the year. The values other than the ones given in tables 5.2 and 5.3 can be computed through linear interpolation.

The solar heat gain of a centre break disconnector is computed under the following assumptions and conditions:

Assumptions:

- The sun is the only source of input energy
- System is in thermal equilibrium

- The disconnector is designed such that at rated current, the temperature rise is equal to the maximum allowable temperature rise.

Table 5.4 Data to evaluate the sun effect

Conditions
α_s =0.25
A= 900mm x 70mm
Contact resistance =75μΩ
Rated current= 3150A
Latitude = 52 degrees north (Delft)
Atmosphere = clear
Date = 10 June
Time = Noon
Ambient air temperature = 25ºC
Maximum temperature rise =65ºC

Analysis

$P_{sun} = 0.25AQ_s$

Using table 5.3 to determine the solar latitude

From table 5.2 the amount of heat received by the contact is obtained by interpolation

Q_s=1004 W/m^2

Thus

P_{sun} = 15.81 W

Assuming the disconnector is operating under full load, the power generated by the load current is:

P=I²R = 744.2W.

Compared to the heat generated under full load, the influence of the sun can be ignored. However, this is different when the disconnector is operating at a percentage of its full load. The effect of the sun heating is presented in table 5.5. In practice most of the disconnectors operate under very small load, and from the results presented in table 5.5 it can be seen that the influence of sun decrease with increasing load. At operating loads less than 40% the influence of the sun cannot be ignored.

Table 5.5 effect of the sun on the temperature rise at the contact

Load [%]	I^2R[W]	Psun[W]	% heat due to sun	ΔTcontct[°C]	ΔT°[C] due to sun
10	7.44	15.81	68	0.65	3.72
20	29.77	15.81	34.69	2.60	3.72
30	67	15.81	19.10	5.85	3.72
40	119.07	15.81	11.72	10.40	3.72
50	186.05	15.81	7.83	16.25	3.72
60	268.0	15.81	5.57	23.4	3.72
70	364.65	15.81	4.16	31.85	3.72
80	476.3	15.81	3.21	41.6	3.72
90	602.8	15.81	2.56	52.65	3.72
100	744.2	15.81	2.08	65	3.72

The temperature correction for solar radiation can be determined using the approximation of reference [28]. According to this reference the maximum temperature rise of a black painted surface with absorption coefficient of 0.97 is 15 °C at incident solar radiation of 1044 W/m^2 midsummer at noon. On the basis of the results of reference [28]a formula for the temperature rise due to solar heating for the contact can be derived.

The temperature rise of an object of different colour under the same condition will be a fraction of this temperature (Stefan-Boltzmann law) and can be given as:

$$\Delta T_{sun} = \frac{\varepsilon_{objct}}{0.97} 15 \quad (5.35)$$

In the case where the incident radiation on the object is different from1044 (W/m^2) the temperature rise must also be corrected for this value. The temperature rise due to sun heating is then:

$$\Delta T_{sun} = \frac{\varepsilon_{objct}}{0.97} \frac{Q_s}{1044} 15 \quad (5.36)$$

Applying this to the example presented above gives a temperature rise of 3.72 °C. This is the value of the maximum temperature that the sun would add to the system described above. For a silver coated contact operating under 40% of its rated load, the temperature rise due to the load should be 10.40°C. But because of the sun the temperature rise is 14.12°C, which is a very high temperature rise for a 40% load. The sun is responsible for more than a quarter (26.3%) of the total temperature rise of the contact. From table 5.4 the contribution from the sun to the total power input is 11.72% whereas the sun's contribution to the temperature rise is twice as much. This is due to the fact that relation between the temperature and power dissipation is neither linear nor square because of the different heat transfer modes.

The forgoing discussion has dealt with the effects of wind, sun, ambient temperature and load on the contacts temperature. To be able to account for the effects of these factors on the temperature, correction factors have been presented. On the basis of the correction the contacts temperature and temperature rise can now be written as:

$$T_{contactcorrectedw,I,Ambtemp,sun} = \Delta T_{\max} (\tfrac{I_m}{I_r})^n (\frac{V}{v_n})^{0.27} + T_{ma} + \quad \Delta T \frac{\varepsilon_{objct}}{0.97} \frac{Q_s}{1044} 15 \, (\frac{V}{v_n})^{0.27} \quad (5.37)$$

$$\Delta T_{contactcorrected,w,I,Ambtemp,sun} = \Delta T_{\max} (\tfrac{I_m}{I_r})^n (\frac{V}{v_n})^{0.27} + \Delta T \frac{\varepsilon_{objct}}{0.97} \frac{Q_s}{1044} 15 \, (\frac{V}{v_n})^{0.27} \quad (5.38)$$

A formula to calculate the temperature rise due to the sun radiation is provided by equation 5.35. The third column of table 5.4 shows the ratio of the sun heating to heating by the load current. It is seen that the effect of the sun decrease with increasing load. Even though, the above calculation shows that, the temperature rise due to the sun is high and must be accounted for; there are two cases where the effect of solar heating can be neglected.

1. When the normal losses due to the load and resistance are much higher as compared to the effect of sun heating then the effect of sun heating can be ignored

2. The wind speed is more than 4. 5m/s[28]. Wind speeds higher than 4.5m/s will completely off set the sun effect and therefore the effect of solar heating can be completely ignored.

It has been argued that the temperature of the contact is also affected by its resistance. The maximum temperature rise above rated ambient as presented by the IEC standard is based on new contacts, which have the lowest resistance. When the contact has been in service for a while, its resistance will increase due to the formation of oxides at the surface or due to thermal stress (see paragraph2.2). This will have some effect on the contacts temperature. The effect of the resistance on the temperature and how to account for it is the subject of the next paragraph.

5.1.4 Contact resistance and temperature correlation

In the preceding paragraphs the correlation between the load current and temperature, effect of wind and sun has been dealt with. The next step is to find the resistance temperature relation. From Joules' law the amount of power dissipated into the contact is proportional to the resistance and to the square of the load ($P=I^2R$). This implies that, the power is a linear function of the resistance. Consequently the contacts temperature will depend on the contact resistance. However it cannot be said whether the temperature will also be a linear function of the resistance as the heat dissipation by radiation and convection are not linear function of the temperature.

If the ratio of the contacts resistance at temperature T to rated contacts resistance at maximum temperature is written as

$$\frac{R_{contact}}{R_{ratedcontact}} = \frac{\Delta T_{contact}}{\Delta T_{\max}} \quad (5.39)$$

Then, the temperature of the contact corrected for resistance can be written as:

$$T_{contactcorrectedforresistnace} = \Delta T_{\max} \frac{R_{contact}}{R_{ratedcontact}} + T_{amb} \quad (5.40)$$

The effect of the contacts resistance on its temperature rise is shown in figures 5.5. The computation of the resistance is done for 4 different values. From the norm of the contacts resistance criteria if the contact is less than 105 % (1.05R) of its initial value, then the condition of the contact is classified as good. The other 3 values, 1.2R is the fair boundary, any value above this is termed poor, and 2R is also shown to illustrate how the temperature of the contact will rise above its maximum value. From this figure it is clear that the contacts resistance curves move away from the rated value curve as the resistance get higher. The temperature rise at the contact seems to increases linearly with the

resistance. For example at full load the temperature rise of R= 2Rrated is 130°C, twice the value of the rated resistance.

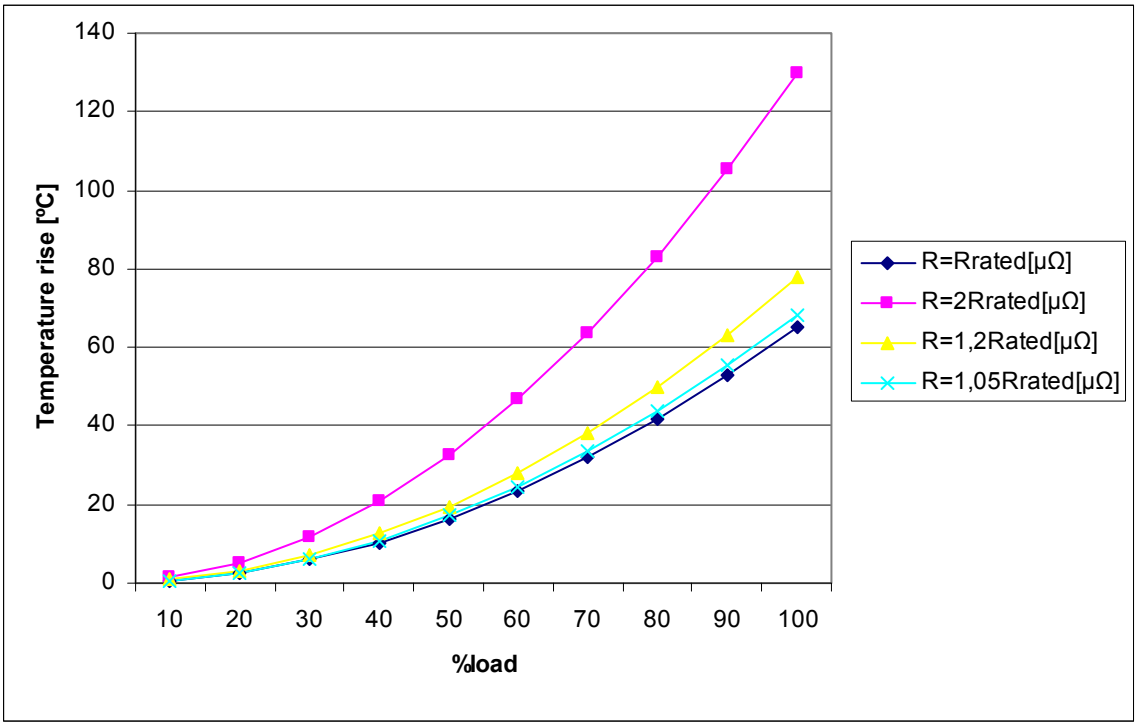

Figure 5.5contacts temperature rise as function of percentage rated load for different values of contacts resistance at 20°C ambient temperature.

5.1.5 Temperature and temperature rise formulas corrected for all influencing factors

Now that all the factors affecting the temperature at the contact have been studied an equation to calculate the temperature and temperature rise can be derived. The formula for the contacts temperature corrected for load, wind, sun, and ambient is:

$$Tc_{contact} = \Delta T_{\max}\left(\frac{I_m}{I_r}\right)^n \left(\frac{V}{v_n}\right)^{0.27} + \frac{\varepsilon}{0.97}\frac{Q_s}{1044}15\left(\frac{V}{v_n}\right)^{0.27} - T_{ambient} \qquad (5.41)$$

The temperature rise is the temperature at the contact minus the ambient temperature, which is

$$\Delta Tc_{contact} = \Delta T_{\max}\left(\frac{I_m}{I_r}\right)^n \left(\frac{V}{v_n}\right)^{0.27} + \frac{\varepsilon}{0.97}\frac{Q_s}{1044}15\left(\frac{V}{v_n}\right)^{0.27} \qquad (5.42)$$

The factors that affect the temperature of the contact have been reviewed in the preceding paragraphs and the formulae to calculate the temperature and temperature rise of the contact has been derived. In the next paragraph these factors are used as the input for the thermal model to evaluate the condition of the contact. The role of the resistance on the contact is left out of the formulas due to the fact that, the resistance is the unknown parameter whose value will be estimated using the temperature data.

5.2 Input data thermal model

Now that the factors affecting the temperature have been evaluated, the input data for the thermal model can be selected as:

- Load current
- Wind speed.
- Solar heating
- Rated current
- Measured ambient temperature

Figure 5.6 shows the inputs and output of the thermal model. Note that the resistance is not part of the input. This is due to the fact that, the resistance in practise is not known and one of the goal of this thesis is to calculate the numerical value using the temperature data. This will be dealt with in the next chapter

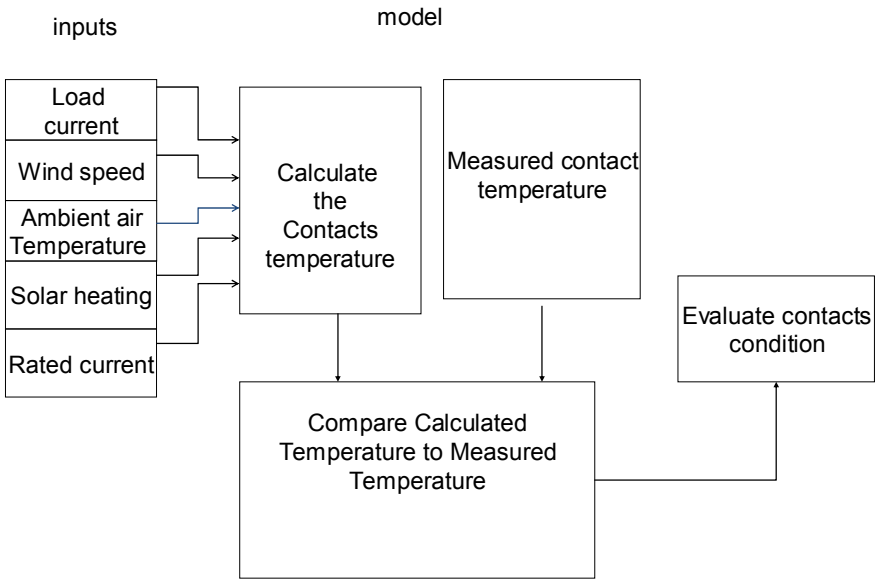

Figure 5.6 block diagram of the thermal model

5.2.1 Assessing the condition of the contact based on temperature rise

The data acquired from the temperature measurements need to be analyzed to assess the condition of the contacts. In chapter 3 it was said that the delta T criteria can be used to assess the condition of the contact. However, criteria, guidelines and standards for temperature rise ratings are based on full load and under predefined environmental conditions. Since most equipment do not operate at full load in real life systems and the ambient condition at the time of measurement may differ from the standard specified ambient conditions, these deviations from standard specified condition must be accounted for. These corrections have been done in sections 5.1.1 through 5.1.4. The condition of the main contact is established by comparing its measured temperature to the calculated maximum temperature. The maximum calculated temperature gives an indication whether the contact is operating within its temperature limits.

The delta T temperature ratings for this thesis are listed in Table 5.7.[4] .Note that in this table the measured contacts temperature is assumed to be higher than calculated temperature. Because when the measured temperature is less than the calculated temperature the contact is operating within its temperature limits and therefore considered to be in good condition. When the measured temperature is greater than the

calculated temperature then there is an indication of abnormality, the extend of this temperature difference is investigated with the help of the delta T criteria [29].

For bolted bare copper contacts the limit is 35°C [5]. This value is used to investigate this model the results are shown in figure 5.9.

Table 5.7 Delta-T criterion to assess the condition

$T_{mcontact}$- $Tc_{contact}$	condition
1°C–3°C	good
4°C–15°C	fair
>15°C	poor

Where $T_{mcontact}$ = the measured temperature of the contact [°C]
$Tc_{contact}$ = the calculated temperature of the contact corrected for wind, load, sun ambient temperature and resistance [°C]
The measured temperature rise corrected for weather condition and ambient temperature is compared to the calculated total allowable temperature rise also corrected for ambient temperature, load current and weather conditions. Comparing the measured temperature of the object to the maximum allowable temperature rise is basically comparing the temperature rise of the contact to a new contact operating under the same conditions as the contact. Figure 5.7 illustrates the basic idea of the thermal model and the regions for the condition are shown in figure 5.8. From figure 5.8 it can be seen that a 25 degrees Celsius temperature rise at 60% load is less severe than at 40% load this is another reason why the load is so important for the severity ratings of the contact.

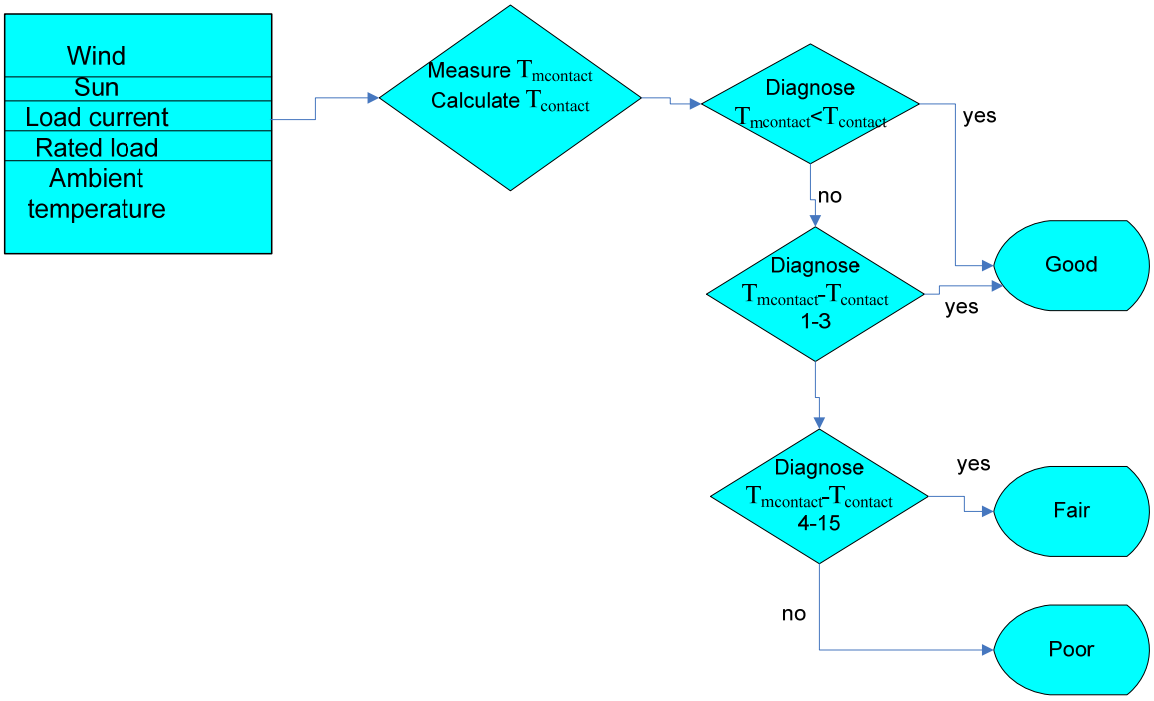

Figure 5.7 flowchart of thermal model

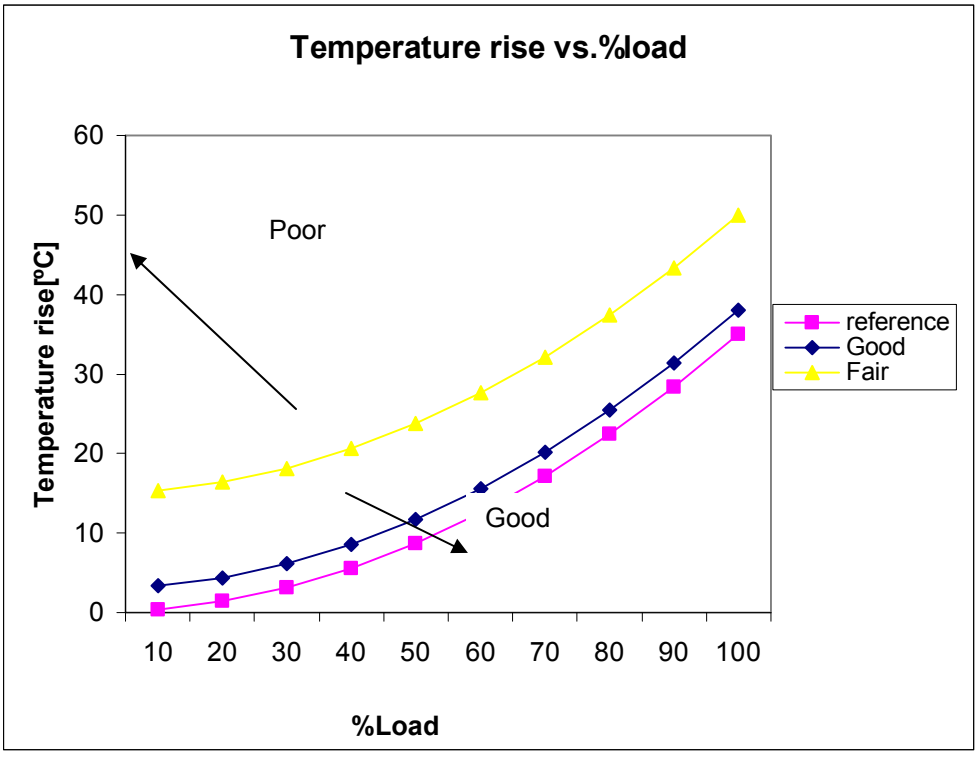

Figure 5.8 Plots showing the three regions of the thermal model

6. Resistance Model (off-line)

The heating due to current flow between the contacts is determined by Joule's law which is $P=I^2R$. Thus for a given load current, the contacts resistance determines the heating of the contact and for this reason must be regarded as an important factor.

Unlike the contacts temperature the contact resistance cannot be measured on line. Therefore the data from the thermal model are needed to estimate the off- line contact resistance value. In the thermal model it was shown that the surface temperature depends on:

- Material of the object
- Dimensions of the object
- The weather conditions (ambient temperature, rain, sun and wind)
- The load current.

Since the contact resistance will be evaluated based on its temperature, it becomes a function of the above mentioned parameters as well, which is given in a mathematical form here below

$$R_{contact} = f(dT_{contact}, A, I)$$

The evaluation of the resistance is based on determining the numerical value of the contact using the data from the thermal model. Before using the temperature data to assess the contact resistance it is necessary that all the factors affecting the resistance are expanded in the temperature data. This makes it possible to model the contacts resistance as a function of its temperature. This evaluation method is described in the following subparagraph.

6.1 Relationship between resistance and temperature

Before developing the resistance model it is necessary to review how the temperature affects the resistance of conductors. It is a well-known fact that the resistance of conductors vary with temperature[21]. In a limited temperature range, up to 100 degrees Celsius, the properties of conductors vary linearly with temperature. The resistance of a conductor with uniform cross sectional area can be calculated from its material property,

resistivity. The resistivity is a linear function of the temperature and can be expressed as [30].

$$\rho(T) = \rho_0(1 + a(T - T_o)) \quad (6.1)$$

The resistance of a conductor based on its material property can be expressed as

$$R = \frac{\rho L}{A} \quad (6.2)$$

Since the resistance of a conductor is directly proportional to the resistivity, the resistance of the conductor will also be a linear function of the temperature. This dependency of the electrical resistance on the temperature is expressed by the following equation [9, 11, 21, 30]

$$R(T) = R_0(1 + \alpha(T - T_0)) \quad (6.3)$$

Where:
α = the temperature coefficient and is a material property [$^oC^{-1}$].
ρ= the resistivity [Ω-m].
L=length of conductor[m]
A= cross-section area [m^2]
R (T) =conductor resistance at temperature T [Ω]
R_0= reference resistance at reference temperature T_0 [Ω]

This relation indicates that after some initial value (R0) the contact resistance will increase linearly with the temperature rise. For a silver plated copper contact with the following specifications and operating condition

R_0 = 50μΩ, α= 0.004$^oC^{-1}$ and To = T_{amb} =20°C, the resistance of the contact can be computed using equation 6.3. The results of the computation are listed in table 6.1; figure 6.1 provides the same information in graphic form.

Table 6.1Results of the resistance
Function of temperature

[%Load]	Tcontact [°C]	Rcontact[μΩ]
20	22.6	50.5
30	25.9	51.2
40	30.4	51.1
50	36.3	53.3
60	43.4	54.7
70	51.9	56.4
80	61.6	58.2
90	72.7	60.5
100	85	63

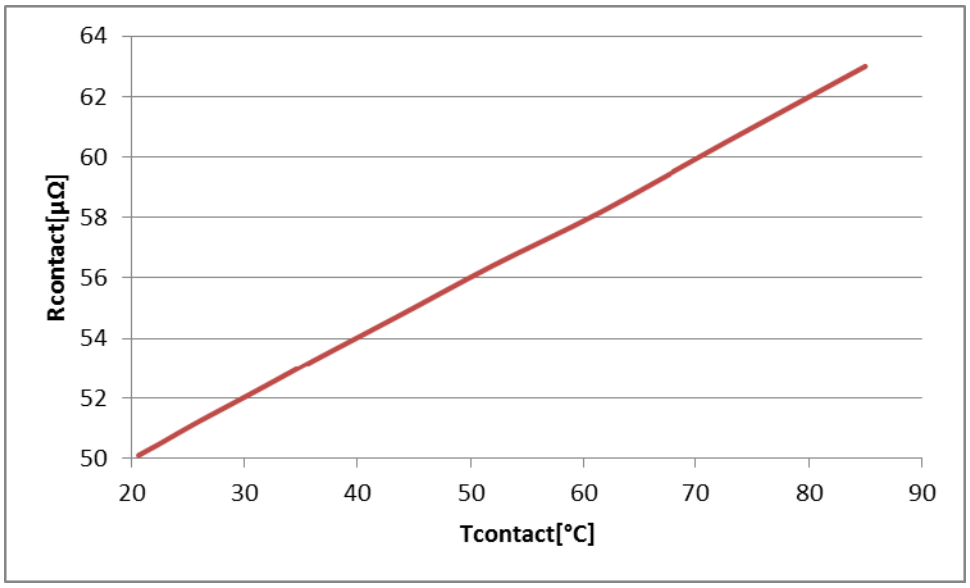

Figure 6.1 contacts resistance as function of its temperature

Note that the minimum temperature is not 0 because minimum temperature of the contact at no load is equal to the ambient temperature. At this temperature the contacts resistance is at its minimum value which is 50μΩ. The results show that the contacts temperature can have a huge impact on its resistance; at full load the increase in the resistance due to its temperature is 26%.

6.2 Method to evaluate the contact resistance

This section will give the method used to evaluate the contacts resistance based on its temperature data. The main goal of this thesis is to relate the online temperature data obtain by means of infrared measurements to the contact resistance. This means determining the off line numerical value of the contacts resistance. This can be done by solving the heat balance equation given by equation 6.4. After the numerical value of the resistance has been determined it can be compared to some predefine reference which can be the contacts resistance value before installation as provided by the manufacturer or the value obtained from previous resistance measurements.

In order to calculate the numerical value of the resistance the heat balance equations must be solved. The steady state heat balance equation for the contact during operation can be expressed as:

$$R(1+\alpha(T_{contact}-T_{amb}))I^2 = P_{convection} + P_{radiation} + P_{conduction} - P_{sun} \qquad (6.4)$$

Where:

$I^2 R(1+\alpha(T_{contact}-T_{amb}))$ = the heat generation in the contact resistance (W)

$P_{conduction} = (Ak/L)(T_{mcontact}-T_{ma})$ is the heat loss due to conduction(W)

$P_{radiation}=\varepsilon\sigma A(T^4_{mcontact} - T^4_{ma})$ is the heat loss due to radiation (W)

$P_{covection} = A\overline{h_L}\ (T_{mcontact}-T_{ma})$ is the heat loss due to convection (W)

$\overline{h_L}$ = the average convection heat transfer coefficient ($Wm^{-2}K^{-1}$).

k = the thermal conductivity (W/mK)

$1+\alpha(T-T_0)$ is the effect of the operation temperature on the resistance.

From equation (6.4) the equation to calculate the off-line numerical value of the contacts resistance when the load current, temperature of the contact and the ambient temperature are known can be derived as:

$$R = \frac{P_{convection} + P_{radiation} + P_{conduction} - P_{sun}}{(1+\alpha(T_{contact} - T_{amb})I^2} \qquad (6.5)$$

Solving equation 6.5 yields the numerical value of the off –line resistance.

6.3 The input data for the resistance model:

The factors affecting the resistance have been described in greater details in the previous section. The variation of temperature with the resistance has also been addressed. Since the resistance will be modelled sorely as a function of temperature the input data of this model are:

- Measured contact temperature
- Measured ambient temperature
- Reference resistance

The flowchart to evaluate the contacts condition is shown in figure 6.2

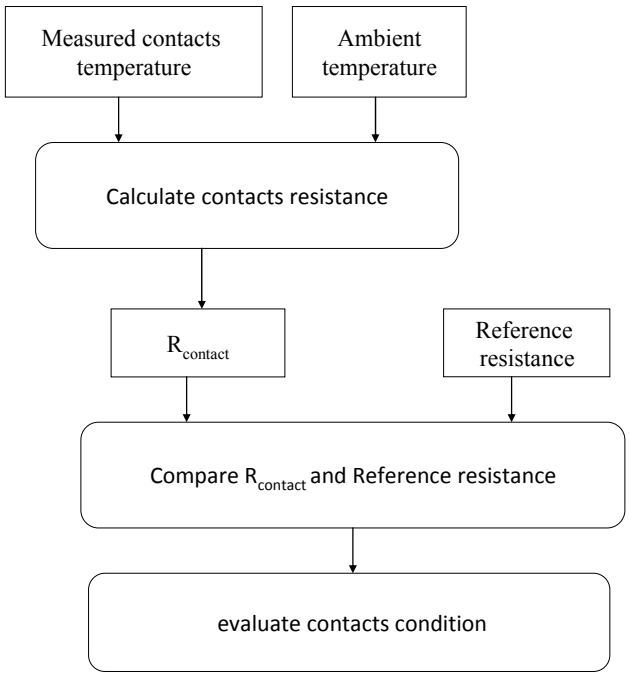

Figure 6.2 flowchart for the off-line method

6.3.1 Condition evaluation of the contact

The condition of the contact is assessed by comparing the calculated resistance value to and using the criteria listed in table 6.2 to analyse its condition. Figure 6.3 shows the evaluation process in a diagram form.

Table 6.2 criteria to assess the condition of the contact

$R_{contact}$ /$R_{refernce}$	Condition
<105%	Good
105-120%	Fair
>120%	poor

Source: KEMA

Just like the thermal model the condition of the contact can fall in one of the three states

- Good
- Fair
- Poor

If from the thermal model the contact has been declared as good for example then, the resistance model also should predict the same outcome. This means that, the percentage rise should not be more than 105%.

In chapter 5 the contact's temperature has been described in greater details. The behaviour of the temperature and temperature rise at the contact has been investigated on the basis of all the factors affecting them. This chapter has explored the possibility of using the temperature data to create a model to determine the resistance of the contact and use the outcome of this model to predict the condition of the contact.

All the investigations so far have been theoretical, and as often is the case theoretical models always work! In order to verify these models, empirical test must be done. Therefore, it is the goal of the next chapters to put the two models to the test by performing experiments.

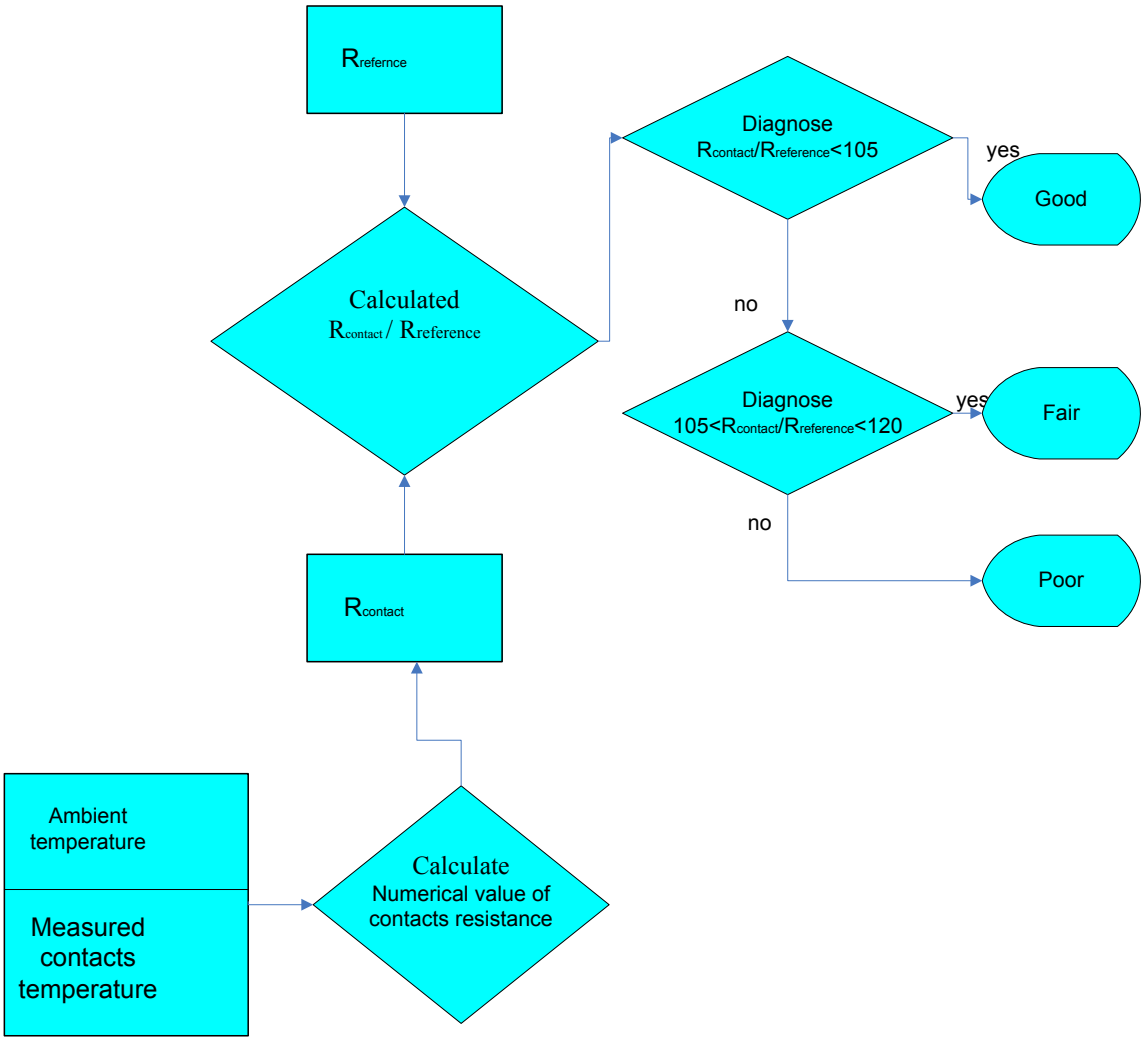

Figure 6.3 flowchart to assess the condition of the contact based on the resistance model

7. Laboratory experiments

To be able to test the validity of the proposed model series of experiments were conducted on samples developed in the high voltage laboratory of Delft University. In chapter 8 the results of the experiments are presented to support the proposed model.

7.1 Goal of the experiments

The experiments were conducted to investigate:

- The load current - temperature behaviour
- Temperature - resistance behaviour
- Effect of wind on the temperature rise
- Effect of solar heating
- Determine the exponent (n) in equation 4.3.
- Since the temperature measurements will be performed by means of infrared camera, the calibration methods motioned in chapter 3 are investigated in order to achieve accurate temperature measurements.

7.2 Test setup

In the previous chapter it was stated that, the contacts condition can be assessed either by its resistance or temperature rise. Therefore two experimental test setups were developed in the laboratory for the temperature and resistance measurements. The sample consists of two metals strips of the same material bolted together in the middle and clamp on a wood. The support and the bolts are made of steel. Thermo-couples were placed on three surface areas of the metal strip.

7.2.1 Test setup for temperature measurements

The temperature rise caused by load variations is measured by means of thermo couples and infrared camera. The surface temperature at the contact and the areas on either side indicated by R_R and R_L in figure 7.1 are measured. The load current will be raised from 150 to 500. The thermo couples were glued onto the three surfaces under investigation. The outputs of the thermo couples are connected to a recorder to display the measured temperature. For the accuracy of the measurement, four thermo couples were placed on the surface of the main contact. The average value of the four temperature readings on the recorder is the measured temperature at the contact. The infrared camera

used was the Fluke Ti50 IR Flex Cam Thermal imager (see picture below). The test set up consists of test object, adjustable current source and inductor for the generation of high current. Figure 7.1 shows the simplified schematic diagram of the test set up. Figure 8.2 illustrates a picture of the aluminium sample with the inductor. The infrared camera and wind meter are shown in figures 7.3. The adjustable current source, the shunt and the recorder are shown in figure 7.4.

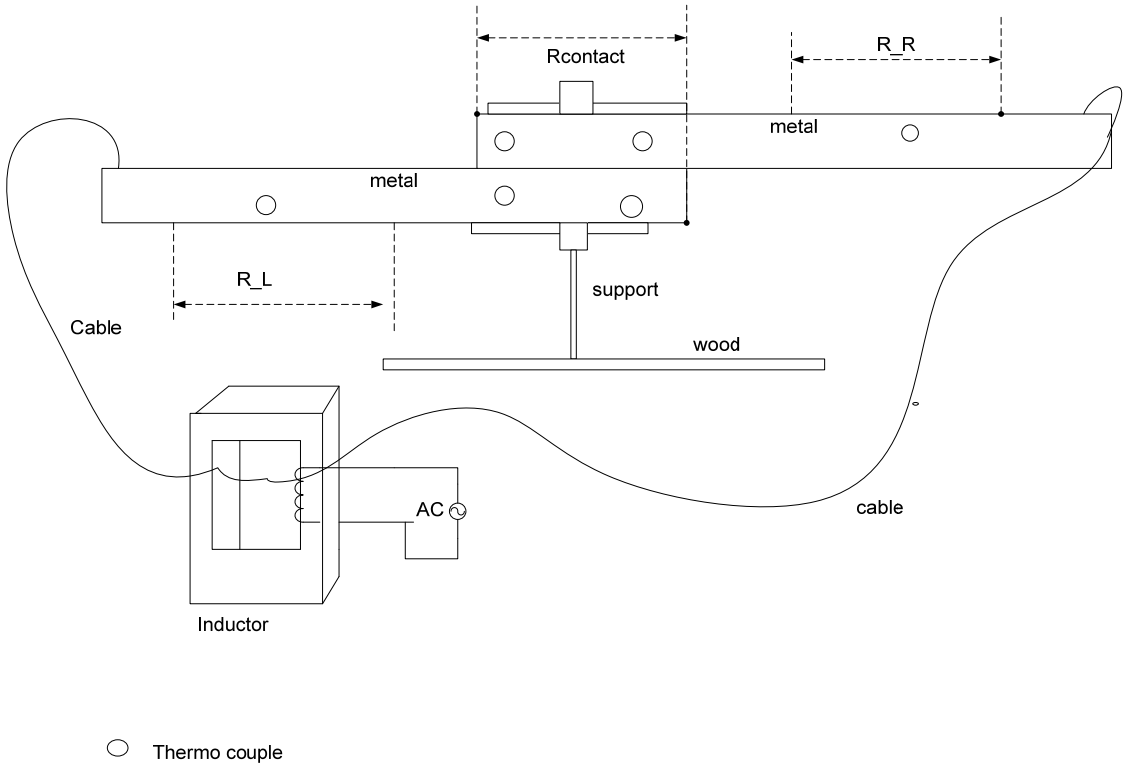

Figure 7.1 Schematic diagram of test setup for temperature measurements

Figure 7.2 picture of test setup for the aluminium sample

Figure 7.3 the Fluke Ti50 infrared camera (left) used for the temperature measurements and the Skywatch Xplorer2 (right) wind meter to record the wind speed

Figure 7.4 the recorder and the variac (adjustable current source) used in the laboratory

The test setup for the resistance measurements are described in the next paragraph.

7.2.2 Test setup for resistance measurements

The resistance of the contact is measured by means of the four points method described in chapter 1. A DC current of approximately 10 amps is applied to the sample, the voltage drop across the contact (see figure 7.5) is measured, and the ratio of the voltage drop across the contact to the current is the resistance of the contact. To eliminate any noise or offsets that may be present the measurements are carried out twice. The terminals are placed as shown in the figure 7.5for the first measurement and then the polarity is reversed for the second measurements. The measured resistance is the average value of

the two measurements. Figure 7.5 shows the setup for the resistance measurements. The DC source used for the current application is shown in figure 7.6.

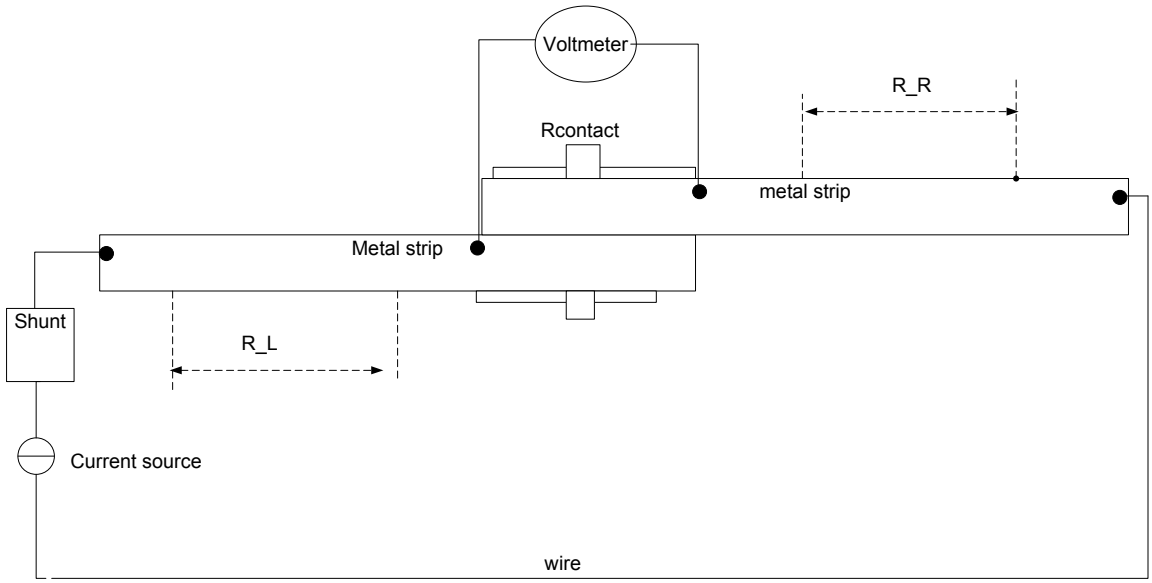

Figure 7.5 Schematic diagram of test setup for resistance measurements

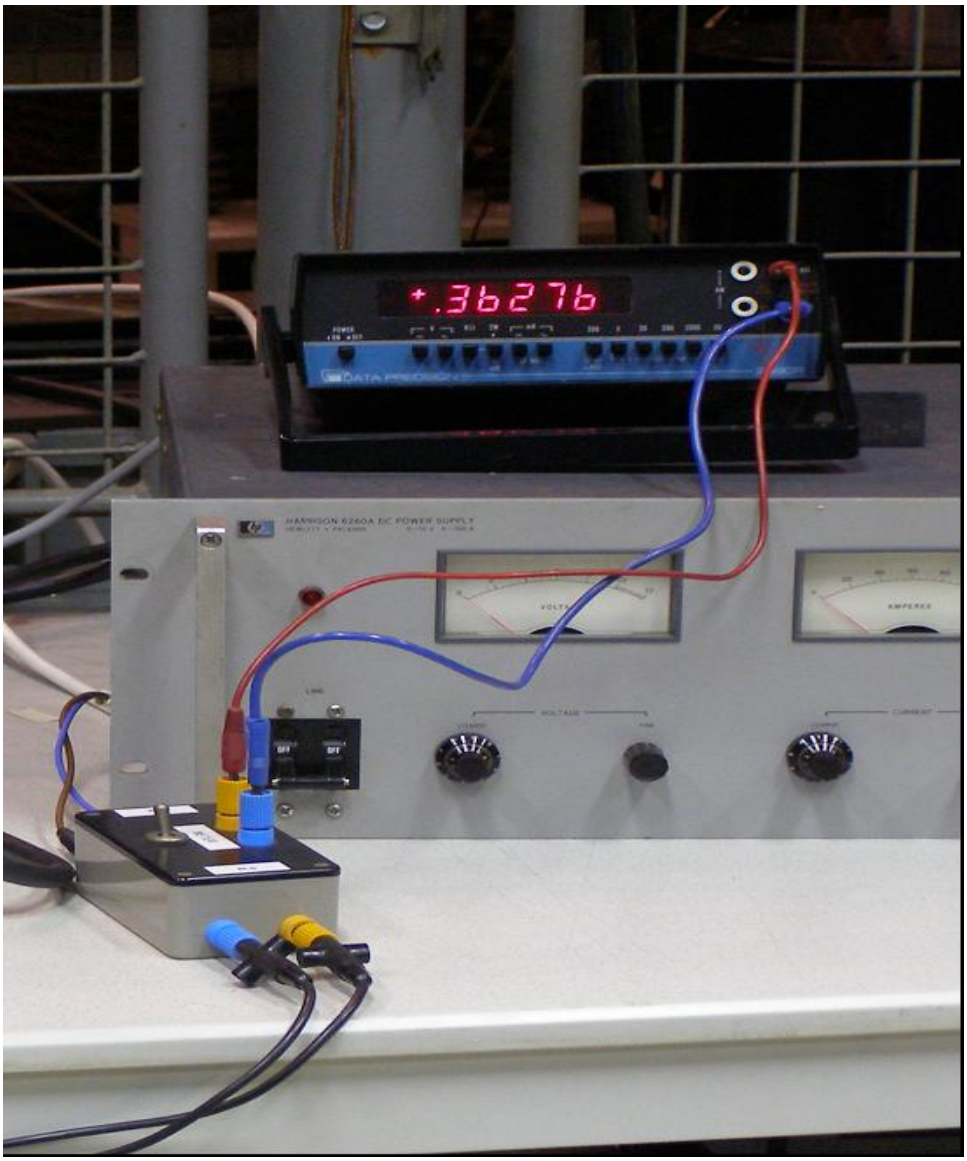

Figure 7.6 DC source and measuring shunt for the resistance measurements

7.3 Test objects

The tests were done on different objects and materials. Disconnector main contacts are usually made of silver-plated copper, hidden in aluminium frame. Therefore, aluminium and copper were the materials used for the investigation. Another interesting consideration is the fact that disconnectors are of the make and break type hence a test object of this kind was also used.

7.3.1 Copper- contact

The sample consists of two metal strips bolted together in the middle and clamped on a wood .The support and the bolts are made of steel. The location where the two strips are

bolted together represents the main contact ($R_{contact}$), which is the main object for the investigation. On either side of the main contact two pieces of strip of same length (R_L and R_R) as the main contact are also presented to give some indication of the temperature distribution of the whole object. Figure 7.7 shows the sample of copper strip.

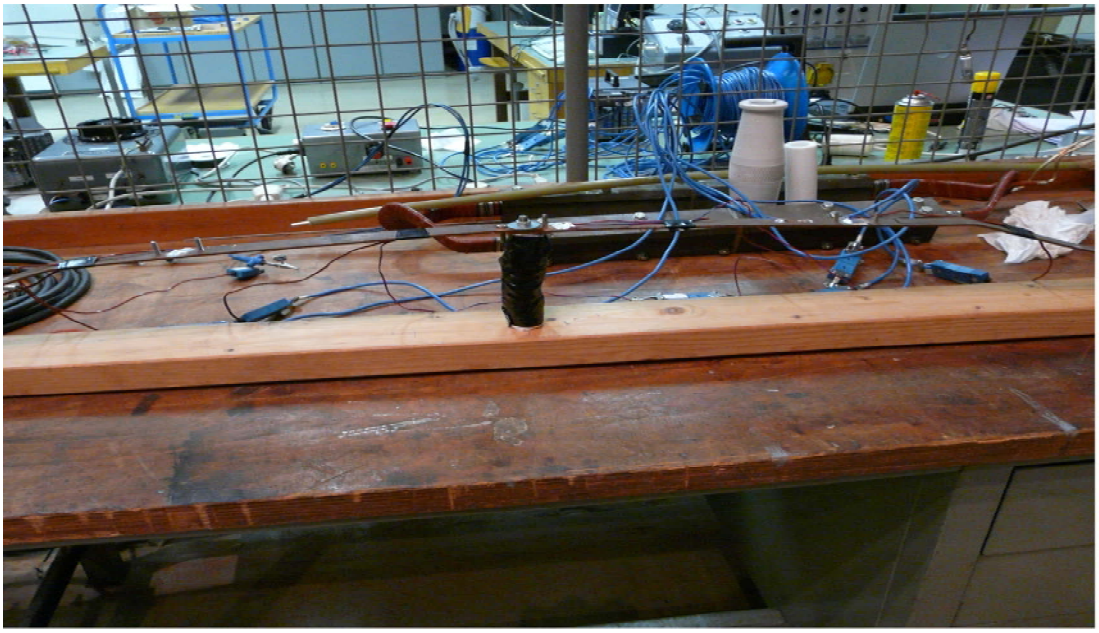

Figure 7.7 a copper strip sample for laboratory investigation

7.3.2 Aluminium contact

The aluminium contact was just like the copper contact the only difference being the material. Figure 7.8 shows a photograph of the aluminium contact.

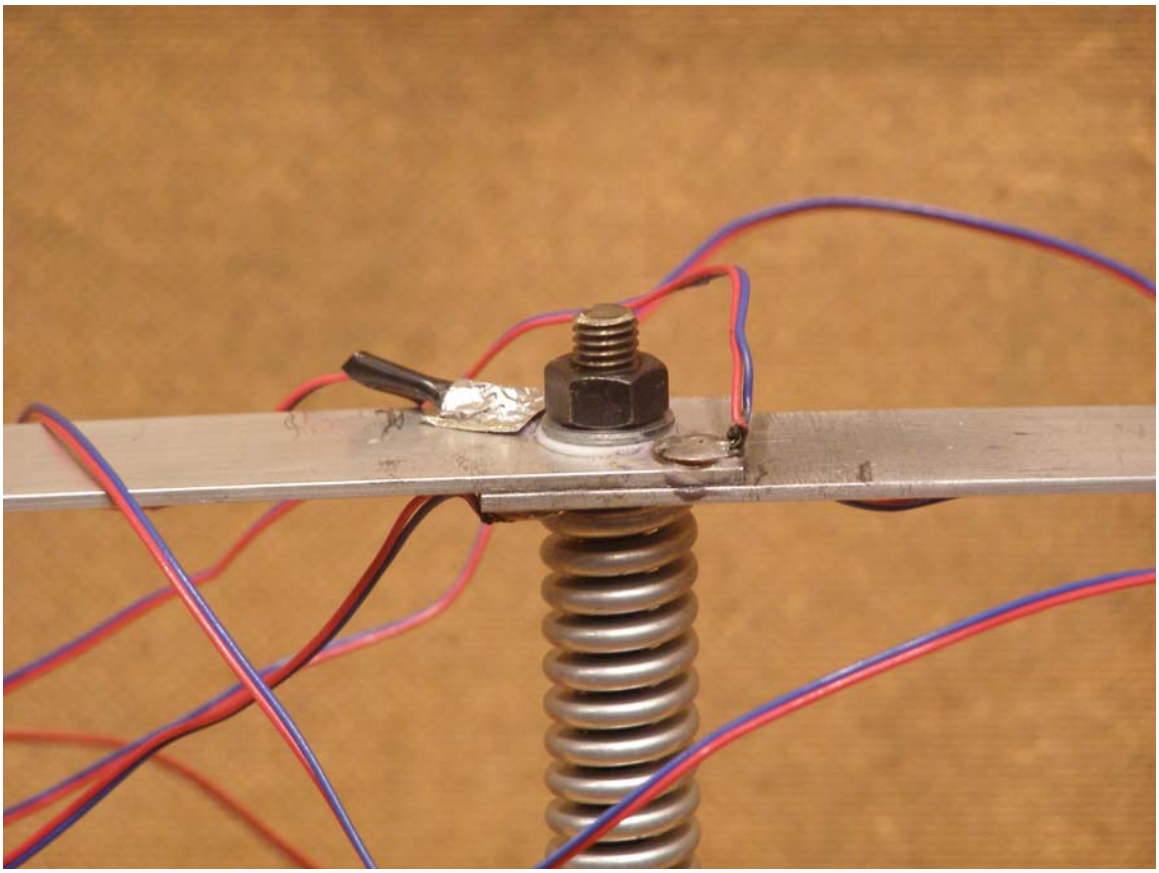

Figure 7.8 aluminium strip sample for laboratory investigation

7.3.3 Mini disconnector

At the time of the experiments there was no disconnector available so instead a mini version of the three phase disconnector shown in figure 7.9 and 7.10 was used.

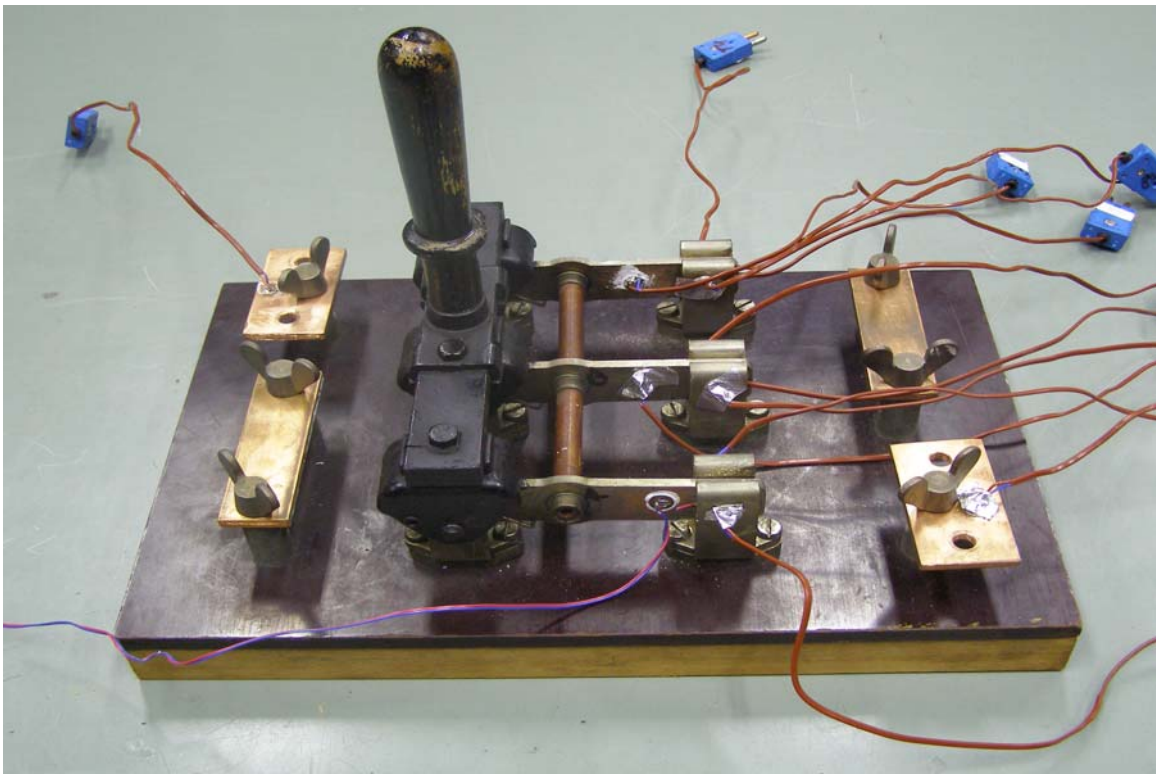

Figure 7.9 three phase mini disconnector for laboratory investigation (closed position)

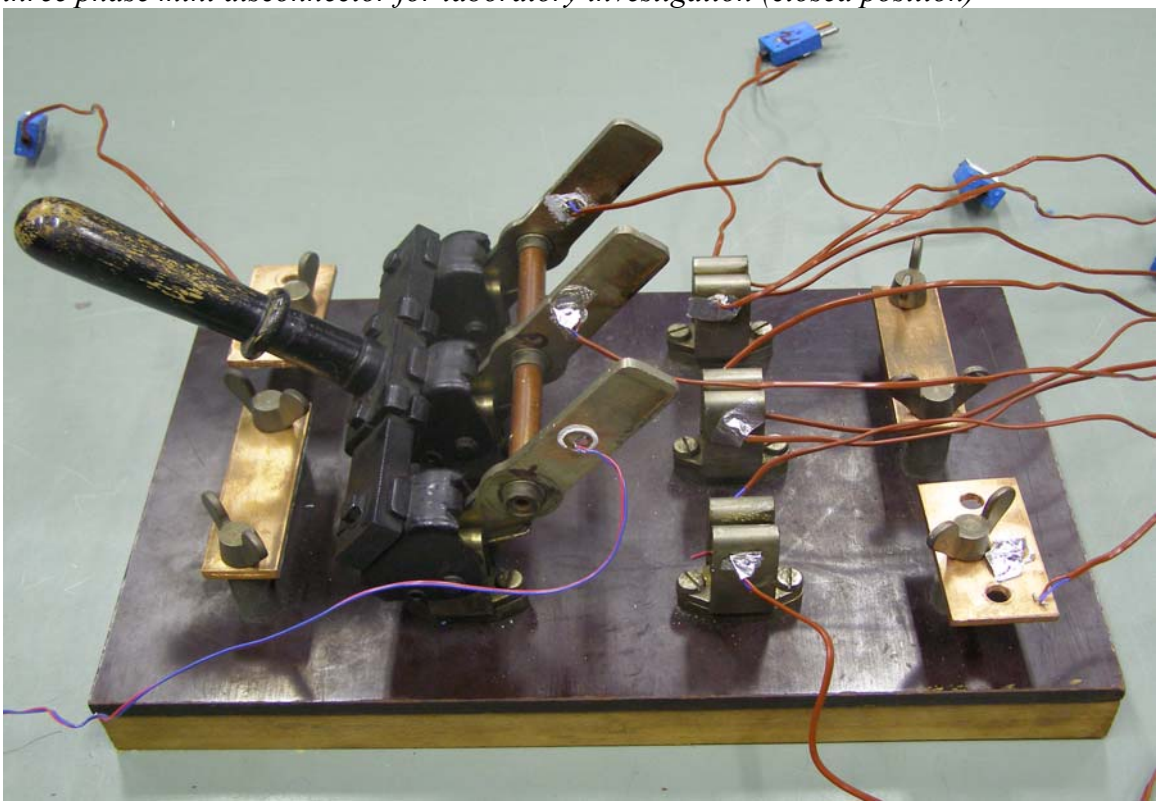

Figure 7.10 *three phase mini disconnector for laboratory investigation (open position)*

8. Measurements and results copper sample

In this section the results of the different measurements performed on the copper sample are presented. Likewise the calculations will also be given.

8.1 Measurements and results for the determination of the exponent (n)

The first measurements series were performed on a copper contact to investigate and determine the exponent (n) in eq. 5.2 section 5.1.1. Before load current was applied the initial contact resistance was measured and registered. The temperature rise caused by load current variations were also recorded and registered. The current was applied continuously. When current is applied it is held constant till the temperature has reached its thermal equilibrium, before raising the current to the next level. That is, when the temperature rise has stabilized. Figure 8.1 shows the flowchart to determine the exponent. Conditions for these measurements are presented in table 8.1.

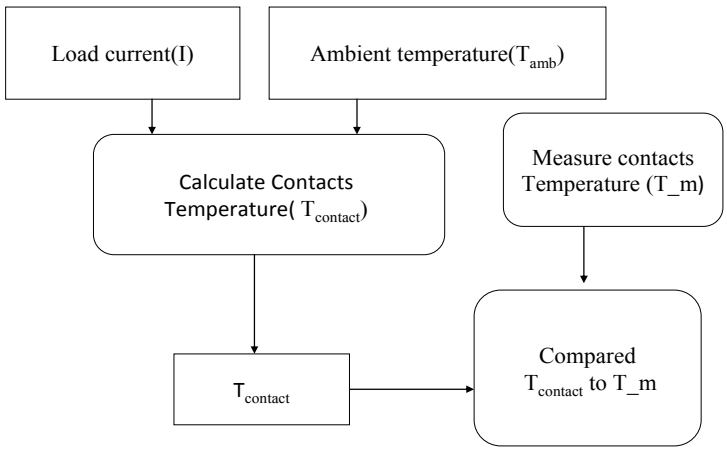

Figure 8.1 Flowchart of temperature rise due to load variations measurement

Table 8.1 measurements conditions

Ambient temperature[°C]	Load current[A]	Resistance Before measurements[μΩ]	Resistance After measurements[μΩ]
18.6[°C]	150-300	13.17	13.17

8.1.1 Results and analysis of the value of the exponent (n)

In the equations to calculate the temperature and temperature rise at the contact it was stated that the value of the exponent equals 2, this is a theoretical value. Therefore the actual value of the exponent (n) has to be determined before proceeding with other measurements. This was done by keeping the contacts resistance fairly constant and changing the load current. The value of the exponent is found by solving equations 5.3 and 5.5 for different values of n. For the accuracy, the experiment was repeated. The results of the first measurements are presented in table 8.2 together with the average mean error and standard deviation. In figure 8.2 the results of the experiment are presented in graphical form. Figure 8.3 shows the power curves fit to the data using the trend line feature of Microsoft Excel, the equations for the fitted curves and the goodness of fit (R^2) are also shown.

Table 8.2 measurement results to determine the exponent

	I[A]	150.6	225.6	300.2		
	Measured Temperature rise [°C]	10.03	21.95	37.1		
Calculated Temperature rise [°C]					Error	
					mean	Standard deviation
	n=1.8	10.03	20.76	36.71	0.53	0.50
	n=1.9	10.03	21,62	37.77	0.33	0.34
	n=2	10.03	22.69	38.67	0.77	0.79

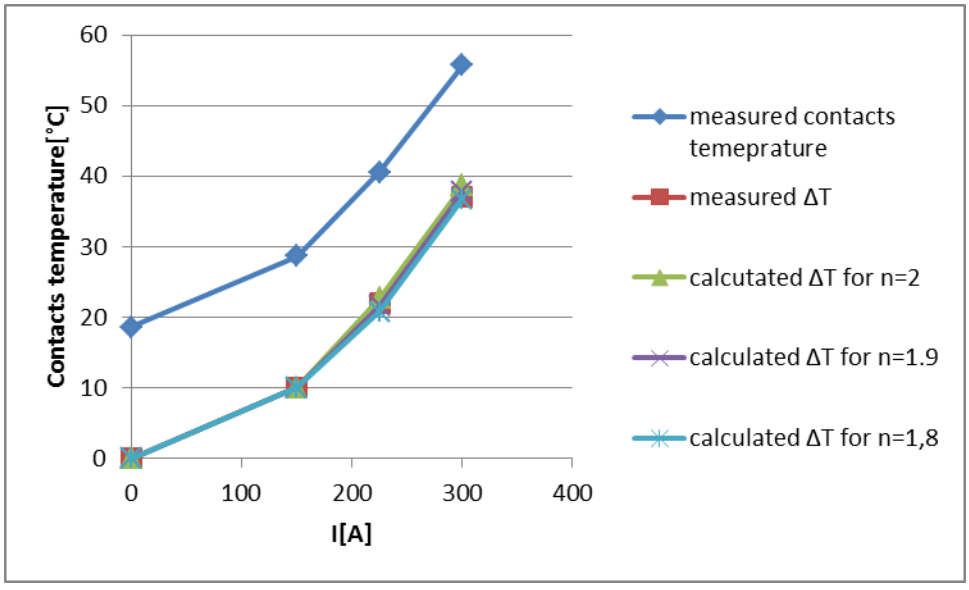

Figure 8.2 plots of various values of the exponent and the actual measured values

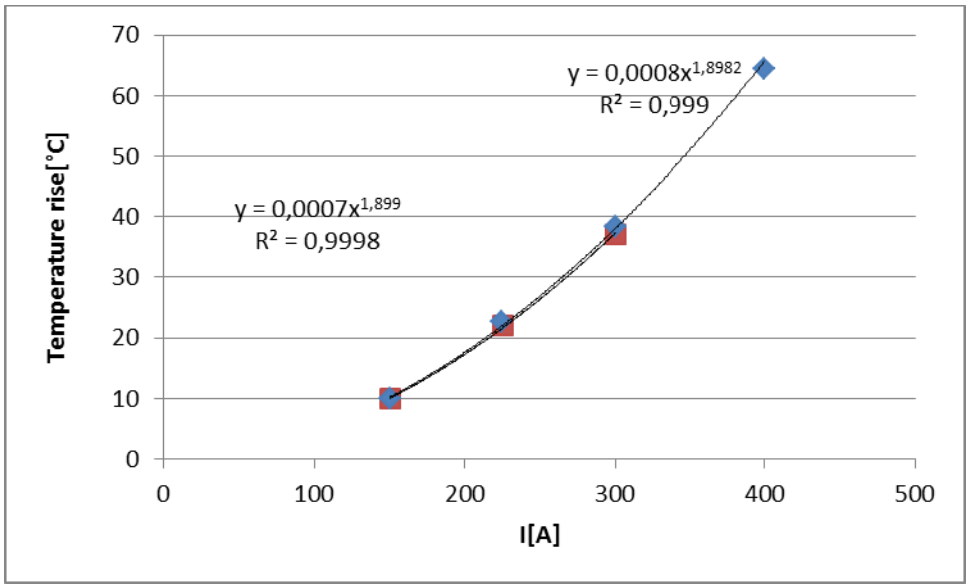

Figure 8.3 power curves fit to experimental data to determine the value of the exponent

From the results presented in table 8.2 and fitted curves it is clear that the value of n is 1.9. This value has the smallest mean error and the goodness of fit is almost 1(the closer the R^2 is to one the better the fit) therefore, n = 1.9 is used for future calculations of the temperature.

8.2 Temperature and temperature rise due to load variations

To evaluate the load temperature behaviour the resistance of the contact was kept fairly constant at 13.59 μΩ and the load current was varied from 150-400 amps. The ambient temperature at the time of measurements was 20°C. The results are presented in figure 8.4. The different colours in the figure represent the measured temperature, measured temperature rise, calculated temperature and calculated temperature rise of the contact.

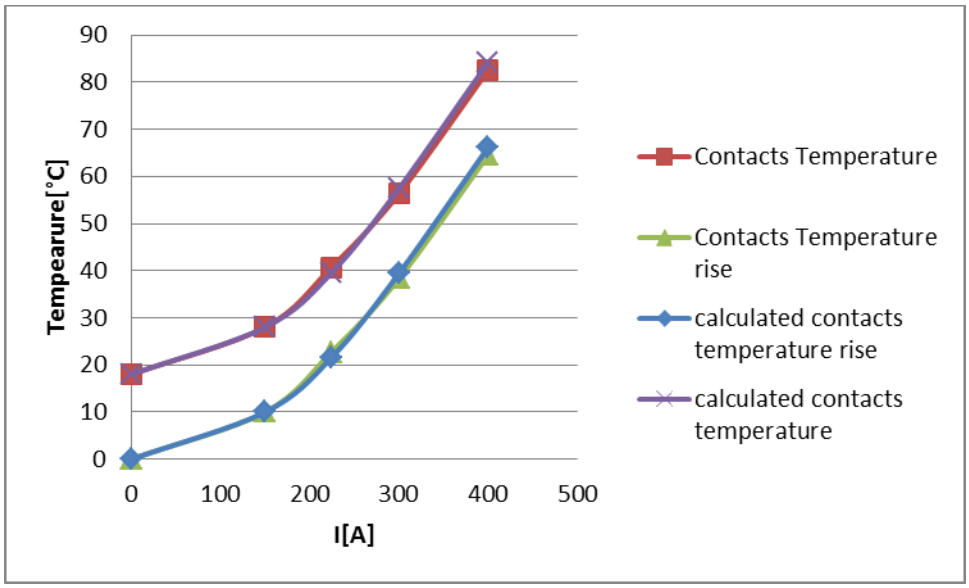

Figure 8.4contacts temperature and temperature rise as function of load current

The measurements results show that, the higher the load the higher the temperature rise. The reason for this is explained by Joule's law. In chapter 5 it was stated when current passes through a contact with resistance R heat is generated. The generated heat due to load current is a square function of the load current thus, as the load increases the heat dissipated into the contact will also increase, this will translate into the temperature of the contact rising. Furthermore the temperature rise in turn is a power function of the load current which is to the 1.9^{th} power from the previous section. The calculated values are also depicted in the figure indicated by the legend calculated.

8.3 Measurements and results temperature and temperature rise due to resistance variation

The resistance measurements were performed in accordance with the method described in section 7.2.2. In this section the following are investigated:

- The resistance of the contact due to temperature variation; hot resistance measurements
- The temperature rise due to resistance variations
- In addition to this the calculated results are compared to the measurements results

The measurements results and conditions are presented in paragraphs 8.3.1 and 8.3.2 respectively.

8.3.1 Results hot resistance measurements

As mentioned in chapter 6, the resistance of the contact varies with the contacts temperature. If the temperature variations are within the normal operating range the variation of the resistance with the temperature will be linear (eq.6.3). Since the resistance model also uses the resistance to predict the condition of the contact, it is useful to verify the statement through measurements.

These measurements were carried out to fulfil the following goal:
To see if the resistance can be measured while the test sample is still hot and to get some data to which the calculated resistance values can be compared. So, after every load application the load current is switched off for a short while so that the resistance can be measured. The measurements conditions and results are presented in tables 8.3 and 8.4 respectively. Figure 8.5 shows the measured and calculated resistance as a function of the temperature.

Table 8.3 Measurements conditions

Ambient temperature T_{ma} [°C]	Load current I[A]	Resistance measurements	Temperature Coefficient α [°C^{-1}]
18	150-400	Before every load change	0.004

Table 8.4 Measurement results

I[A]						Mean error	Standard deviation
Temperature rise[°C]	0	10	22.68	38.33	64.5		
Measured contact resistance [μΩ]	13.59	13.75	13.91	15.72	16.5		
Calculated contact resistance [μΩ]	13.59	13.62	14.31	15.21	16.8		
Error	0	-0.13	0.4	0.51	0.3	0.012	0.36

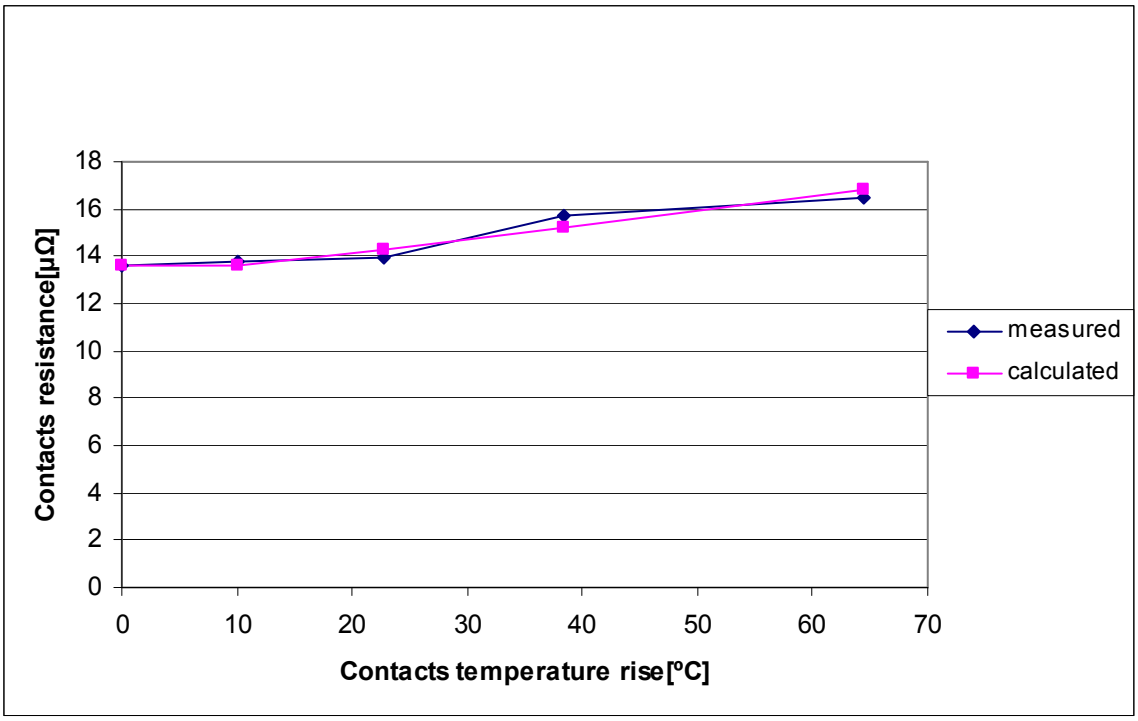

Figure 8.5 the effect of temperature on the resistance

The calculated and measured curves both show a linear relation between the temperature and resistance. The small deviations between the calculated values and measured values can be attributed to the fact that when the current is switched off the temperature of the contact begins to fall rapidly therefore the exact temperature at which the measurements were made differs from the temperature used for the calculations. After the measurements were done, the contact was left to cool off to the ambient temperature and the resistance after the contact has cooled to ambient temperature the resistance was measured, it was the same as before the measurements. This means that the resistance of the contact is influenced by its temperature.

8.3.2 Measurements and Results of the contacts resistance

As mentioned at the beginning of chapter 6 if the load is kept constant the resistance of the contact will determine the heat generated at the contact.
In order to evaluate how the increase in resistance affects the temperature rise, the load was kept constant and the resistance changed.
The resistance of the contact was varied in three different ways:

1) The contact surface area was decreased by lowering the pressure holding the contact together.
2) A semiconducting material (Elastosil M 4601-A) was applied at the contact, which serves as a tarnish layer at the contact area.

3) The contact was deliberately burned out by applying low pressure at the contact (loosening the bolts holding the contact together) and then applying current to it.

The results are shown in figure 8.4. The different colour lines in the figure indicate different load current.

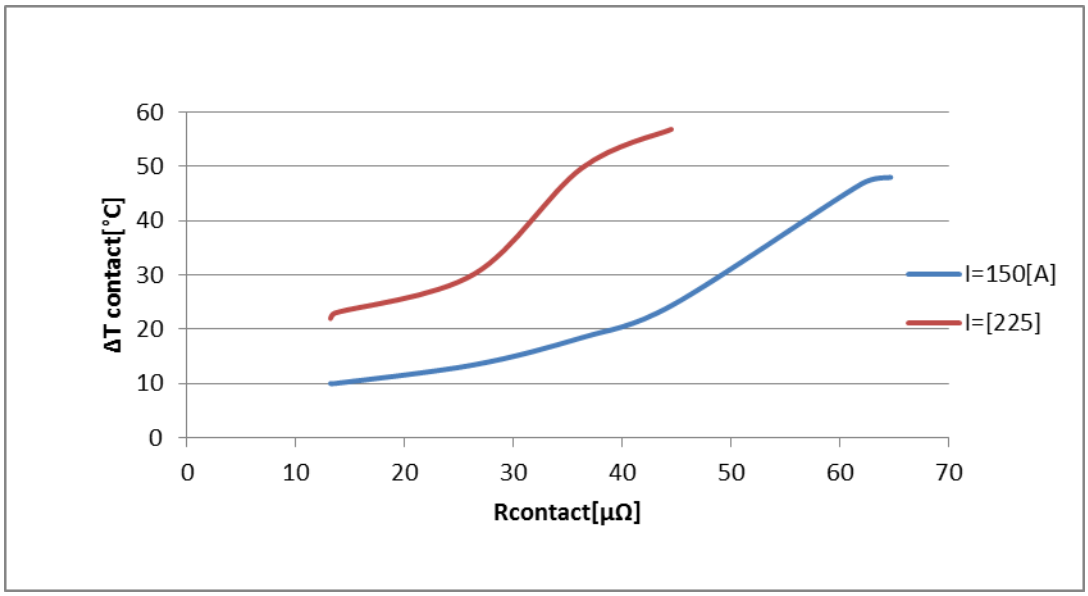

Figure 8.6 temperature rises as function of contacts resistance at two loads.

In figure 8.6 the contacts temperature rise is shown as a function of resistance. It is seen that the temperature rise increases with increasing resistance. This is due to the fact that if the load current is fixed the resistance determines the power dissipated into the contact (chapter 6). Therefore if the contacts resistance is increased the heat generated at the contact will also increase consequently the temperature will also increase. For example at constant load of 150 amps and a resistance of 13.6 μΩ, the temperature rise is 10°C if the resistance is increased to 26.4 μΩ, the temperature rise is 13.4°C. The resistance has doubled but the temperature rise didn't double; the difference is 3.4°C; this is because the temperature rise is not a linear function of the resistance. If the heat loss was due to conduction alone then the temperature rise would have been a linear function of the resistance, the nonlinearity is caused by the heat losses due to convection and radiation. On the other hand if the load is increased, for example from 150 amps to 225 the temperature rise curve moves from the blue line to the red line.

The basic idea of this thesis is to determine the resistance of the contact based on its temperature rise and load current therefore, the temperature rise is plotted as function of the load for different values of the resistance this is depicted in figure 8.7 where different colour line represent different values of the contacts resistance.

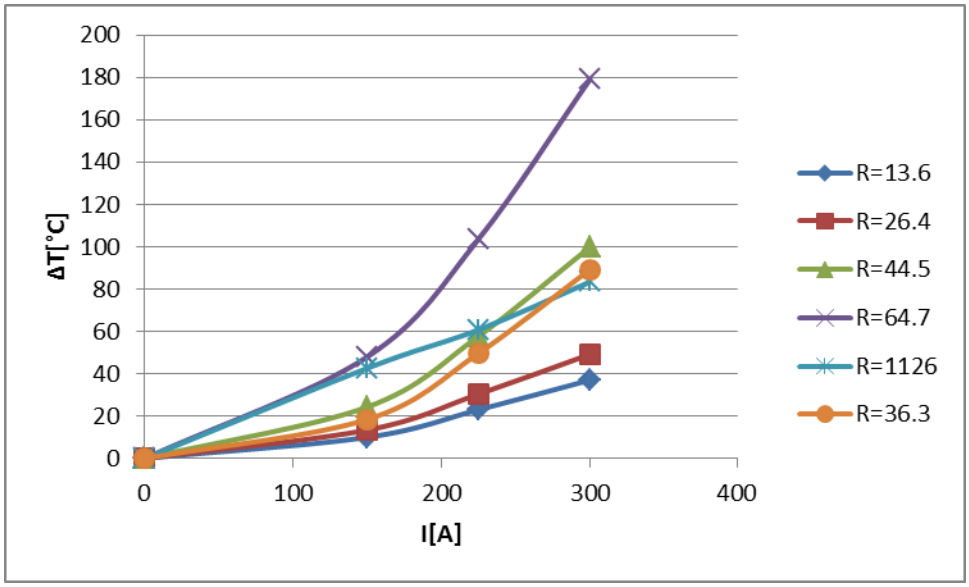

Figure 8.7 temperature rise as funtion of load current for various resistance values

1) From this figure it is observed that at constant load the higher resistance have higher temperature rise.
The figure also shows the higher the load the higher the temperature rise up to a point. There is a point where, when the load is raised farther the temperature rise of a contact with higher resistance is less than that of a resistance 25 times less. This was found in the measurements carried out with an initial resistance of 44.5 and 1126 μΩ.
At 150 amps load current the temperature rise for the 1126 μΩ resistance was 42.7 °C (turquoise line) and that for the 44.5 μΩ Resistance was 24.35°C(green line). The resistance with higher value has the higher temperature rise as expected. When the load current is raised from 150 to 300 amps the temperature rise for the higher resistance is less than that of the lower resistance, the green curve is above the turquoise curve. Further investigation of the contact showed that the contact area had welded together and as a result has reduced the contacts resistance significantly. The measured resistance after the test was half the initial value, 644 μΩ. The reason for this is that, when current passes through the contact the temperature of the contact will increases (Joules law), the temperature rise in turn will cause an increase in the contacts resistance (results from 8.3.1), in this case the is 17%, which will lead to even higher temperature rise and as results soften the material of the contact locally thereby increasing the contacts area and reducing its resistance (chapter 6 eq6.2). This is why it is important to diagnose the condition of the contact before it reaches the stage whereby the influence of its temperature becomes detrimental to the resistance.

The results from the previous measurement with load variations showed that the temperature rise is function of the load current to the 1.9^{th} power. The results from the

temperature rise due to resistance variations show that resistance characterised by higher values produce the most heat and thus have higher temperature rise.
Based on these findings the following can be done:

1) When the load and temperature rise are known for a given resistance, extrapolation can be made to find the temperature rise of the contact for other load currents. This is done for four different resistance values; 13.6, 26.4, 36.3 and 44.5 μΩ the results are shown in figure 8.8, the different line colours represents different resistance values.

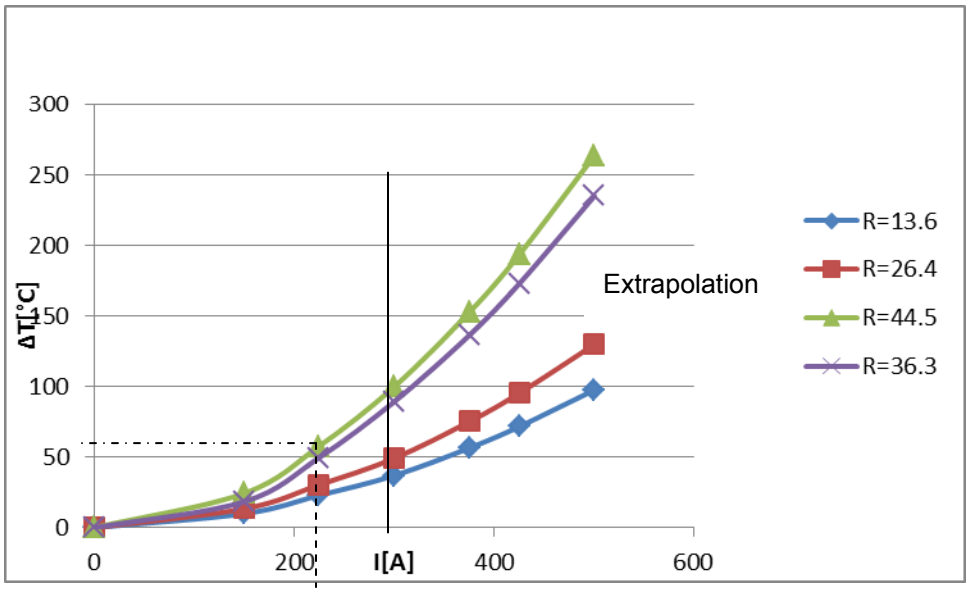

Figure 8.8 extrapolation of the relation between temperate rise and load current

2) When the temperature rise and the load current are known as often is the case with online measurements the off-line numerical value of the contacts resistance (which is the point of intersection between the straight lines drawn from the temperature axis and the current axis, dashed lines in fig 8.8) can be determined using equation 6.8.

To be able to solve equation 6.8 the contact is modelled as two horizontal plates with heated surface up for the top plate and for the bottom plate, the hot surface is facing down. The off-line resistance were calculated using MATLAB (see appendix), for the consistency of the calculation the load was changed three times for every resistance. And for the convenience of comparison four resistance calculations were made to see whether or not the difference between the actual and the calculated values were resistance dependent. The results are presented in tables 8.6a, b, c and d. The dimensions of the sample and the constant properties are given in table 8.5.

Table 8.5 constant parameters and sample dimensions for copper sample

Thermal conductivity = 401W/mk
Emissivity=0.78 the highest value found for copper
Temperature coefficient = 0.004°C^{-1}
Sample dimensions in mm: 25x3x1987 (width x thickness x length)
Contacts dimensions in mm:25x3x31.5 (width x thickness x length)

Table 8.6 a calculated offline resistance of a copper contact of 13.6μΩ at 18°C *ambient temperature*.

		Contacts resistance[μΩ]			
I[A]	$T_{contact}$[°C]	measured	calculated	Measured /calculated	
150.1	28	13.6	5.5	2.5	
224.4	40.68	13.6	5.3	2.6	
300.2	56.33	13.6	7.0	1.9	
		error		mean	2.3
				std	0.4

Table 8.6 b calculated offline resistance of a copper contact 0f 26.4μΩ at 18.3°C *ambient temperature*.

		Contacts resistance[μΩ]			
I[A]	$T_{contact}$[°C]	measured	calculated	Measured/calculated	
150	31.75	26.37	12.6	2.1	
250	55.1	26.37	15.5	1.7	
300	67.5	26.37	12.9	2	
		error		mean	1.9
				std	0.2

Table 8.6 c calculated offline resistance of a copper contact 0f 36.3μΩ at 19.6°C ambient temperature.

		Contacts resistance[μΩ]			
I[A]	$T_{contact}$[°C]	measured	calculated	Measured – calculated	
150	38.05	36.3	27.5	8.8	
200	64.85	36.3	35.7	0.6	
250	82.78	36.3	31.5	4.8	
		error		mean	4.7
				std	4.1

Table 8.6 d calculated offline resistance of a copper contact with 44.5 μΩ at 20.4°C ambient temperature.

		Contacts resistance[μΩ]			
I[A]	$T_{contact}$[°C]	measured	calculated	Measured-Calculated	
150	44.75	44.5	41.3	4.2	
200	67.53	44.5	43.9	0.6	
225	78.23	44.5	42.5	2	
		error		mean	2.3
				std	1.8

The results show that the calculated values deviate significantly from their actual values for contacts with low resistance. The deviation varies from 1.7 to 2.5 times less than the actual values. For the higher resistance the difference between the calculated values and the measured values are between 0.6 and 8.8. The explanation for these deviations from the original values is as follows:

- The relations of the convection heat transfer are very complex because of the number of variables upon which convection depends.

- The Rayleigh (Ra_L) number for the convection heat transfer for a horizontal plate with heated surface facing down in the laminar region is in the range of $10^5 \le Ra_L \le 10^{10}$ as given by equation 5.15.The range of the Raleigh number for the calculation fell out of this range. Since there was no convection heat equation found for Rayleigh number less than 10^5, it was assumed that the equation could be used for the calculations.

- For the lower resistance values, the difference between the contacts temperature and the temperature in the neighbourhood on either side of the contact was small (less than 2°C) the contact had the lowest temperature of the three areas (see fig. 7.1).

- Properties such as emissivity and the temperature coefficient that were taken to be constant for the calculations are also temperature dependent.

Although, for the two lowest resistances the calculated values deviate significantly from the measured values it is seen that for the higher resistance the model seems to be accurate with an accuracy of 5%. For each resistance the range of the Raleigh number was different, the closer the range of the Raleigh found for the calculation came to the given range, the better the prediction of the off-line resistance value. A summary of the range of the Raleigh number found for the calculations are given below:

-For 13.4 μΩ: $262 \le Ra_L \le 807$

-For 26.37 μΩ: $342 \le Ra_L \le 951$

-For 36.3 μΩ: $443 \le Ra_L \le 10^3$

-For 44.5 μΩ: $551 \le Ra_L \le 10^3$

Since the other properties used for the calculations are same for each contact resistance it can be concluded that the convection heat transfer correlation for lower plate is the greatest contributor to the error.

8.4 Measurements and Results solar heating

The effect of the sun heating was tested by placing the sample in the sun for three hours. Before the sample was placed in the sun, a black tape of high emissivity (0.95) was placed on two small surfaces very close to the contact, one on the left and the other on the right side of the contacts surface indicated by R_LB and R_RB respectively. The sample was then left in the sun for three hours after which the temperatures of the contact, the

areas indicated by R_R and R_L (see figure 7.1) and the areas with black tape were recorded. The measurement results are presented in table 8.7. The ambient temperature at the time of measurement was 24.3 degrees Celsius there was no wind during the measurement.

Table 8.7 results solar heating

	Temperature rise in degrees Celsius			emissivity
	Measured values	**Calculated values**		
		Eq. 5.34	***Eq.5.35***	
Contact	14.3	11.8	8.6	0.76
R_RB	12.9	14.7	10.7	0.95
R_R	11.5	11.8	8.6	0.76
R_LB	14.9	14.7	10.7	0.95
R_L	14.2	11.8	8.6	0.76

The calculated results are also presented in the table under the heading calculated values. The values were obtained using formula 5.34 and 5.35. Equation 5.34 gives the maximum value of the temperature rise corrected only for objects emissivity and 5.35 gives the temperature rise corrected for objects emissivity and incident heat flux.
The heat flux (Q_s) was found to be 757W/m^2 and the solar altitude was 24 degrees. The influence of the sun can have a huge impact on the temperature ratings of the contact. For example in figure 8.9 the temperature rise of the contact with a resistance of 13.6 μΩ at 150 amps load is 10°C. If the contacts temperature had been measured during this time the temperature rise would have been 24.3 °C (10+14.3), thus suggestion that the resistance of the contact is 44.5μΩ.
Thus the temperature rise measured on a clear day at noon in the summer must be corrected with the temperature rise calculated with equation 5.34; corrected with the maximum temperature rise due to the sun because this value is the closest from the table to the actual measured value with an accuracy of 17%. And in all other cases when the sun is present and the sky is clear the measured temperature rise at the contact must be corrected with the temperature rise calculated with 5.35.

9. Results aluminium sample

The measurements results of the aluminium sample are the subject of this chapter. In addition to the measurements results, the calculated results are also given.

9.1 Determination of the exponent (n) of aluminium sample

The method used to determine the exponent for the copper sample was also used for this sample. The load current was raised from 150 to 250 amps in steps of 50 amps. The temperature of the contact was recorded and registered after the temperature rise had stabilized. The results are shown in table 9.1.The calculated values of the temperature rise for different values of the exponent and the measured values together with the absolute mean error and standard deviation are also listed in the table 9.1. In figure 9.1 results of fitting the measured data with power regression, using the trend line feature of Microsoft Excel is presented.

Table 9.1 measurement results to determine the exponent of aluminium sample

	I[A]	150	200	250		
	Measured Temperature rise [°C]	28.2	47.6	75		
Calculated Temperature rise [°C]					Error	
					mean	Standard deviation
	n=1.8	10.03	20.76	36.71	1.35	1.75
	n=1.9	10.03	21,62	37.77	0.35	1.71
	n=2	28.2	50.1	74.4	0.66	1.66

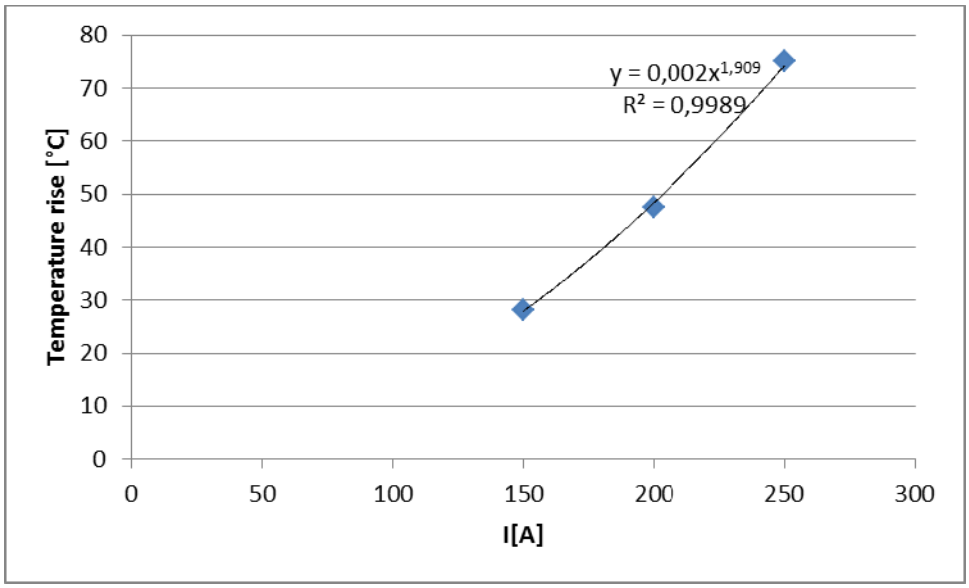

Figure 9.1 power curves fit to measurement data to determine the value of the exponent

From table 9.1, 1.9 has the smallest mean error and the power regression curve also estimates the value of the exponent to be 1.9 thus, it can be assumed that the value of exponent for this sample is also 1.9; consequently this value is used for future calculations.

9.2 Load current and temperature rise measurements

The measurements were conducted under an ambient air temperature of 20°C. The load was raised from 0-250 amps in steps of 50 amps; the contacts temperature was recorded and registered. The measurements results and calculated values are presented is figure 9.2. The colour lines represent calculated and measured temperature rise.

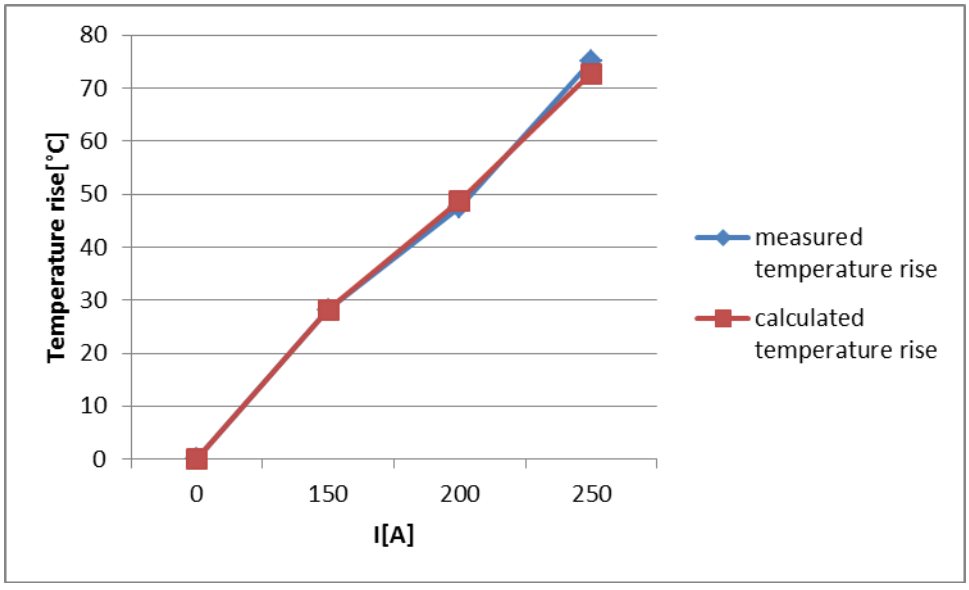

Figure 9.2 contacts temperature rise as function of load

The plots show that the temperature rise increases with increasing load this is due to the Joule heating.

9.3 Measurements and results on influence of the wind

The effect of the wind was investigated at different load current as well as at different wind speeds to find the correlation between the wind speed and the temperature rise. For the wind a fan was used to produce wind over the surface, the wind speed was measured three times using the Skywatch Xplorer the average value of three measurements is the measured wind speed. The manufacturer of this states it +/-3% accurate. The wind speed varied between 0-4m/s and the applied load current was 150 and 250 amps. The flowchart for the wind effect investigation is given in figure 9.3. The results of the measurements are depicted in figure 9.4.

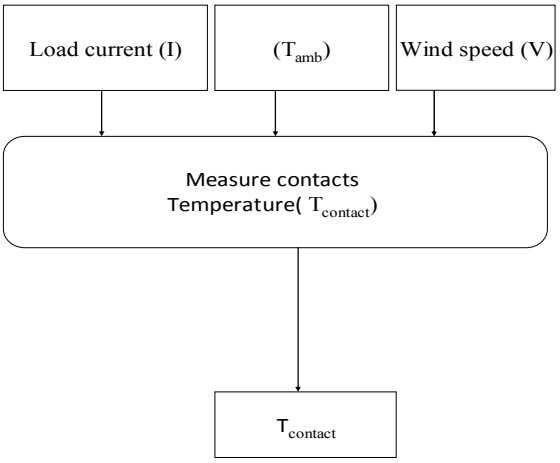

Figure 9.3 Flowchart to investigate the wind effect

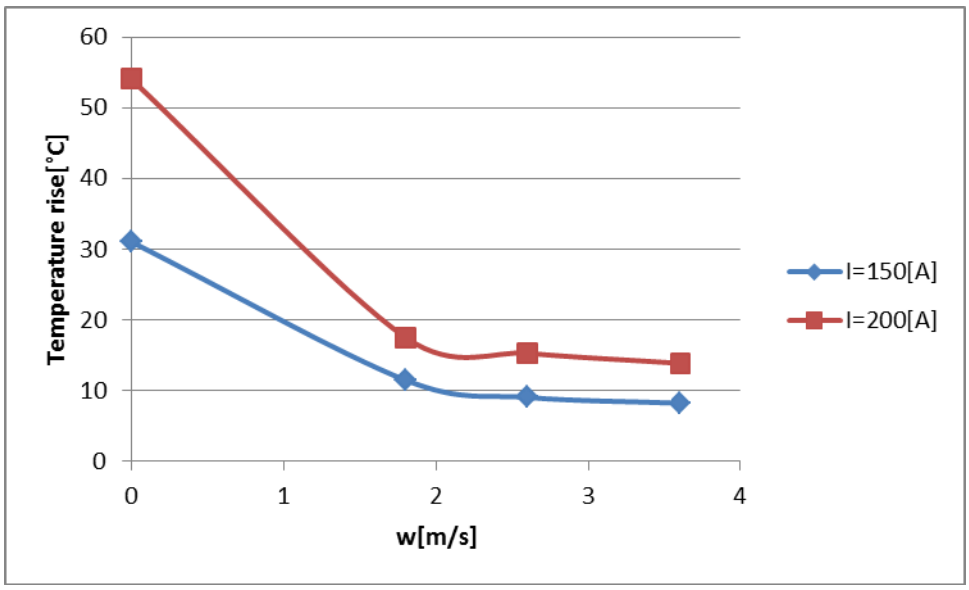

Figure 9.4 Temperature rise as function of wind speed for two power levels

The results show the wind has a huge effect on the temperature rise, even for lower wind speeds. For example at 150 amps load the temperature rise is 31.0 °C at no wind. At wind speed 1.8m/s the temperature rise is 11.45°C a reduction of almost 20°C. This means that the contact will appear normal during inspection. The cooling of the wind is also power dependant, for example at 1.8m/s wind speed the reduction of the temperature rise at 150 is 20°C and at 200amps the reduction is 36.6°C more than three times the reduction at 150 amps.

In chapter 5 it was mentioned that the wind influence on the temperature rise is of the form w^m where w is the wind speed and m an exponent that must be determined. On the basis of this, power regression is used to fit the data obtained by measurement. The results are presented in figure 9.5, the temperature rise at no wind are shown separately in the figure because of the power fit to the data.

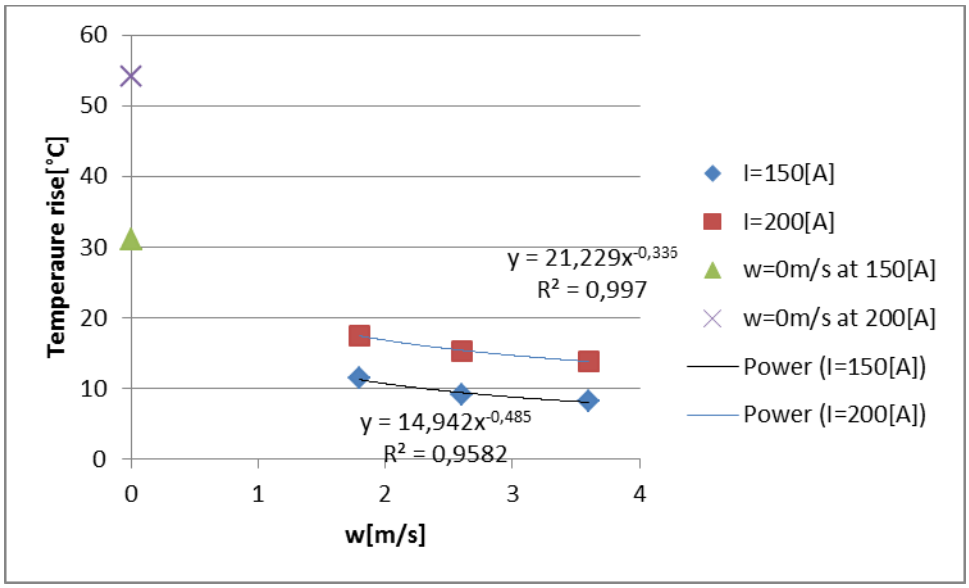

Figure 9.5 variation of contacts temperature rise with speed

The above figure shows each power level has different exponents thus making the wind effect power dependent. This is not a surprising result because the wind effect originates from convective cooling (chapter 5) whose variables are also temperature dependant. The exponent of 200 amps load is 0.485 and the exponent of 150 amps load is 0.336, the exponent at 200 amps load is higher than at 150 amps load. It can be concluded that the wind cooling is higher for higher loads.

9.3.1 Wind correction for aluminium sample

To compensate for the wind the data from the wind speed measurements are evaluated. The wind correction is the ratio of temperature rise at no wind to temperature rise with wind. The results are shown in figure 9.6.

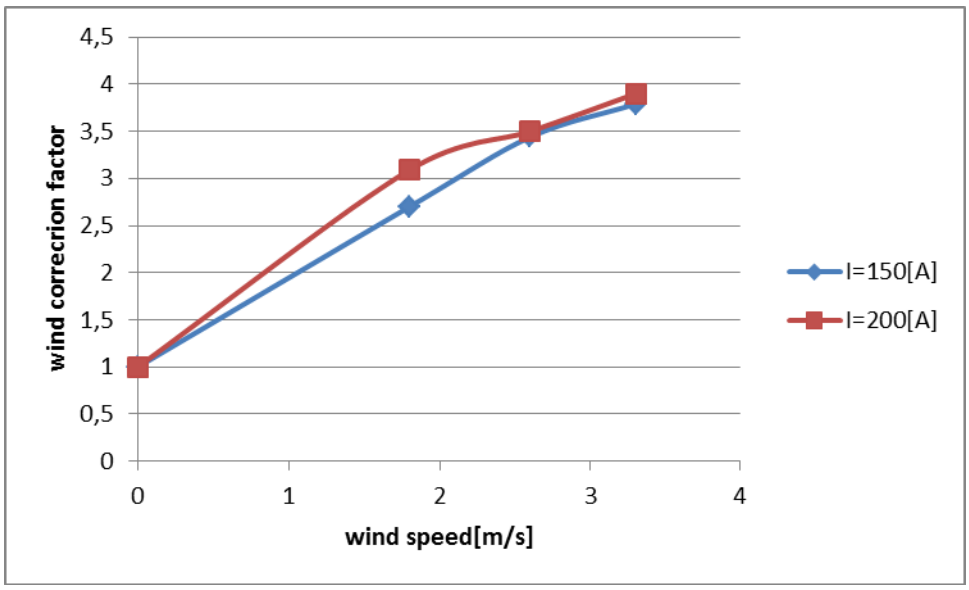

Figure 9.6 calculated wind correction factor

The plot of figure 9.6 shows the wind correction factor for 2 different power levels. Each power level produces a different correction curve and the correction also varies with the wind speed which makes the wind correction factor power and wind speed dependant. Therefore if the power and the wind speed are known the temperature rise can be corrected for by multiplying the measured temperature by the correction factor corresponding to that particular power level and wind speed. The figure also shows that the curves diverge at lower wind speeds with discrepancy at a wind speed of 2.6m/s; this can be attributed to measurement error.

Since the effect of the wind is a power function of the wind speed, regression can be used to fit the data obtained by computing the ratio temperature rise at no wind to temperature rise with wind see figure 9.7. Note that the zero wind speed is left out because of the power fit to the data. By means of interpolation correction factors for other wind speeds can be calculated. However, the interpolation is only meaningful when the wind speed is within the given range. Beyond this range it is possible that the system might be in the turbulent region, or that the system is no longer operating under steady state conditions. This means that, the heat capacity of the object must also be considered in the heat calculations which will make the calculation even more complex.

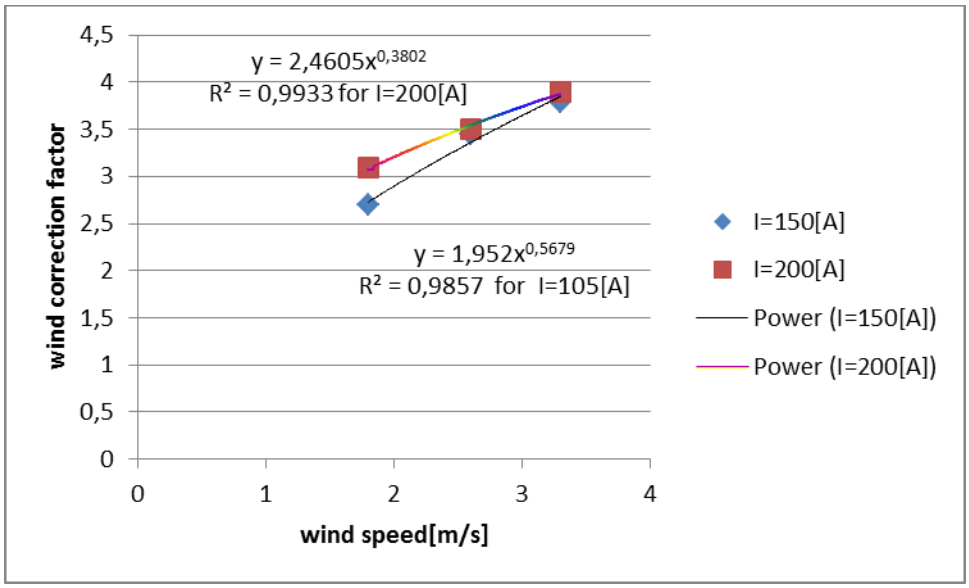

Figure 9.7 power fit to measments data

9.3.2 Offline contact resistance aluminuim sample

The same calculation and evaluation method used for the copper sample are also used for this sample. The constant parameters and the dimension of the sample are listed in table 9.2, the results of the measurements and calculations are presented in tables 9.3 a and b.

Table 9.2 *constant parameters and sample dimensions for aluminium sample*

Thermal conductivity = 237W/mk
Emissivity=0.06 the highest value found for aluminium
Temperature coefficient = $0.004°C^{-1}$
Sample dimensions in mm: 30x3x1940(width x thickness x length)
Contacts dimensions in mm:30x3x31(width x thickness x length)

Table 9.3 a results of offline resistance estimation of aluminium contact of 50 μΩ resistance

		Contacts resistance[μΩ]			
I[A]	$T_{contact}$[°C]	measured	calculated	Measured/calculated	
150	49.2	49.6	11.4	4.4	
200	68.6	49.6	9.2	5.1	
250	96	49.6	7.6	6.5	
		error		mean	5.3
				std	1.3

Table 9.3 a results of offline resistance estimation aluminium contact of 75 μΩ resistance

		Contacts resistance[μΩ]			
I[A]	$T_{contact}$[°C]	measured	calculated	Measured/calculated	
150	51.5	74.6	31.5	2.3	
200	73.7	74.6	27.6	2.7	
250	96.5	74.6	20.4	3.7	
		error		mean	2.9
				std	0.7

From both tables it is clear that the calculated values deviate significantly from the actual values. The deviation ranges from 2.3 to 6.5. Just like with the copper contact, the contact was not the source of the overheating; the temperature on the left and right side of the contact were higher than the contacts temperature.

10. Mini disconnector

The mini disconnector developed in the laboratory was also tested in the same way as the two previously motioned samples. The ratings of the mini disconnector were:

- Rated current: 200A
- Rated AC voltage: 500V
- Rated DC voltage 250V

Just like the other samples the first set of measurements were to determine the value exponent in the temperature calculations.

The disconnector contact was a nickel plated copper contact. Since the contact consists of two different materials the following assumptions are made:

1. The properties of nickel are used for the surface characteristics, the radiation from opaque bodies is instigated with a few microns of the surface, therefore radiation properties such as emissivity is characteristic of nickel rather than copper[20].
2. For the internal parameters the properties of copper are taken, this is because the percentage of nickel is less than 1 as a result the temperature coefficient of this sample will be practically the same as of pure copper [21]. According to this reference if the percentage of copper is less than 100% the temperature coefficient (α) of copper can be determined a $n\alpha$ where n= the percentage copper

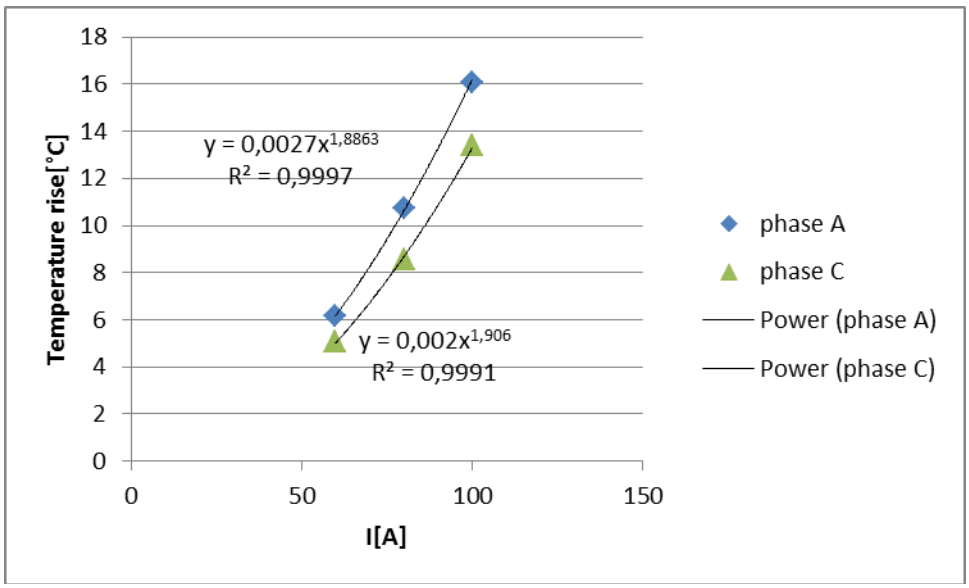

Figure 10.1 power curves fit to experimental data to determine the value of the exponent

From figure 10.1 the exponent can be taken to be 1.9 which is the same as the copper sample discussed in chapter 8. This is in agreement with assumption 2.

10.1 Load current and temperature rise measurements.

For this set of measurements the load was raised from 30% load to full load.
The thermal model described in chapter 5 was applied to this sample to investigate the temperature distribution of the three phases. For this experiment the contacts resistance of each phase was different. The measured contacts resistance were 134, 52, 79 micro ohms for phase A, B and C respectively. The results are shown in figure 10 .2.

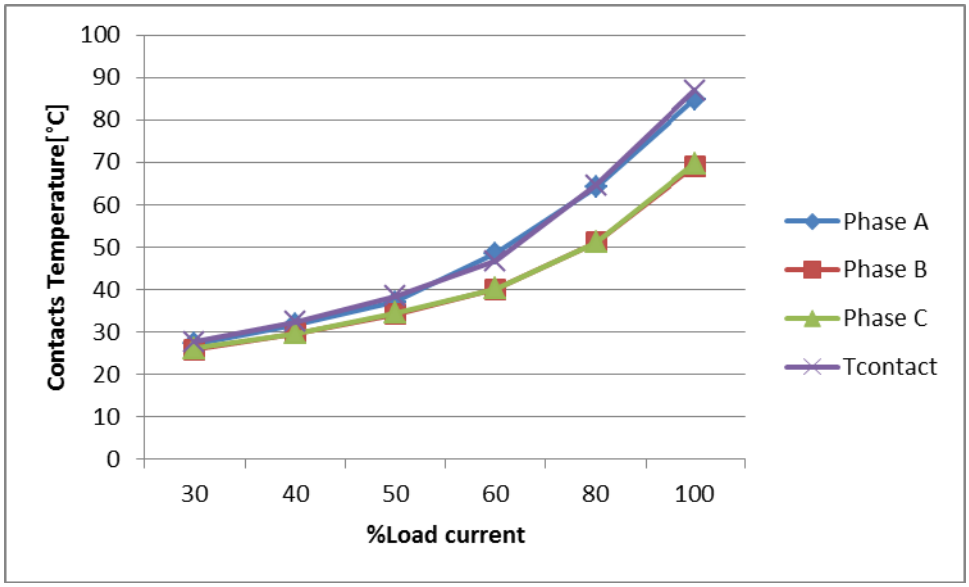

Figure 10.2 contacts temperature as funtion of persentage load current

The different colours represent different phase and the calculated contacts temperature. The curves in figure 10.2 show that phase A has the highest temperature which was expetect, as phase A has the highest resistances. The temperature of the other two phases are far below the norminal temperature which is represented by the legend $T_{contact}$. The temperature of phase A on the other hand is very close to this temperaure.The temperature results show that, although the contacts resitance of Phase A is almost 3 times higher than the resistance of fase B the temperture rise of Phase A is not 3 times as high as phase B. This result is not completely surprising from previous results it is known that the contact resistance is not a linear function of the temperture rise due to radition and convection heat losses.

10.2 Influence of the sun

The contribution of the sun on the temperature rise was also investigated for this sample. The results are shown in table 10.1. From the table, the maximum temperature of the test

object is 6.5°C which is almost three times less than the measured value. The highest emission coefficient found for nickel in test book within temperature range of this project is 0.41. But higher values 0,59 at 650 degrees Celsius and 0.86 at 1255 degrees Celsius have been documented in the literature [22]. Although these temperatures are very high, from the measurements results the value of 0.86 seems to be more the suitable value for the emissivity.

Table 10.1 the effect of solar heating calculted for 2 different values emissivity of nickel

	Contacts temperature rise in degrees Celsius				
	Measured values	**Calculated values**			
		Eq. 5.34		***Eq.5.35***	
		ε=0.41	**ε=0.86**	**ε=0.41**	**ε=0.86**
Phase A	16.2	6.5	13.3	4.7	9.6
Phase B	14.5	6.5	13.3	4.7	9.6
Phase C	13.6	6.5	13.3	4.7	9.6

10.3 Offline resistance calculations

The temperature data obtained are used to calculate the offline resistance. This is done by solving for R in equation 6.8. To this end the disconnector contact is modelled as a vertical plate. The conditions and dimensions of the contacts are listed in table 10.2. The results of the offline resistance calculations are presented in table 10.3

Table 10.2 constant parameters and sample dimensions for mini disconnector

Thermal conductivity = 237W/mk
Emissivity=0.41
Temperature coefficient = $0.004°C^{-1}$
Contacts dimensions in mm:25x3x50(width x thickness x length)

Table 10.3 results offline resistance measurements and calculations.

		Phase Contact resistance[μΩ]					
		A		**B**		**C**	
		measured	*calculated*	*measured*	*calculated*	*measured*	*calculated*
	%load						
	30	109.5	115	52	50.1	79	80.3
	50	109.5	115.7	52	50.1	79	84.6
	60	109.5	118	52	59.3	79	75.6
	80	109.5	118	52	53.9	79	78.6
	100	109.5	105	52	60.6	79	76.7
error	mean	6.6		4.4		3	
	std	1.8		3.3		1.4	

From table 10.3 it is clear that the calculated values are very close to the measured values.

10.3.1 Temperature correction

The effect of temperature on the resistance was described in chapter 6 which stated that the resistance of conductors increases with increasing temperature. Thus to eliminate the addition resistance caused by the temperature rise the resistance must be corrected for this effect. The effect of temperature rise on the resistance is shown in table 10.4

Table 10.4 effect of temperature on the resistance

	Phase Contact resistance[μΩ]					
	A (109.5)		**B(52)**		**C(79)**	
%load	*Uncorrected*	*corrected*	*uncorrected*	*corrected*	*uncorrected*	*corrected*
30	118	115	51.8	50.1	82	80.3
50	123	115.7	53.2	50.1	89.6	84.6
60	131.6	118	63.5	59.3	81.1	75.6
80	139.2	118	60.1	53.9	87.5	78.6
100	131.8	105	71.9	60.6	91.3	76.7

The resistance measured before the test is given in brackets next to the phase in the column heading. The results show that without resistance correction the estimated values would be much higher without the correction. The correction factor is the term: $1/(1+\alpha(T_{contact}-T_{ma}))$

10.4 Model verification

The condition assessment models developed in chapters 5 and 6 are now applied to this sample to test the validity of the models.

10.4.1 Condition Assessment based on the thermal model

With this model the measured contacts temperature is compared to the calculated maximum allowable temperature of the contact corrected for load current and ambient temperature. The simplified flow chart of the thermal model is given in figure 10.4.The results are shown in table 10.5; the subscript m indicates measured values. Figure 10.5 shows the results in graphical form.

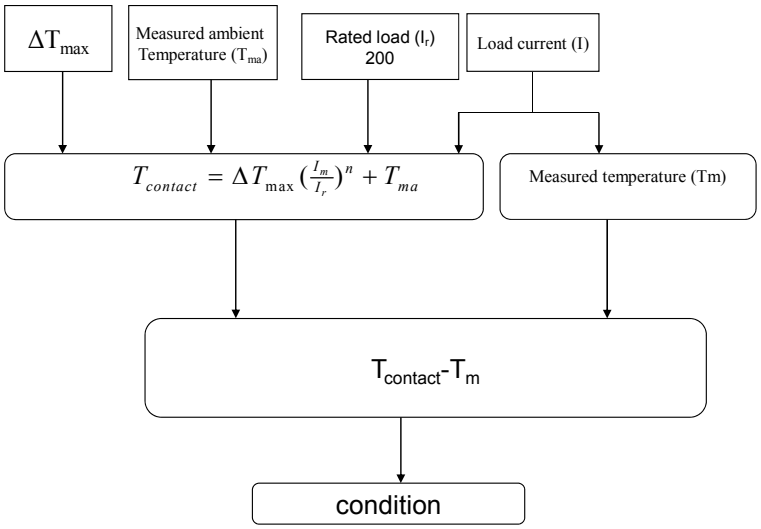

Figure 10.3 simplified flowchart of thermal model ΔT_{max} = 65ºC and n=1.9

Table 10.5 results of measured and calculated contacts temperature

	Phase contacts temperature								
%Load	**A(Rcontact=109.5μΩ)**			B**(Rcontact=52μΩ)**			**C(Rcontact=79μΩ)**		
	$T_{Ccontact}$	$T_{mcontact}$	*|ΔT|	$T_{Ccontact}$	$T_{mcontact}$	*|ΔT|	$T_{Ccontact}$	$T_{mcontact}$	*|ΔT|
30	27.6	27.5	0.1	27.6	26.2	1.4	27.6	26.2	1.4
50	38.41	38	0.41	38.41	34.1	4.40	38.41	34.4	4.40
60	46.7	49.7	0.2	46.7	40	6.7	46.7	40.2	6.5
80	64.5	64.4	0.1	64.5	51.1	13.4	64.5	51.1	13.4
100	87	86.9	0.1	87	69.1	17.9	87	69.7	17.6

*ΔT= Tmcontact - TCconact

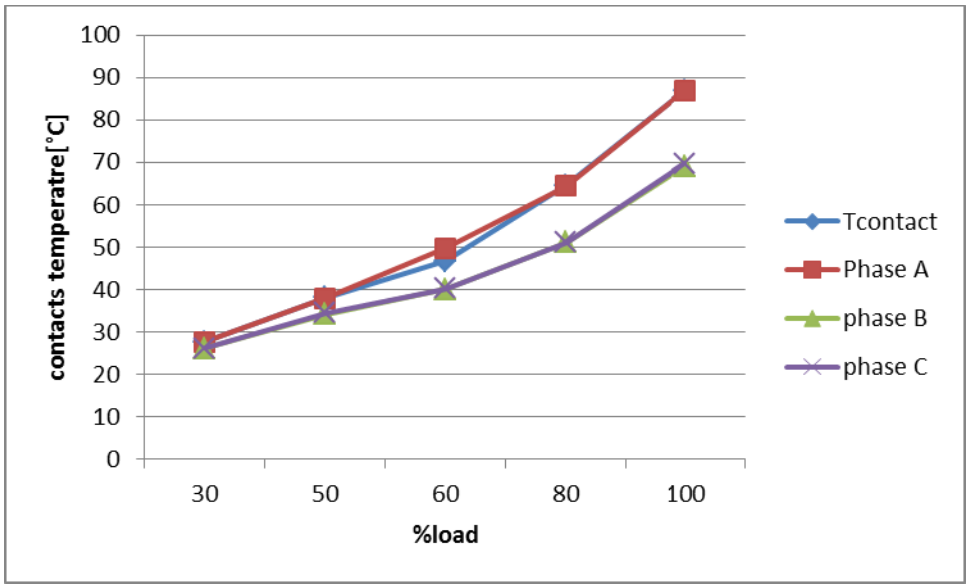

Figure 10.4 measured contacts temperature against maximum allowable contacts temperature (Tcontact)

The results presented in figure 10.5 shows that regardless of the load current the measured contacts temperature of each phase is below the maximum allowable temperature. This implies that all three contacts are in good condition. This result is very strange since the resistance of the contact of phase A is more than twice as that of phase B. Also the temperature differences between phase B and C are practical zero, while the resistance of phase C is higher than that of phase B.

10.4.2 Condition assessment based on resistance model

The resistance model as described in chapter 6 uses the calculated numerical value of the contacts resistance to assess the condition of the contact.

This method uses in addition to the data from the thermal model a reference to evaluate the condition of the contact. Figure 10.5 illustrates the evaluation process. The results are given in table 10.7

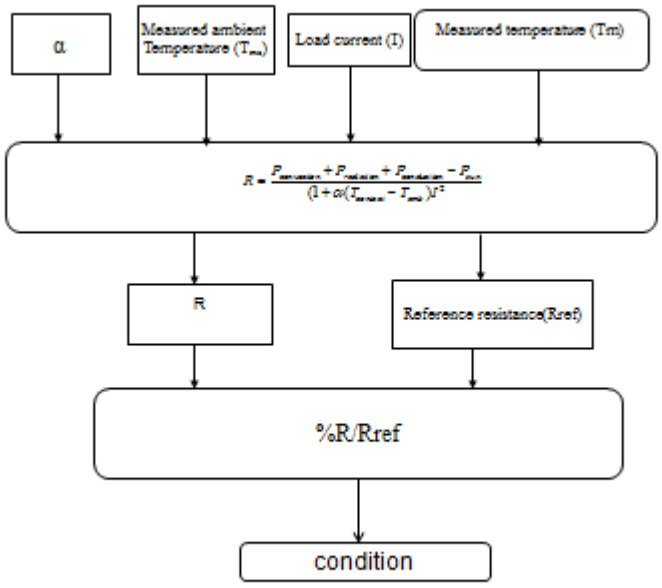

Figure 10.5 model to evaluate the contacts condition according to off-line method

The contacts resistance of phase B is chosen as reference resistance to evaluate the condition of the contacts of phase A and C.

Table 10.7 calculations results

	$\%R/R_{ref}$	
%Load	**A(Rcontact=109.5μΩ)**	**C(Rcontact=79μΩ)**
30	221.2	154.4
50	222.5	162.7
60	226.9	145.4
80	226.9	151.2
100	201.9	147.5

According to the criteria to analyse the contacts condition (see table 6.2) when the value of R/Rref is greater than 120% the condition of the contact is declared poor. From the results of table 10.7 all the values in the second and third column are greater than 120%. Hence the contacts of phase A and B are poor. While the thermal and on-line evaluation models have failed to detect the poor condition of these contacts, this model on the other hand has managed to predict that the contacts of phase A and C are in the poor condition.

Conclusion based on the results from chapter 8, 9 and 10 the following conclusions can be drawn:

- 1. Although, with smaller resistance of the contact, the resistance model couldn't predict the off-line numerical value it managed to predict that the contact was in good condition by estimating its value to be lower.

- 2. The resistance model is accurate when the contact is the source of heating of the device. The estimated value of the off-line numerical value was pretty close to the actual value.

11. Infrared camera measurements

The infrared measurements were done indoors as well as outdoors, using the Fluke Ti50 IR FlexCam Thermal Imager with fusion. (See fig 7.3). The system consisted of a scanning camera with vanadium oxide detector of wave length 8-14 μm. According to the manufacturer the system has thermal sensitivity of ≤ 0.070 at 30ºC. The camera had 320x240 Focal plane array detector and the 1.3mrad spatial resolution with 23° horizontal and 17° vertical FOV.

For the indoor measurements the experimental samples developed in the laboratory discussed in chapters 7 through 10 were used, the experiments were done in the high voltage laboratory of University of Delft. For the outdoor measurements, the disconnectors contacts in the substations of TenneT TSO bv were the samples.

11.1 Laboratory experiments with infrared camera

The goal of this experiment is to investigate the following:

- The role of emissivity on the temperature measurement
- The role of the distance and the angle between the camera and the object
- The impact of background reflections on the measurements

11.1.1 Determining the emissivity value

The emissivity values were determined in accordance with the calibration methods described in chapter 3.The values were determined when the temperature of the sample was higher than the surrounding temperature. In chapter 3 it was showed that the radiated energy from an object is a function of its temperature and its emissivity and the reflected energy is a function of its reflectance and temperature. Since the transmitted energy from opaque body is zero the energy measured by the camera is a sum of the emitted and reflected energy by the object. Therefore if the object is at the same temperature as its surroundings the energy measured by the camera can be expressed as:

$$W_{cam} = \varepsilon W(T_{amb}) + \rho W(T_{amb}) \quad (11.1)$$

Where $\varepsilon W(T_{amb})$ is the energy emitted by the object and $\rho W(T_{amb})$ is the energy reflected off the object at the same temperature T_{amb}. Since the reflectivity (ρ) is $1-\varepsilon$, equation 11.1 then becomes:

$$W_{cam} = \varepsilon W(T_{amb}) + (1-\varepsilon) W(T_{amb}) \quad (11.2)$$

This simplifies to:

$$W_{cam} = W(T_{amb}) \qquad (11.3)$$

Equation 11.3 shows that the measured radiant energy by the camera is only a function of the temperature which means the camera will always measure $W(T_{amb})$ regardless of the emissivity. This is the reason why the temperature of the object must be higher than its surroundings.

Calibration at ambient temperature was performed on the minidisconnector. A point was placed on a surface of the contact area and the camera was tuned until the temperature of the point was the same as the ambient temperature. The value of the emissivity found was 88. Figure 11.1 shows the temperature of the point calibrated at ambient temperature of 19°C; the object was not loaded. The visible image is presented in figure 11.1a, figure 11.1b shows is the original image of the calibration. Figures c and d are the simulated thermograms for different values of emissivity. There is no difference between the simulated thermograms and the original thermogram. All three thermograms give the same temperature; 19°C. This is correct as the ambient temperature has not changed. Therefore the calibration must be done on loaded object which has higher temperature than the ambient temperature.

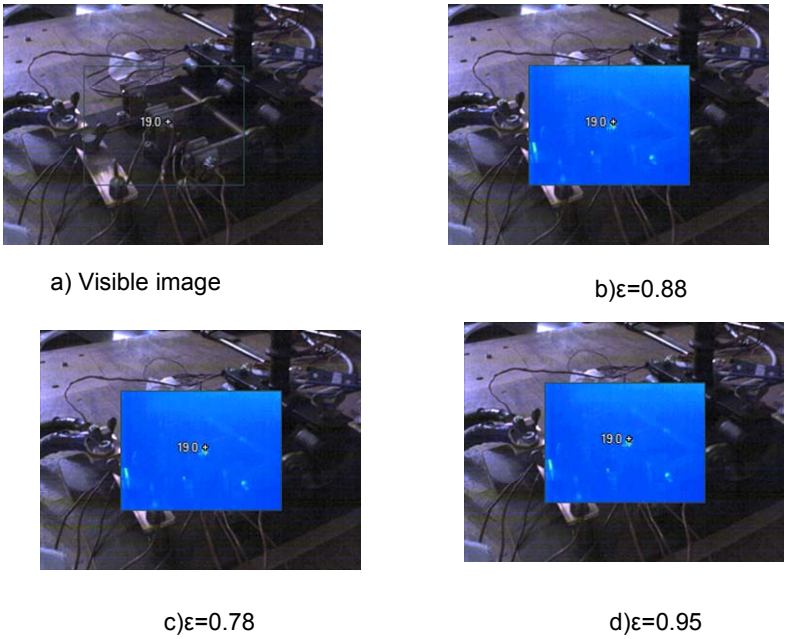

a) Visible image

b)ε=0.88

c)ε=0.78

d)ε=0.95

Figure 11.1 effect of emissivity calibration with target object at the same temperature as the background

- **Determination of the emissivity value according to the contact method described in chapter 3.2.3**

A thermocouple was placed on a small surface area of the disconnector contact. The thermocouple was connected to a recorder, at 60% load the contacts temperature was 36.4°C and the value of the emissivity was 0.55. After the calibration the load was raised from 60% to 100%, the images were recorded and analysed using the Smartview software, the results are presented in table 11.1 where Tc represent the thermocouple, Tmin,Tavg and Tmax are the minimum, average and maximum temperature of the contact measured by the camera, std is the standard deviation. The difference between the temperature measured by the infrared and the thermocouples are very little. This means the error caused by emissivity is less; the temperature reading from the camera will be more accurate.

Table 11.1 calibration based on the contact method at 19°C ambient temperature

		Temperature by IR camera				
I[A]	**Tc[°C]**	**Tmin[°C]**	**Tavg[°C]**	**Tmax[°C]**	**std**	**Tc-Tavg**
200	57	32.4	57.4	77.6	8.36	-0.4 ± 8.36
240	69.5	33.4	68.1	96.7	12.4	1.4 ± 12.4

- **Determination of the emissivity from lookup table**

The minidisconector had an oxidized surface therefore the emissivity value given by the lookup table is 0.42. This value is used to simulate the images recorded from the above calibration. The results are presented in table 11.2.

Table 11.2 simulated results with ε=0.42 at 19°C ambient air temperature

		Temperature by IR camera				
I[A]	**Tc[°C]**	**Tmin[°C]**	**Tavg[°C]**	**Tmax[°C]**	**std**	**Tc-Tavg**
200	57	37.2	68.2	91.8	10.31	11.2 ± 8.36
240	69.5	33.4	87.1	<110	x	17.6

- **Determination of emissivity based on black tape method**

A black tape of emissivity 0,95 was placed on the copper sample close to the contacts area, two thermocouples were also placed at the contact surface to measure and record the contacts temperature for the sake of comparison. The calibration was done at 150 amps load current and at 24°C ambient temperature .The value found for the emissivity of the copper sample was 0.52. The results are presented in table 11.3. The values given the in the second column are the average values of the two thermocouples plus the standard deviation.

Table 11.3 Black tape calibration

		Temperature by IR camera				
I[A]	**Tc[°C]**	**Tmin[°C]**	**Tavg[°C]**	**Tmax[°C]**	**std**	**Tc-Tavg[**°C]
200	53.1 ± 0,14	39,8	50,5	64,2	5,75	2.7 ± 5.61
240	63 ± 0.07	43,5	59,6	75,8	9,62	3.4 ± 9.13

The following conclusions can be drawn from the three results:

- The calibration with the thermocouples gave the best results for the emissivity, the difference between the temperature measured by the thermocouples and the camera were the least from the three calibration methods.
- The worst was the lookup table methods this method gave the largest error.
- The errors increased as the temperature of the object also increased these results are seen by all three methods.

11.1.2 Effect of distance and angle on the measurements

When the object is examined from a long range, the object appears to be colder but the ambient temperature stays the same which will cause the camera to read a lower temperature. This is due to the fact that the area seen by the camera at long range becomes wider and as result, the camera will detect other objects surrounding the target object. The energy from the target object spreads out and energy from the other objects surrounding the target starts mixing with the target objects energy. This will affect the objects temperature, because the surrounding temperature is colder than the objects temperature, the temperature of the hot spot will be less than it should be. When the distance is further increased the hot spot may go entirely unnoticed.

Distance object to camera

The effect the distance from camera to object was investigated by placing a thermocouple at the surface of the copper sample for comparison. Image of the sample were taken at three different objects to camera distances. The images analysed, using the centre point feature of the SmartView software .The ambient temperature at the time of measurement was 23 °C. The results are shown in table 11.4.The data in the first column are the values from the centre point analysis and in the second columns, the temperature measured by the thermocouple (TC) are presented.

Table11.4Effect of distance object to camera

Distance[m]	**Tcp[ºC]**	**TC[ºC]**
0.5	57	63
1	45.1	63
1.5	23.9	63

From the results the following are observed:
-The temperature difference between the minimum and maximum distance is 33.1°C
-The temperature difference between the thermocouple and the minimum distance is 3°C
- The temperature difference between the maximum distance and the thermocouple is 39.1°C.
The above results show that the farther the object is from the camera the less accurate will the results be. At the minimum distance, the accracy of the measurement is 5% compared to the 53% accuracy at maximum distance.

Angle between object and camera

To investigate the effect of angle between camera and object, the aluminium sample was loaded with 150 amps. A thermocouple was placed at the surface of the sample for comparison. The angle from object to camera was varied from 0 to 90 degrees; 0 degrees angle is defined as the position directly in front of the object (see fig11.2 position 1). Images of the sample were made and analysed, using the centre point feature of the SmartView software .The ambient temperature at the time of measurement was 20 °C. The results are shown in table 11.5.The data in the first column are the values from the centre box analysis and in the second columns, the temperature measured by the thermocouple (TC) are presented.

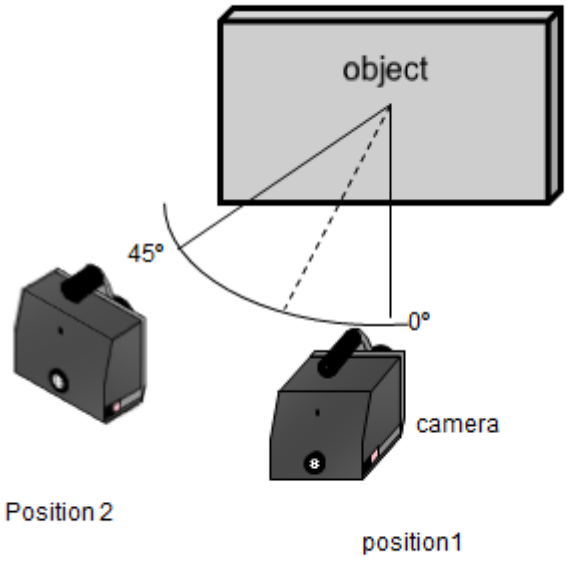

Figure11.2 illustration of angle of camera to object

Table 11.5Angle between camera and object at 0.5m distance with ambient air temperature at 20.4ºC

Angle[degrees]	**Tcp[ºC]**	**TC[ºC]**
0	51.9	51.4
30	82.2	51.4
45	40.2	51.4
60	25.2	51.4
90	25.1	51.4

Using the temperature of the centre point analysis it is seen that:
- The temperature difference between the minimum and maximum camera angle is 26.8 ºC.
-The temperature difference between the minimum angle and the thermocouple measurement is 0.5 ºC
-The temperature difference between the maximum angle and the value measured by the thermocouple measurement is 26.3 ºC.
-The temperature difference between the minimum angle and the maximum angle is practically the same as the temperature difference between the thermocouple and the minimum angle.

From the results it can be concluded that the angle between the camera and object is a factor that must be considered in infrared measurements. The best results are obtained at an angle of 0 degrees.

11.1.3 Effect of reflections from the background

Reflections enhance the temperature of the object and lead to the wrong temperature reading. During the experiment in the laboratory the temperature of the copper sample was taken with the light switched on and the light switched off, the results are shown in figure 11.3.

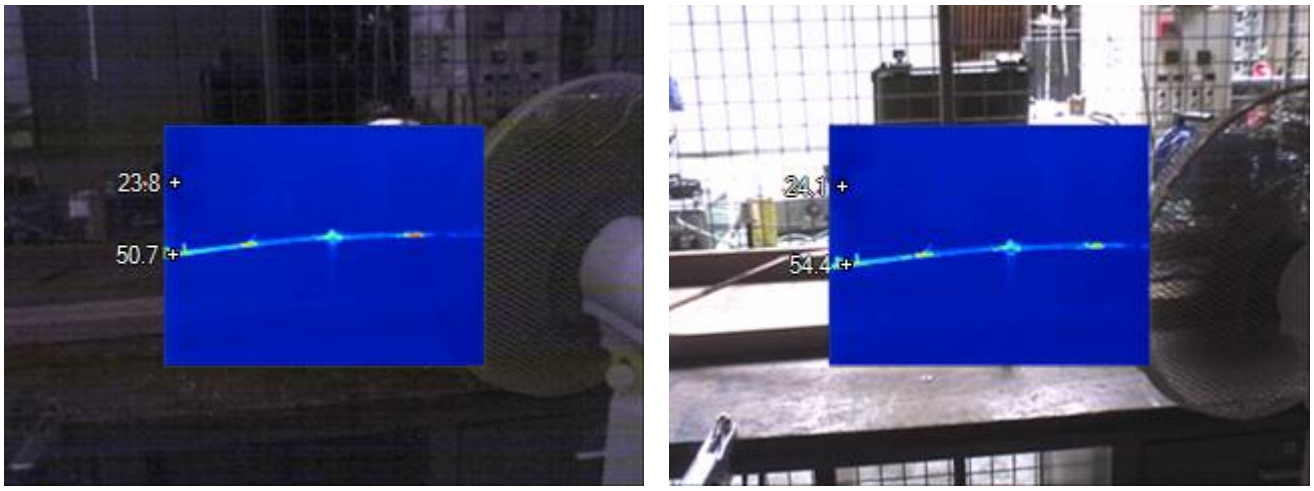

a) light off b) light on

Figure 11. 3Effect of reflections on the temperature.

The hotspot feature of the SmartView software was used to mark the hottest spot of the object. In the figure on the left the temperature, the hottest spot is 50.7 ºC and form the right picture the hottest spot is about 4 ºC higher. From chapter 3 it is shown that the camera calculates the object temperature based on the amount of radiation energy the camera received from the object. From the left picture the energy leaving the objects surface is higher due to the big light.

11.1.4 Data Analysis of laboratory experiment with infrared

The effect of distance and angle are explained by the field of view (FOV) and the spatial resolution (IFOV) of the camera.

FOV
This is the largest area that the camera can see at set distance often given in horizontal degrees (H) by vertical degrees (V), describing the resolution in the horizontal and vertical direction (see fig. 11.5). The formula for the FOV as function of distance is given as [14]:

HxV [m^2] (11.1)

Where
$H = d\sin(horizontal\,\deg rees)$ [m], $V = d\sin(vertical\,\deg rees)$ [m] , d= distance from object to camera[m] and sin is the sine function. This means that as the distance increases the area seen by the camera will become wider. The FOV of the Fluke Ti50 is 23° horizontal x 17° vertical with these optics the FOV can be plotted as a function of distance. The result is shown in the top plot of figure 11. From the plot it clear as the distance gets longer, the area seen by the camera gets wider.

IFOV is the smallest detail within the FOV that the camera can see at a set distance. Therefore the Fluke Ti50 with 320 by 240 focal plane array at distance d can detect a detail of[14]:

$dHrad = dVrad$ [m2] (11.2)

Where

$Hrad = d\sin(\frac{23\pi}{180*320})$ is the spatial resolution in the horizontal direction(m)

$Vrad = d\sin(\frac{17\pi}{180*240})$ is the spatial resolution in the vertical direction(m).

In the bottom plot of figure 11.x the result of the IFOV as function of distance is presented. The curve shows that the smallest detail detectable by the camera gets wider as the distance to the object increases. For example at 0.3 meters distance the IFOV is $1.396x10^{-7}m^2$ while the IFOV is $5.58310^{-7}m^2$ at 0.6m. This is 4 times bigger than the IFOV at 0.3m, thus at 0.6 meters details smaller than $5.58310^{-7}m^2$ will not be detected by The angle at which the camera is placed is also a factor. The wider the angle the wider the area viewed by the camera.

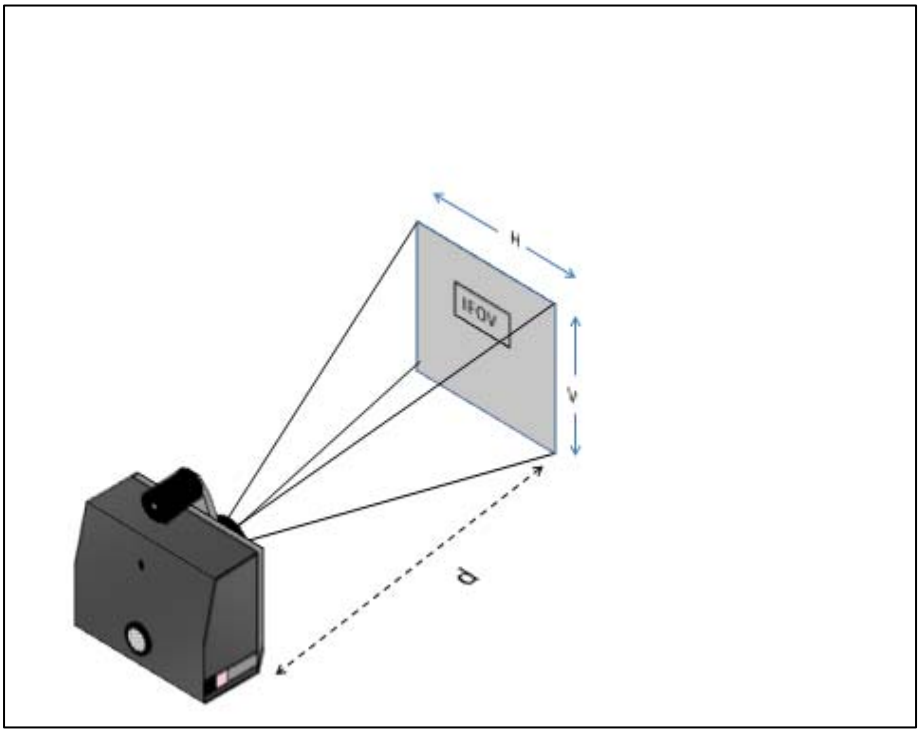

Figure 11.4 Illustration of distance of camera to object

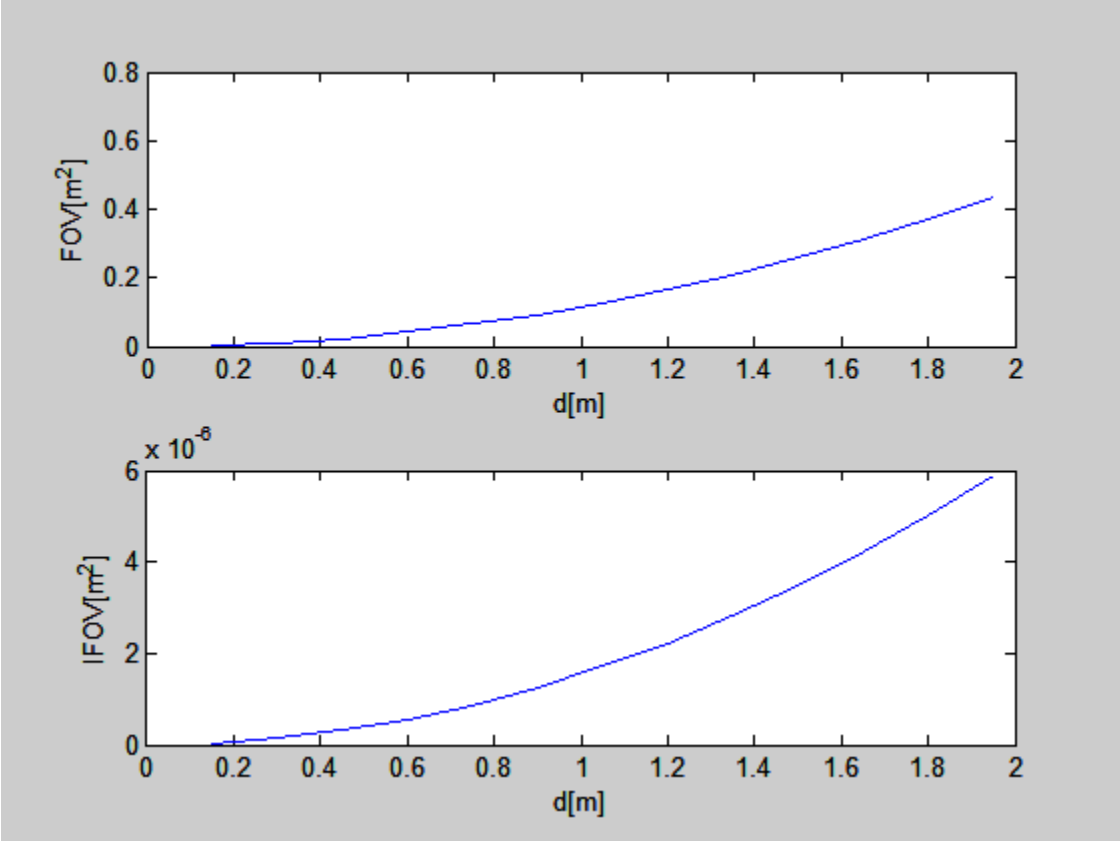

Figure 11.5 field of view as function of distance

IFOV is the smallest detail within the FOV that the camera can see at a set distance

11.2 On-line measurements

The on-line measurements were conducted at two substations of TenneT TSO, one outdoor station and one indoor station. In this section the thermal model developed in chapter 5 will be applied. The resistance model will not be applied here due to the fact that the dimensions of the disconnectors are unknown.

11.2.1 Outdoor substation

The first inspection was carried out at the 150kV outdoor substation on a double side break disconnectors. The rated current of the disconnector was3150A, the resistance was not measured. From the thermal model the Total allowable temperature at the time of measurements was calculated using the equation 5.2. The results are given in the last column of table 11.5. The ambient temperature at

the time of measurements was 30°C, the ambient temperature used for the calculation was 20°C because the emissivity value used by the infrared camera to measure the temperature of the contact was 0.95 this value is associated with ambient temperature of 20°C, to make the comparison more meaningful the, ambient the for the thermal model must also be set to 20 °C. The images of the three contacts were taken and the rectangle box feature was used to mark the whole contact area for the analysis of the temperature at the contact. The results are presented in table11.5. The column headings represent measurement number, minimum, average and maximum temperature of the contacts, the standard deviation, and the ambient temperature used to analyse the contacts temperature the calculated maximum value of the contacts temperature and the load current. A0 and A1 indicate the two contacts of the double side break disconnector.

Table 11.5 results outdoor measurements

No	**Tmin[ºC]**	**Tavg[ºC]**	**Tmax[ºC]**	**std**	**Tamb°C**	**T_cal[**°C]	**I[A]**
1							120
A0	20.6	5.1	29.9	19.33	20	20.1	
A1	-19	5.5	28.9	17.09	20	20.1	
2							380
A0	-12.4	6.8	33.5	17.9	20	20.9	
A1	-11.9	6.9	34.5	17.85	20	20.9	
3							120
A0	-21.2	5.3	13.98	13.98	20	20.1	
A1	-19.2	5.3	12.64	12.64	20	20.1	

To assess the condition of the contact the thermal model compares the measured valued to the calculated values of the contacts temperature. If the measured value of the contacts temperature is less than the calculated value the, the contact is in good condition. Using the average values it is seen that the measured temperatures are far less than the calculated values hence the contacts are in good conditions.

11.2.2 Indoor substation

The second measurements were performed at the150 kV indoor substation on a double side break disonnectors. The rated current of the disconnector was 2kA. Two disconnectors contacts from two different sections were measured. For each section only the contacts that were in the shadows could be measured and for each disconnectors, only one main contact was measured because there was too much reflection on the other

contact due to the sun rays through the stations window. Since there was no way of calibrating the camera, different values for emissivity are used to determine the contacts temperature. The value of emissivity are taken from table 3.1(chapter 3) and from the manufacturer. Who states that the emissivity of the object can be set to 0.95 and the background temperature to 20°C. The contact temperature was calculated using eq.5.2, chapter 5, the load current at the time of measurements were 37A for section 2 and 58 A for section 3. The results are presented in table 11.6 a and b for section 2 and 3 respectively.

Table 11.6a results section 2 at

ε	**Tmin[ºC]**	**Tavg[ºC]**	**Tmax[ºC]**	**std**	**Tamb[°C]**	**T_cal[**°C]
0.04	-12	-8.1	12.6	6.4	21.5	21.5
0.07	-2.9	5.3	13.1	2.52	21.5	21.5
0.11	6.3	11.8	18.4	1.8	21.5	21.5
0.95	19.9	20.4	21	0.20	20	20

Table 11.6b results Section 3

ε	**Tmin[ºC]**	**Tavg[ºC]**	**Tmax[ºC]**	**std**	**Tamb**[°C]	**T_cal[**°C]
0.04	-7.7	6.6	6.6	7.07	21.1	21.6
0.07	-2.9	13.2	13.2	3.91	21.5	21.6
0.11	6.3	6.3	16.3	2.33	21.5	21.6
0.95	19.9	20.5	21	0.25	20	20

Using the average values of the rectangle marker feature of the software it can be seen that:

-For both section 2 and section 3 the maximum measured temperature is at emissivity 0.95

-The average temperature at emissivity 0.95 is used to for comparison for the condition assessment. The value found at 0.95 is close to the actual value if for example the disconnector was unloaded, the temperature of the contact will be close to the temperature of its environment.

- Comparing the average temperature at emissivity value of 0.95 with the calculated values shows that the difference is less than 4ºC. There for the contacts of the contacts are in good stage.

11.3 Conclusions and recommendations infrared camera measurements

The conclusion drowns from the experimental and field measurements are:
The infrared camera is not capable of taking accurate temperature measurements due to the following factors:

- **The emissivity of the object.**

This can have a huge impact on the temperature reading and is the largest source of error in the temperature measurements.

- **The distance from camera to object**

The camera software does not incorporate object distance to be taken into account. The results show that, the distance between the object cannot be ignored. If the distance is too long the sees a wider area and smaller details are missed which can leads to lower temperature reading.

- **Angle of camera to object**

This has an effect on the temperature reading but not as much as the objects distance to camera. The best angle is 0 degrees. This will reduce the background of the object with this angle the other objects from the targets surrounding can be minimized.

- **Reflections**

Reflection cannot be avoided unless the measurements are done in complete darkness. However reflection can be reduced by performing temperature measurement before sunrise or after sunset and preferably when the sky is not clear.

Recommendations
Reference[4] recommended that in order to perform thermographic inspection with reasonable accuracy the following must be considered:

- The device under investigation must be in service and preferably under high load.
- The person conducting IR scanning surveys must be able to distinguish between excessive temperature due faulty equipment and excessive temperature due to reflections and solar gain.
- Environmental factors such as wind, rain, snow and the sun must be avoided.

The author seconds the first two statements and recommends in addition the following

- Sun

  If the sun cannot be avoided the measured temperature must be corrected with the method described in section 5.1.3 using either equations 5.34 or 5.35.

- Wind

Power stations owner or operators must perform wind test on their equipment at different power levels and create a chart with wind correction factors.

During thermographic inspection the thermographer must have a wind meter to measure the wind speed and correct for wind using the chart created for that particular equipment.

- Emissivity

The emissivity error can be minimized by:

1) The emissivity value must be determined through calibration at high load using the contact method.
2) Or equipment must be painted black, this way the emissivity value of 0. 95 can be used

- Angle between camera and object

The angle between the camera and object should be preferably 0 degrees

- Distance between object and camera

Use cameras that allows the distance from object to camera to be entered in the calculations the.

- The thermograms must be simulates with different values of emissivity to minimize the error caused by emissivity

12. Conclusions and recommendations

In this study a model has been presented to estimate the offline numerical value of the contact resistance, using the temperature data obtained online, resistance model. This model is based on a steady state heat transfer calculations. Next to this model is a thermal model used to investigate the factors which have effect on the contacts temperature.

12.1 Conclusions

Resistance model

The model has been verified through measurements in the laboratory. From the measurements results it was found that:

- When the resistance of the contact is high the model can estimate the off-line resistance value with 6% accuracy.
- For contacts with medium resistance the accuracy of the model is 8%
- When the resistance of the contact is low the model fails to estimate the offline numerical value of the contacts resistance, the prediction form the model is in the range 2 to 5 time less than the offline value of the contacts resistance.
- The convection heat transfer correlations found in the literature for horizontal plate with heated surface downwards are specified for Rayleigh number in the range of 10^5 to $10^{10,}$ the values found for the calculation were in the range of 262-807 for the very low resistance and 551-10^3 for the high resistance. This presented a huge challenge for the accuracy of the calculations and was the main source of error.

Thermal model:

- The thermal model on its own as proposed by this thesis was not able to predict the correct condition of the contact in some cases. However, when it is used in conjunction with the resistance model the condition of the contact can be predicted.
- Environmental conditions have huge impact on the temperature of the contact. The study showed that in some cases the sun can add up to 16°C to the contacts temperature.
- The wind cooling is power dependent and therefore making it impossible to find one wind correction factor for all loads.

IR camera:

- The Fluke Ti50 does not incorporate distance to object to be taken into account, although the distance from object to camera plays an important role in the temperature measurements.

- The most important parameter influencing the temperature measurements is the emissivity value. The error caused by this can be reduced by calibrating the object at higher loads, using a contact method.

12.2 Recommendations

The resistance model presented in this thesis was not tested on a real-life disconnector contacts. It is recommended that further research be done using real life disconnect contacts.

Appendix A

Equations for solar latitude and solar declination

$$Hc = arc\sin\{\cos(Lat)\cos(\delta)\cos(\omega) + \sin(Lat)\sin(\delta)\}$$
$$\delta = 23.4583\sin\{\tfrac{284+N}{365}360\}$$
$$Q_s = A + BH_c + CH_c^{\,2} + DH_c^{\,3} + EH_c^{\,4} + FH_c^{\,5} + GH_c^{\,6} \quad (1.1)$$

N= day of the year
δ =solar declination
Lat =latitude in degrees

Table A1 coefficient for equation

Clear atmosphere	
A	-42.2391
B	63.8044
C	-1.9220
D	$3.46921\text{x}10^{-2}$
E	$-3.6118\text{x}10^{-4}$
F	$1.943181\text{x}10^{-6}$
G	$-4.07608\text{x}10^{-9}$
Industrial atmosphere	
A	53.1821
B	14.2110
C	6.6138
D	$-3.1658\text{x}10^{-2}$
E	$5.4654\text{x}10^{-4}$
F	$-4.3446\text{x}10^{-6}$
G	$1.3236\text{x}10^{-8}$

Appendix B

Detailed data and MATLAB script code for calculation

Data for copper sample

R=13.6	Measured temperature[ºC]				
I[A]	T_contcat	T_low	T_up	T_left	T_right
150.1	28	28.05	27.95	24.40	28
224.4	40.68	40.85	40.50	42.30	40.60
300.2	56.33	56.50	56.15	57.50	56.20

R=26.4	Measured temperature[ºC]				
I[A]	T_contcat	T_low	T_up	T_left	T_right
150	31.75	31.8	31.7	31.7	31.2
250	54.43	53.3	52.2	53.3	52.2
300	67.5	67.35	67.65	66.4	66

R=36.3	Measured temperature[ºC]				
I[A]	T_contcat	T_low	T_up	T_left	T_right
150	38.05	38	38.1	37.3	35.6
200	64.85	64.7	65	62.8	60
250	82.78	82.50	83.03	79.3	77

R=44.5	Measured temperature[ºC]				
I[A]	T_contcat	T_low	T_up	T_left	T_right
150	44.75	44.85	44.65	42.8	41.3
200	67.53	67.55	67.5	63	60.8
225	78.23	79	77.45	73.4	70.3

Data mini disconnector

I[A]	TA[ºC]		TB[[ºC]		TC[ºC]		Tma[ºC]
	contact	blade	contact	blade	contact	blade	Tam
60	27.5	25.8	28.8	21.78	26.2	26.08	21
100	37.95	37.1	34.05	33.94	34.4	34.06	21
120.1	49.7	48.5	40	39.86	40.1551.169.7	39.7	22
160	64.35	63.3	51.1	68.46		50.22	
200	86.65	83.4	69.05	68.46		68.28	

MATLAB script code for copper

```
clc
clear
format long g
fprintf ('computing contact resistance value');
T_contact=input ('\nenter contacts temperature ( deg C):');
T_contactu=input ('\nenter upper contacts temperature ( deg C):');
T_contactd=input ('\nenter lower contacts temperature ( deg C):');
T_amb=input ('enter ambient temperature ( deg C):');
T_L=input ('enter temperature left (deg C):');
T_R=input ('enter temperature Right (deg C):');
 I=input ('enter Load current I(A):');

%%%%%%%%%%%%%%%%%%%%%%%%%%%%%%%%%%%%%%%%%
% conversion from Celcuis to Kelvin
%%%%%%%%%%%%%%%%%%%%%%%%%%%%%%%%%%%%%%%%%%%%%%%%%%%%%%%%%%%%%%%%%%%%%%
T_contactK = T_contact+273;%convert contacts temperature from Celsius
to Kelvin
T_ambK =T_amb + 273;%convert ambient temperature from Celsius to Kelvin
T_LK=T_L +273;%convert left side temperature from Celsius to Kelvin
T_RK= T_R+273;%convert right side temperature from Celsius to Kelvin
T_contactKu = T_contactu+273;%convert upper contact temperature from
Celcius to Kelvin
T_contactKd = T_contactd+273;%convert lower temperature from Celsius to
Kelvin
%%%%%%%%%%%%%%%%%%%%%%%%%%%%%%%%%%%%%%%%%%%%%%%%%%%%%%%%%%%%%%%%%%%%%%%%
%%%%%%%%%%%%
%linear interpolation for air properties
%%%%%%%%%%%%%%%%%%%%%%%%%%%%%%%%%%%%%%%%%%%%%%%%%%%%%%%%%%%%%%%%%%%%%%%%
%%%%%%%%%%%%%%%
T_f= (T_contactK +T_ambK)/2;%film temperature
Vf=[11.44 15.89 20.92 26.41];% table for kinematic viscosity
Kf=[22.3 26.3 30.0 33.8];% table thermal conductivity
Mu=[159.6 184.6 208.2 230.1];% table for kinnemat
T= [250 300 350 400];% temperature range for interpolation
pr=[0.720 0.707 0.700 0.690];%table Prantl number
Pr=interp1(T,pr,T_f);%interpolation at film temperature for Prantl
k_f=(interp1(T,Kf,T_f))/1e+3;%interpolation at film thermal
conductivity
```

```
vf=(interp1(T,Vf,T_f))/1e+6;%interpolation at film temperature
kinnematic viscosity
mu=(interp1(T,Mu,T_f))/1e+7;%interpolation at film temperature for
epsi=input ('enter emissivity:');
A_total=31.5e-3*25e-3;
k=401; %thermal conductivity copper
g=9.8;%gravitational acceleration
alfa=0.004;%temeprature coefficient of copper
beta =1/(T_f) ;% thermal expansion coefficient
A=3e-3*25e-3;%conduction surface area
A_hole=pi*(4.25e-3)^2;%
A_contact= A_total -  A_hole;
L_c=0.305;%coduction length
L1 =A_contact/(2*(25e-3 + 31.5e-3));%characteristic length=A/perimeter
delta= 5.67e-8 ;%Boltzman constant
Grhoff=(g*(T_contactK-T_ambK)*beta*L1^3)/vf^2;
Ra=Grhoff*Pr;% Raleigh number
Nuss_L=0.59*Ra^(1/4);%hot surface facing up
Nuss_d=0.27*Ra^(1/4);%hot surface facing down
h_convL=Nuss_L*k_f/L1;% heat transfer
h_d = Nuss_d*k_f/L1;
p_convL= h_convL*A_contact*(T_contactK-T_ambK);%heat loss due to
convection hot up
p_convd= h_d*A_contact*(T_contactK-T_ambK);%heat loss due to convection
hot down
P_condu= k*A*(T_contactKu-T_RK)/L_c;%heat loss due to conduction right
side
P_condd= k*A*(T_contactKd-T_LK)/L_c;%heat loss due to conduction up
P_rad=delta*epsi*A_contact*((T_contactK^4)-(T_ambK^4));
PoutL= p_convL+ P_rad;
PoutD= p_convd+ P_rad;
P_cond1=P_condd+P_condu;
P_tot=PoutL+PoutD+P_condu+P_condd;
fprintf ('\nheat loss due to radiation=%0.2f W',P_rad);
fprintf ('\nheat loss due conduction = %0.4f W',P_cond1);
fprintf ('\ntotal heat loss = %0.4f W',P_tot);
R_contact= P_tot/((1+alfa*(T_contactK-T_ambK))*I^2);
R_contact1= P_tot/I^2;% uncorrected resistance for temperature
fprintf ('\nvalue contact resistance= %0.2e \n',R_contact);
```

MATLAB script code for Minidisconnector

```
clc
clear
format long g
fprintf ('computing contact resistance value');
T_contact=input ('\nenter contacts temperature (deg C):');
T_Blade=input ('\nenter blade temperature ( deg C):');
T_amb=input ('enter ambient temperatutre( deg C):');
I=input ('enter Load current I(A):');
% V=input ('enter wind speed(m/s):');
%%%%%%%%%%%%%%%%%%%%%%%%%%%%%%%%%%%%%%%%%%%%%%%%%%%
% linaer interpolation
T_contactK = T_contact+273;
T_ambK =T_amb + 273;
T_b=T_Blade +273;
T_f= (T_contactK +T_ambK)/2;
Vf=[11.44 15.89 20.92 26.41];
Kf=[22.3 26.3 30.0 33.8];
Mu=[159.6 184.6 208.2 230.1];
T= [250 300 350 400];
pr=[0.720 0.707 0.700 0.690];
Pr=interp1(T,pr,T_f);
k_f=(interp1(T,Kf,T_f))/1e+3;
vf=(interp1(T,Vf,T_f))/1e+6;
mu=(interp1(T,Mu,T_f))/1e+7;
epsi=input ('enter emissivity:');
A_total=31.5e-3*25e-3;
k=401; %thermal conductivity copper
g=9.8;
alfa=0.004;
beta =1/(T_f) ;
A=5e-3*25e-3;%conduction area
A_contact=50e-3*25e-3; %surface area
L_c=87.5e-3;%conduction path
L=50e-3;%characteristic length
delta= 5.67e-8 ;%Boltzman constant
Grhoff=(g*(T_contactK-T_ambK)*beta*L^3)/vf^2;
Ra=Grhoff*Pr;
Nuss_L=0.59*Ra^(1/4);
h_convL=Nuss_L*k_f/L;
p_cond= k*A*(T_contactK-T_b)/L;
P_conv=h_convL*A_contact*(T_contactK-T_ambK);
P_rad=delta*epsi*A_contact*((T_contactK^4)-(T_ambK^4));
Pout= 2*(P_conv+ P_rad);
P_tot=Pout+p_cond;
fprintf ('\nheat loss due to convection=%0.4f W',P_conv);
fprintf ('\nheat loss due to radiation=%0.2f W',P_rad);
fprintf ('\nheat loss due conduction = %0.4f W',p_cond);
fprintf ('\ntotal heat loss = %0.4f W',P_tot);
R_contact= P_tot/((1+alfa*(T_contactK-T_ambK))*I^2);
R_contact1= P_tot/I^2;
fprintf ('\nvalue contact resistance= %0.2e \n',R_contact);
```

Reference

1. Faulkenberry, L.M. and W. Coffer, *Electrical Power Distribution And Transmission*. 1996: Prentice-Hall.
2. Ryan, H.M., *High voltage engineering and testing*. 2nd ed. 2001, London: The institution of Electical Enineers.
3. Aksyonov, Y.P., et al., *On-line & off-line diagnostics for power station HV equipments.* IEEE Int conference, 28 October 99
4. Gill, P., *Electrical power Equipment Maintenance and Testing*. 1998: CRC press.
5. Cigre , W.G., *User Guide For Application of Monitoring and Diagnostic Techniques for switching equipments for rated voltage of 72.5kV and above.* August 200.
6. Lindquist, T.M. and L. Bertling, *Hazard Rate Estimation for High-Voltage Contact Using Infrared Thermography.* IEEE, 2008.
7. Braunovic, M., et al., *Estimation of remaining life remaining life of power connections using infrared thermography.* IEEE 2009.
8. M.Muhr, et al., *Thermography of aged contacts of high voltage equipments.* Elektrotechnik & informationtechnik, December 2006.
9. Braunovic, M., N.K. Myshkin, and V.V. konchits, *Electrical Contacts fundamentals, Applications and Technology*. 2007: CRC Press
10. P.B.Joshi and P.Ramakrishhnan, *Materials for Electrical and Electronic contacts*. 2004, Enfield,New Hampshire: Science Publishers,Inc.
11. Slade, P.G., *Electrical contacts principles and application*. 1999, New York: Marcel Dekker Inc.
12. Kreith, F. and M.S. Bohn, *Principles of heat Transfer*. 1986: Harper & Row, Publishers.
13. Filippakou, M.P., C.G. Karagiannopoulos, and P.D. Bourkas, *Thermal fatigue of the contact/conductors system in emergency load panels.* IEEE, 1996.
14. Minkina, w. and S. Dudzik, *Infrared Thermograpy Errors and uncertainties*. 2009, Chichester: John Wiley & Sons Ltd.
15. Fan, C., F. Sun, and L. Yang, *Investigation on nondestructiveEvaluation of pipelines using infrared thermography.* IEEE, 2005.
16. Schmidt, F.W., R.E. Henderson, and C.H. Wolgemuth, *Introduction to Thermal Sciences*. 1984: John Wiley &Sons.Inc.
17. Incropera, F.P. and D.P. DeWitt, *Fundamentals of Heat and Mass Transfer*. 4th ed. 1996: John Wiley &Sons.Inc.
18. Lindquist, T.M., L. Bertling, and R. Eriksson, *Estimation of disconnector contact condition for modelling the effect of maintenance and ageing* IEEE.
19. Rathore, M.M. and R.R.A. kapuno, *Engineering heat trasfer*

2nd ed. 2011: Jones and Barlett.

20. SmartView, *End users guid.*

21. Fink, D.G. and H.W. Beaty, *Standard handbook for electrical engineers*. 14th ed. 2000, New York: McGraw-Hill.
22. Raznjevic, K., *Handbook of thermodynamic Tables and charts*. 1976, New York: McGraw-Hill.
23. Grover, P., *Applying ASI/IEEE/NEMA Temperature Standards To Infrared Inspections.* 1979.
24. 62271-1, I., *High-voltage switchgear and control gear - Part1: Common specifications* 2007.
25. 738-2006, I.S., *IEE Standard for calculating the Current-Temperature of Bare Overhead Conductors.* 30 Junuary 2007.
26. Santori, E., *Convection coefficient equations for forced air flow over flate surfaces.* Solar Energy, 2006.
27. Duffie, J.A. and W.A. Beckman, *Solar Engineering of thermal processes*. Third ed. 2006, Hoboken, New Jersey: John Wiley&Sons,Inc.
28. C37.24, A.I., *IEEE Guide for Evaluating the Effect of Solar Radiation on Outdoor Metal Enclosed Switchgear.* 1986.
29. Perch-Nielsen, T. and J.C.Sorensen, *Guidelines to thermographic inspection of electrical installations.* 1994.
30. M.A.Laughton and D.F. Warne, *Electrical Engineer's Reference Book,* . sixteenth Edition ed.